PREPARATION AND EVALUATION OF ORAL NANOPARTICULATE DRUG DELIVERY SYSTEM OF ATORVASTATIN CALCIUM

A THESIS SUBMITTED TO

GAUHATI UNIVERSITY, GUWAHATI, ASSAM

IN THE PARTIAL FULFILLMENT OF THE REQUIREMENT

FOR THE DEGREE OF

MASTER OF PHARMACY

IN

PHARMACEUTICS

SUBMITTED BY

Ranjit Konwar

Roll no. MP/11/01

GU Registration no. 051069 of 2008-09

Under the supervision of

Dr. Suvakanta Dash (Principal, GIPS)

Dr. Abdul Baquee Ahmed (Asst. Professor, GIPS)

JUNE, 2013

GIRIJANANDA CHOWDHURY INSTITUTE OF PHARMACEUTICAL SCIENCE

HATHKHOWAPARA, AZARA, GUWAHATI-781017, KAMRUP, ASSAM (INDIA)

GIRIJANANDA CHOWDHURY INSTITUTE OF PHARMACEUTICAL SCIENCE (GIPS)

(A unit of Shrimanta Shankar Academy)
Approved by AICTE & PCI, New Delhi, affiliated to Gauhati University, N.H. 37, Hathkhowapara, Azara, Guwahati-781017
Telephone: (0361) 2843405
Email: gips_guwahati@rediffmail.com

CERTIFICATE

This is to certify that the thesis entitled **"Preparation and Evaluation of oral nanoparticulate drug delivery system of Atorvastatin calcium"** submitted to Gauhati University for the partial fulfilment of the Master of Pharmacy (Pharmaceutics) is a faithful record of bonafide and original research work carried out by **Ranjit Konwar**, with registration no 051069 of 2008-09 & Roll no - MP/11/01 during the academic session 2011-2013 at Pharmaceutics laboratory/Department of Girijananda Chowdhury Institute of Pharmaceutical Science (GIPS) under my supervisions and guidance.

I wish him all success in his life.

Signature of Guide
Dr. Abdul Baquee Ahmed
[Asstt Prof. (Pharmaceutics), GIPS]

Signature of Guide
Prof (Dr.) Suvakanta Dash
[Principal, GIPS]

CONTENTS

List of Tables

List of Figures

LIST OF ABBREVIATIONS

ABBREVIATIONS	FULL FORMS
FTIR	Fourier Transform Infrared Spectroscopy
SEM	Scanning Electron Microscopy
DSC	Differential scanning calorimetry
PXRD	Powder X-ray Diffractometer
rpm	Revolution per minute
mg	Miligram
Hrs	Hours
Min	Minutes
Sec	Seconds
w/v	Weight/ volume
µg/mc	Microgram
^{0}C	Degree centigrade
%	Percentage
I.P.	Indian Pharmacopoeia
U.S.	United states of Pharmacopoeia
B.P.	British Pharmacopoeia
DMSO	Dimethyl sulfoxide
PhEup	European Pharmacopoeia
USPNF	National Formulary, United states of Pharmacopoeia

SD	Standard Deviation
LOQ	Limit of Quantification
LOD	Limit of Detection

Dedicated to

My Beloved family

GIRIJANANDA CHOWDHURY INSTITUTE OF PHARMACEUTICAL SCIENCE (GIPS)

(AUnit of ShrimantaShankarAcademy)

Approved by AICTE, New Delhi, Affiliated to GauhatiUniversity

N.H. 37, Hathkhowapara, Azara, Guwahati-781017

Telephone: (361) 2843405,09957184005(Principal) E-mail:
gips_guwahati@rediffmail.com

CERTIFICATE

This is to certify that the project entitled "Preparation and Evaluation of oral nanoparticulate drug delivery system of Atorvastatin calcium" has been approved by the IAEC, GIPS with the animal and number as per condition given below:

1. Proposal number:- Mph-2
2. Approval No:- *GIPS/IAEC/MPH/20013/2*
3. Date of approval: - 3. 5.2013
4. Expiry date:- 3.6.2013
5. Species of animal used:- Rabbit
6. No of Animal permitted:- 6 (six only)

GIRIJANANDA CHOWDHURY INSTITUTE OF PHARMACEUTICAL SCIENCE AZARA, GUWAHATI-17

Chairman, IAEC, GIPS
(Dr. Suvakanta Dash)

Dr. Suvakanta Dash M. Pharm, Ph. D.
Principal
Girijananda Chowdhury Institute
of Pharmaceutical Science
Azara, Guwahati - 17

ACKNOWLEDGEMENT

Research is a never ending process involving a team of persons striving to attain newer horizons in the field of sciences. This study would not have been completed without the encouragement and co-operation of my teachers, parents, friends, well-wishers and relatives. I take this opportunity to express my deep gratitude to one and all.

I consider myself most lucky and privileged to work under the guidance of Dr. Abdul Baquee Ahmed, Asst. Professor, Dept. of Pharmaceutics, GIPS, Azara, Guwahati. His discipline, principles, simplicity, caring attitude and provision of fearless work environment will be cherished in all walks of my life. I am very much grateful to him for his valuable guidance and everlasting encouragement throughout my course.

I sincerely thank Dr. Suvakanta Dash, Principal, GIPS, Azara, Guwahati for his inspiration and for being a great facilitator.

I express my sincere gratitude to my teachers Asst. Professor Dr. Bipul Nath and Bhanupratap Sahu, GIPS,Azara, Guwahati, for their meticulous guidance and encouragement provided to me for the completion of my dissertation work. Also my sincere thanks to other teaching faculty for their timely help.

I wish to express my deepest gratitude to Dr. Debasis Chowdhury, IASST, Boragaon, Guwahati, for his help in providing me SEM and Zeta potential analysis facility in completing the work.

I am very thankful to Ozone Pharmaceutical, Amingaon, Guwahati, for generous gift sample of Atorvastatin Calcium and Amlodipdine Bisylate.

My heartfelt thanks to my friends Samir, Ratul, Utpal, Jatin, Popy, Adiya, Somi, Pranab, Sanjay, Shiekh Sofiur, Pranjal, Tapash, Anupam, Trailokya for their support who by their honest opinions and diligence kept me lively.

I express my sincere thanks to Bipul Sarma, GIPS, Azara, Guwahati, for his help in performing HPLC and all other analytical work in completing my work.

Last,.....but not at least, I wish to express my gratitude towards " god-almighty" and my father and mother who gave me the strength and courage to fulfil my dream and has showered upon me their choicest blessings.

Thankful I ever remain.....

Date:

Place: Azara, Guwahati **Ranjit Konwar**

GIRIJANANDA CHOWDHURY INSTITUTE OF PHARMACEUTICAL SCIENCE (GIPS)

(A unit of Shrimanta Shankar Academy)
Approved by AICTE & PCI, New Delhi, affiliated to Gauhati University,
N.H. 37, Hathkhowapara, Azara, Guwahati-781017
Telephone: (0361) 2843405
Email: gips_guwahati@rediffmail.com

DECLARATION BY THE CANDIDATE

I hereby declare that this dissertation/ thesis entitled **"Preparation and Evaluation of Oral Nanoparticulate Drug Delivery System of Atorvastatin Calcium"** is a bonafied and genuine research work carried out by me under the supervision and guidance of **Dr. Abdul Baquee Ahmed**, Asst. Professor, Dept. of Pharmaceutics, GIPS, Hathkhowapara, Azara, Guwahati-781017.

Date:

Place: Azara, Guwahati, Assam **Ranjit Konwar**

Regd. No. 051069

Chapter 1

Introduction

1.1. ORAL ROUTE OF DRUG DELIVERY

1.2. NANOPARTICULATE DRUG DELIVERY SYSTEM

1.3. HYPOLIPIDAEMICS

1.4. AIM AND OBJECTIVES

1.5. PLAN OF WORK

1. INTRODUCTION

1.1. ORAL ROUTE OF DRUG DELIVERY

Oral ingestion is the most convenient and commonly employed route of drug delivery due to its ease of administration, high patient compliance, cost effectiveness, least sterility constraints and flexibility in the design of dosage form. As a result, many of the generic drug companies are inclined more to produce bioequivalent oral drug products. However the major problem with the design of oral dosage forms lies with their poor bioavailability. The oral bioavailability depends on several factors including aqueous solubility, drug permeability, dissolution rate, first pass metabolism and susceptibility to efflux mechanisms. The most frequent causes of low bioavailability is attributed to poor solubility and low permeability.[1]

Nearly 40% of new drug candidates exhibit low solubility in water, which leads to poor oral bioavailability, high intra and inter subject variability, and lack of dose proportionality. Thus, for those drugs, the absorption rate from the lumen of the gastrointestinal tract is controlled by dissolution. Hence, producing suitable formulations is essential to improve the solubility and bioavailability of such drugs. One of the most popular and commercially viable formulations approaches for these problem is nanoparticulate system which have attracted considerable attention from pharmaceutical scientist who want to increase the oral bioavailability of such poorly water soluble drugs.

1.2. NANOPARTICULATE DRUG DELIVERY SYSTEM

1.2.1. Introduction

Nanoparticles are defined as particulate dispersions or solid particles with a size in the range of 10-1000nm. The drug is dissolved, entrapped, encapsulated or attached to a nanoparticle matrix. Depending upon the method of preparation, nanoparticles, nanospheres or nanocapsules can be obtained. Nanocapsules are systems in which the drug is confined to a cavity surrounded by a unique polymer membrane, while nanospheres are matrix systems in which the drug is physically and uniformly dispersed. In recent years, biodegradable polymeric nanoparticles, particularly those coated with hydrophilic polymer such as poly(ethylene glycol) (PEG) known as long-circulating particles, have been used as potential drug delivery devices because of their ability to circulate for a prolonged period time target a particular organ, as carriers of DNA in gene therapy, and their ability to deliver proteins, peptides and genes. The major goals in designing nanoparticles as a delivery system are to control particle size, surface properties and release of pharmacologically active agents in order to achieve the site-specific action of the drug at the therapeutically optimal rate and dose regimen.

Though liposomes have been used as potential carriers with unique advantages including protecting drugs from degradation, targeting to site of action and reduction toxicity or side effects, their applications are limited due to inherent problems such as low encapsulation efficiency, rapid leakage of water-soluble drug in the presence of blood components and poor storage stability. On the other hand, polymeric nanoparticles offer some specific advantages over liposomes. For instance, they help

to increase the stability of drugs/proteins and possess useful controlled release properties [2, 3, 4].

The advantages of using nanoparticles as a drug delivery system include the following:

- Particle size and surface characteristics of nanoparticles can be easily manipulated to achieve both passive and active drug targeting after parenteral administration.
- They control and sustain release of the drug during the transportation and at the site of localization, altering organ distribution of the drug and subsequent clearance of the drug so as to achieve increase in drug therapeutic efficacy and reduction in side effects.
- Controlled release and particle degradation characteristics can be readily modulated by the choice of matrix constituents. Drug loading is relatively high and drugs can be incorporated into the systems without any chemical reaction; this is an important factor for preserving the drug activity.
- Site-specific targeting can be achieved by attaching targeting ligands to surface of particles or use of magnetic guidance.
- The system can be used for various routes of administration including oral, nasal, parenteral, intra-ocular etc.

In spite of these advantages, nanoparticles do have limitations. For example, their small size and large surface area can lead to particle-particle aggregation, making physical handling of nanoparticles difficult in liquid and dry forms. In addition, small particles size and large surface area readily result in limited drug loading and burst

release. These practical problems have to be overcome before nanoparticles can be used clinically or made commercially available[5, 6].

1.2.2. Preparation of Nanoparticles:

Nanoparticles can be prepared from a variety of materials such as proteins, polysaccharides and synthetic polymers. The selection of matrix materials is dependent on many factors including: (a) size of nanoparticles required; (b) inherent properties of the drug, e.g., aqueous solubility and stability; (c) surface characteristics such as charge and permeability; (d) degree of biodegradability, biocompatibility and toxicity; (e) Drug release profile desired; and (f) Antigenicity of the final product[7].

Nanoparticles have been prepared most frequently by three methods: (A) dispersion of preformed polymers; (B) polymerization of monomers; and (C) ionic gelation or coacervation of hydrophilic polymers. However, other methods such as supercritical fluid technology and particle replication in non-wetting template have also been described in the literature for production of nanoparticles. The latter was claimed to have absolute control of particle size, shape and composition, which could set an example for the future mass production of nanoparticles in industry[8].

A. Dispersion of preformed polymers:

Dispersion of preformed polymers is a common technique used to prepare biodegradable nanoparticles from poly (lactic acid) (PLA); poly (D,L-glycolide),PLG; poly (D, L-lactide-co-glycolide) (PLGA) and poly (cyanoacrylate) (PCA)[9,10,11]. This technique can be used in various ways as described below.

A.1. Solvent evaporation method: [12]

In this method, the polymer is dissolved in an organic solvent such as dichloromethane, chloroform or ethyl acetate which is also used as the solvent for dissolving the hydrophobic drug. The mixture of polymer and drug solution is then emulsified in an aqueous solution containing a surfactant or emulsifying agent to form an oil in water (o/w) emulsion. After the formation of stable emulsion, the organic solvent is evaporated either by reducing the pressure or by continuous stirring. Particle size was found to be influenced by the type and concentrations of stabilizer, homogenizer speed and polymer concentration. In order to produce small particle size, often a high-speed homogenization or ultrasonication may be employed.

A.2. Spontaneous emulsification or solvent diffusion method: [13]

This is a modified version of solvent evaporation method. In this method, the water miscible solvent along with a small amount of the water immiscible organic solvent is used as an oil phase. Due to the spontaneous diffusion of solvents an interfacial turbulence is created between the two phases leading to the formation of small particles. As the concentration of water miscible solvent increases, a decrease in the size of particle can be achieved. Both solvent evaporation and solvent diffusion methods can be used for hydrophobic or hydrophilic drugs. In the case of hydrophilic drug, a multiple w/o/w emulsion needs to be formed with the drug dissolved in the internal aqueous phase.

B. Polymerization method: [14]

In this method, monomers are polymerized to form nanoparticles in an aqueous solution. Drug is incorporated either by being dissolved in the polymerization medium

or by adsorption onto the nanoparticles after polymerization completed. The nanoparticle suspension is then purified to remove various stabilizers and surfactants employed for polymerization by ultracentrifugation and re-suspending the particles in an isotonic surfactant-free medium. This technique has been reported for making polybutylcyanoacrylate or poly (alkylcyanoacrylate) nanoparticles. Nanocapsule formation and their particle size depend on the concentration of the surfactants and stabilizers used.

C. Coacervation or ionic gelation method: [15]

Much research has been focused on the preparation of nanoparticles using biodegradable hydrophilic polymers such as chitosan, gelatine and sodium alginate. Calvo and co-workers developed a method for preparing hydrophilic chitosan nanoparticles by ionic gelation. The method involves a mixture of two aqueous phases, of which one is the polymer chitosan, a di-block co-polymer ethylene oxide or propylene oxide (PEO-PPO) and the other is a polyanion sodium tripolyphosphate. In this method, positively charged amino group of chitosan interacts with negative charged tripolyphosphate to form coacervates with a size in the range of nanometer. Coacervates are formed as a result of electrostatic interaction between two aqueous phases, whereas, ionic gelation involves the material undergoing transition from liquid to gel due to ionic interaction conditions at room temperature.

D. Production of nanoparticles using supercritical fluid technology: [16]

Conventional methods such as solvent extraction-evaporation, solvent diffusion and organic phase separation methods require the use of organic solvents which are hazardous to the environment as well as to physiological systems. Therefore, the supercritical fluid technology has been investigated as an alternative to prepare

biodegradable micro- and nanoparticles because supercritical fluids are environmentally safe.

A supercritical fluid can be generally defined as a solvent at a temperature above its critical temperature, at which the fluid remains a single phase regardless of pressure. Supercritical CO_2 (SC CO_2) is the most widely used supercritical fluid because of its mild critical conditions (Tc = 31.1 °C, Pc = 73.8 bars), non-toxicity, non-flammability, and low price. The most common processing techniques involving supercritical fluids are supercritical anti-solvent (SAS) and rapid expansion of critical solution (RESS). The process of SAS employs a liquid solvent, eg. methanol, which is completely miscible with the supercritical fluid (SC CO_2), to dissolve the solute to be micronized; at the process conditions, because the solute is insoluble in the supercritical fluid, the extract of the liquid solvent by supercritical fluid leads to the instantaneous precipitation of the solute, resulting the formation of nanoparticles. RESS differs from the SAS process in that its solute is dissolved in a supercritical fluid (such as supercritical methanol) and then the solution is rapidly expanded through a small nozzle into a region lower pressure, Thus the solvent power of supercritical fluids dramatically decreases and the solute eventually precipitates. This technique is clean because the precipitate is basically solvent free. RESS and its modified process have been used for the product of polymeric nanoparticles. Supercritical fluid technology technique, although environmentally friendly and suitable for mass production, requires specially designed equipment and is more expensive.

1.2.3. Effect of Characteristics of Nanoparticles on Drug Delivery:

a. Particle size

Particle size and size distribution are the most important characteristics of nanoparticle systems. They determine the *in vivo* distribution, biological fate, toxicity and the targeting ability of nanoparticle systems. In addition, they can also influence the drug loading, drug release and stability of nanoparticles. Many studies have demonstrated that nanoparticles of sub-micron size have a number of advantages over microparticles as a drug delivery system. Generally nanoparticles have relatively higher intracellular uptake compared to microparticles and available to a wider range of biological targets due to their small size and relative mobility. Desai *et.al*; found that 100 nm nanoparticles had a 2.5 fold greater uptake than 1 µm microparticles, and 6 fold greater uptake than 10 µm microparticles in a Caco-2 cell line [17]. In a subsequent study, the nanoparticles penetrated throughout the submucosal layers in a rat *in situ* intestinal loop model, while microparticles were predominantly localized in the epithelial lining. It was also reported that nanoparticles can across the blood-brain barrier following the opening of tight junctions by hyper osmotic mannitol, which may provide sustained delivery of therapeutic agents for difficult-to-treat diseases like brain tumors. Tween 80 coated nanoparticles have been shown to cross the blood-brain barrier. In some cell lines, only submicron nanoparticles can be taken up efficiently but not the larger size microparticles [18].

Drug release is affected by particle size. Smaller particles have larger surface area, therefore, most of the drug associated would be at or near the particle surface, leading to fast drug release. Whereas, larger particles have large cores which allow more drug to be encapsulated and slowly diffuse out. Smaller particles also have greater risk of

aggregation of particles during storage and transportation of nanoparticle dispersion. It is always a challenge to formulate nanoparticles with the smallest size possible but maximum stability [19]. Polymer degradation can also be affected by the particle size. For instance, the rate of PLGA polymer degradation was found to increase with increasing particle size *in vitro*. It was thought that in smaller particles, degradation products of PLGA formed can diffuse out of the particles easily while in large particles, degradation products are more likely remained within the polymer matrix for a longer period to cause autocatalytic degradation of the polymer material. Therefore, it was hypothesized that larger particles will contribute to faster polymer degradation as well as the drug release. However, Panyam *et.al*; prepared PLGA particles with different size ranges and found that the polymer degradation rates *in vitro* were not substantially different for different size particles [20]. Currently, the fastest and most routine method of determining particle size is by photon-correlation spectroscopy or dynamic light scattering. Photon-correlation spectroscopy requires the viscosity of the medium to be known and determines the diameter of the particle by Brownian motion and light scattering properties. The results obtained by photon-correlation spectroscopy are usually verified by scanning or transmission electron microscopy (SEM or TEM).

b. Surface properties of nanoparticles

When nanoparticles are administered intravenously, they are easily recognized by the body immune systems, and are then cleared by phagocytes from the circulation. Apart from the size of nanoparticles, their surface hydrophobicity determines the amount of adsorbed blood components, mainly proteins (opsonins). This in turn influences the *in vivo* fate of nanoparticles[21]. Binding of these opsonins onto the surface of

nanoparticles called opsonization acts as a bridge between nanoparticles and phagocytes. The association of a drug to conventional carriers leads to modification of the drug biodistribution profile, as it is mainly delivered to the mononuclear phagocytes system (MPS) such as liver, spleen, lungs and bone marrow. Indeed, once in the blood stream, surface non-modified nanoparticles (conventional nanoparticles) are rapidly opsonized and massively cleared by the macrophages of MPS rich organs[22]. Generally, it is IgG, complement C_3 components that are used for recognition of foreign substances, especially foreign macromolecules. Hence, to increase the likelihood of the success in drug targeting by nanoparticles, it is necessary to minimize the opsonization and to prolong the circulation of nanoparticles *in vivo*. This can be achieved by (a) surface coating of nanoparticles with hydrophilic polymers/surfactants; (b) formulation of nanoparticles with biodegradable copolymers with hydrophilic segments such as polyethylene glycol (PEG), polyethylene oxide, polyoxamer, poloxamine and polysorbate 80(Tween 80). Studies show that PEG conformation at the nanoparticle surface is of utmost importance for the opsonin repelling function of the PEG layer. PEG surfaces in brush-like and intermediate configurations reduced phagocytosis and complement activation whereas PEG surfaces in mushroom-like configuration were potent complement activators and favoured phagocytosis[23].

The zeta potential of a nanoparticle is commonly used to characterise the surface charge property of nanoparticles. It reflects the electrical potential of particles and is influenced by the composition of the particle and the medium in which it is dispersed. Nanoparticles with a zeta potential above (+/-) 30 mV have been shown to be stable in suspension, as the surface charge prevents aggregation of the particles. The zeta

potential can also be used to determine whether a charged active material is encapsulated within the centre of the nanocapsule or adsorbed onto the surface[24].

c. Drug loading [25]

Ideally, a successful nanoparticulate system should have a high drug-loading capacity thereby reduce the quantity of matrix materials for administration. Drug loading can be done by two methods:

- Incorporating at the time of nanoparticles production (incorporation method)
- Absorbing the drug after formation of nanoparticles by incubating the carrier with a concentrated drug solution (adsorption/absorption technique).

Drug loading and entrapment efficiency very much depend on the solid-state drug solubility in matrix material or polymer (solid dissolution or dispersion), which is related to the polymer composition, the molecular weight, the drug polymer interaction and the presence of end functional groups (ester or carboxyl). The PEG moiety has no or little effect on drug loading. The macromolecule or protein shows greatest loading efficiency when it is loaded at or near its isoelectric point when it has minimum solubility and maximum adsorption. For small molecules, studies show the use of ionic interaction between the drug and matrix materials can be a very effective way to increase the drug loading.

d. Drug release [26]

To develop a successful nanoparticulate system, both drug release and polymer biodegradation are important consideration factors. In general, drug release rate depends on: (1) solubility of drug; (2) desorption of the surface bound/adsorbed drug; (3) drug diffusion through the nanoparticle matrix; (4) nanoparticle matrix

erosion/degradation; and (5) combination of erosion/diffusion process. Thus solubility, diffusion and biodegradation of the matrix materials govern the release process. In the case of nanospheres, where the drug is uniformly distributed, the release occurs by diffusion or erosion of the matrix under sink conditions. If the diffusion of the drug is faster than matrix erosion, the mechanism of release is largely controlled by a diffusion process. The rapid initial release or 'burst' is mainly attributed to weakly bound or adsorbed drug to the large surface of nanoparticles. It is evident that the method of incorporation has an effect on release profile. If the drug is loaded by incorporation method, the system has a relatively small burst effect and better sustained release characteristics. If the nanoparticle is coated by polymer, the release is then controlled by diffusion of the drug from the core across the polymeric membrane. The membrane coating acts as a barrier to release, therefore, the solubility and diffusivity of drug in polymer membrane becomes determining factor in drug release. Furthermore release rate can also be affected by ionic interaction between the drug and addition of auxiliary ingredients. When the drug is involved in interaction with auxiliary ingredients to form a less water soluble complex, then the drug release can be very slow with almost no burst release effect; whereas if the addition of auxiliary ingredients e.g., addition of ethylene oxide-propylene oxide block copolymer (PEO-PPO) to chitosan, reduces the interaction of the model drug bovine serum albumin (BSA) with the matrix material (chitosan) due to competitive electrostatic interaction of PEO-PPO with chitosan, then an increase in drug release could be observed. Various methods which can be used to study the *in vitro* release of the drug are: (1) side-by-side diffusion cells with artificial or biological membranes; (2) dialysis bag diffusion technique; (3) reverse dialysis bag technique; (4) agitation followed by ultracentrifugation/centrifugation; (5) Ultra-filtration or centrifugal ultra-

filtration techniques. Usually the release study is carried out by controlled agitation followed by centrifugation. Due to the time-consuming nature and technical difficulties encountered in the separation of nanoparticles from release media, the dialysis technique is generally preferred.

1.2.4. Applications of Nanoparticulate Delivery Systems:

a. Tumor targeting using nanoparticulate delivery systems

The rationale of using nanoparticles for tumor targeting is based on (1) nanoparticles will be able to deliver a concentrate dose of drug in the vicinity of the tumor targets via the enhanced permeability and retention effect or active targeting by ligands on the surface of nanoparticles; (2) nanoparticles will reduce the drug exposure of health tissues by limiting drug distribution to target organ. Verdun *et.al*; demonstrated in mice treated with doxorubicin incorporated into poly (isohexylcyanoacrylate) nanospheres that higher concentrations of doxorubicin manifested in the liver, spleen and lungs than in mice treated with free doxorubicin[27]. Studies show that the polymeric composition of nanoparticles such as type, hydrophobicity and biodegradation profile of the polymer along with the associated drug's molecular weight, its localization in the nanospheres and mode of incorporation technique, adsorption or incorporation, have a great influence on the drug distribution pattern *in vivo*. The exact underlying mechanism is not fully understood but the biodistribution of nanoparticles is rapid, within ½ hour to 3 hours, and it likely involves MPS and endocytosis/phagocytosis process[28].

Recently Bibby *et.al*; reported the biodistribution and pharmacokinetics (PK) of a cyclic RGD doxorubicin- nanoparticle formulation in tumor bearing mice[29]. Their biodistribution studies revealed decreasing drug concentrations over time in the heart,

lung, kidney and plasma and accumulating drug concentrations in the liver, spleen and tumor. The majority injected dose appeared in the liver (56%) and only 1.6% in the tumour at 48 hrs post injection, confirming that nanoparticles have a great tendency to be captured by liver. This indicates the greatest challenge of using nanoparticles for tumour targeting is to avoid particle uptake by mononuclear phagocytic system (MPS) in liver and spleen. Such propensity of MPS for endocytosis/phagocytosis of nanoparticles provides an opportunity to effectively deliver therapeutic agents to these cells. This biodistribution can be of benefit for the chemotherapeutic treatment of MPS- rich organs/tissues localized tumors like hepatocarcinoma, hepatic metastasis arising from digestive tract or gynaecological cancers, brochopulmonary tumors, primitive tumors and metastasis, small cell tumors, myeloma and leukaemia. It has been proved that using doxorubicin loaded conventional nanoparticles was effective against hepatic metastasis model in mice. It was found there was greater reduction in the degree of metastasis than when free drug was used. The underlying mechanism responsible for the increased therapeutic efficacy of the formulation was transfer of doxorubicin from healthy tissue, acting as a drug reservoir to the malignant tissues[30]. Histological examination showed a considerable accumulation of nanoparticles in the lysosomal vesicles of Kupffer cells, whereas nanoparticles could not be clearly identified in tumoral cells. Thus Kupffer cells, after a massive uptake of nanoparticles by phagocytosis, were able to induce the release of doxorubicin, leading to a gradient of drug concentration, favourable for a prolonged diffusion of the free and still active drug towards the neighbouring metastatic cells.

When conventional nanoparticles are used as carriers in chemotherapy, some cytotoxicity against the Kupffer cells can be expected, which would result in deficiency of Kupffer cells and naturally lead to reduced liver uptake and decreased

therapeutic effect with intervals of less than 2 weeks administration. Moreover, conventional nanoparticles can also target bone marrow (MPS tissue), which is an important but unfavourable site of action for most anticancer drugs because chemotherapy with such carriers may increase myelosuppresive effect. Therefore, the ability of conventional nanoparticles to enhance anticancer drugs efficacy is limited to targeting tumors at the level of MPS-rich organs. Also, directing anticancer drug-loaded nanoparticles to other tumoral sites is not feasible if a rapid clearance of nanoparticles occurs shortly after intravenous administration[31].

b. Long circulating nanoparticles [32]

To be successful as a drug delivery system, nanoparticles must be able to target tumors which are localized outside MPS-rich organs. In the past decade, a great deal of work has been devoted to developing so-called "stealth" particles or PEGylated nanoparticles, which are invisible to macrophages or phagocytes. A major breakthrough in the field came when the use of hydrophilic polymers (such as polyethylene glycol, poloxamines, poloxamers, and polysaccharides) to efficiently coat conventional nanoparticle surface produced an opposing effect to the uptake by the MPS. These coatings provide a dynamic "cloud" of hydrophilic and neutral chains at the particle surface which repel plasma proteins. As a result, those coated nanoparticles become invisible to MPS, therefore, remained in the circulation for a longer period of time. Hydrophilic polymers can be introduced at the surface in two ways, either by adsorption of surfactants or by use of block or branched copolymers for production of nanoparticles.

c. Reversion of multidrug resistance in tumour cells [33]

Anticancer drugs, even if they are located in the tumour interstitium, can turn out to be of limited efficacy against numerous solid tumour types, because cancer cells are able to develop mechanisms of resistance. These mechanisms allow tumours to evade chemotherapy. Multidrug resistance (MDR) is one of the most serious problems in chemotherapy. MDR occurs mainly due to the over expression of the plasma membrane p-glycoprotein (Pgp), which is capable of extruding various positively charged xenobiotics, including some anticancer drugs, out of cells. In order to restore the tumoral cells, sensitivity to anticancer drugs by circumventing Pgp-mediated MDR, several strategies including the use of colloidal carriers have been applied. The rationale behind the association of drugs with colloidal carriers, such as nanoparticles, against drug resistance derives from the fact that Pgp probably recognizes the drug to be effluxed out of the tumoral cells only when this drug is present in the plasma membrane, and not when it is located in the cytoplasm or lysosomes after endocytosis.

d. Nanoparticles for oral delivery of peptides and proteins [34]

Significant advances in biotechnology and biochemistry have led to the discovery of a large number of bioactive molecules and vaccines based on peptides and proteins. Development of suitable carriers remains a challenge due to the fact that bioavailability of these molecules is limited by the epithelial barriers of the gastrointestinal tract and their susceptibility to gastrointestinal degradation by digestive enzymes. Polymeric nanoparticles allow encapsulation of bioactive molecules and protect them against enzymatic and hydrolytic degradation. For instance, it has been found that insulin-loaded nanoparticles have preserved insulin

activity and produced blood glucose reduction in diabetic rats for up to 14 days following the oral administration.

e. Targeting of nanoparticles to epithelial cells in the GI tract using ligands

Targeting strategies to improve the interaction of nanoparticles with adsorptive enterocytes and M-cells of Peyer's patches in the GI tract can be classified into those utilizing specific binding to ligands or receptors and those based on nonspecific adsorptive mechanism. The surface of enterocytes and M-cells display cell-specific carbohydrates, which may serve as binding sites to colloidal drug carriers containing appropriate ligands. Certain glycoproteins and lectins bind selectively to this type of surface structure by specific receptor-mediated mechanism. Different lectins, such as bean lectin and tomato lectin, have been studied to enhance oral peptide adsorption[35]. Vitamin B-12 absorption from the gut under physiological conditions occurs via receptor-mediated endocytosis. The ability to increase oral bioavailability of various peptides (e.g., granulocyte colony stimulating factor, erythropoietin) and particles by covalent coupling to vitamin B-12 has been studied. For this intrinsic process, mucoprotein is required, which is prepared by the mucus membrane in the stomach and binds specifically to cobalamin. The mucoprotein completely reaches the ileum where resorption is mediated by specific receptors[36].

f. Absorption enhancement using non-specific interactions [37]

In general, the gastrointestinal absorption of macromolecules and particulate materials involves either paracellular route or endocytotic pathway. The paracellular route of absorption of nanoparticles utilises less than 1% of mucosal surface area. Using polymers such as chitosan, starch or poly (acrylate) can increase the paracellular permeability of macromolecules. Endocytotic pathway for absorption of nanoparticles

is either by receptor-mediated endocytosis, that is, active targeting, or adsorptive endocytosis which does not need any ligands. This process is initiated by an unspecific physical adsorption of material to the cell surface by electrostatic forces such as hydrogen bonding or hydrophobic interactions. Adsorptive endocytosis depends primarily on the size and surface properties of the material.

If the surface charge of the nanoparticles is positive or uncharged, it will provide an affinity to adsorptive enterocytes though hydrophobic, whereas if it is negatively charged and hydrophilic, it shows greater affinity to adsorptive enterocytes and M-cells. This shows that a combination of size, surface charge and hydrophilicity play a major role in affinity. This is demonstrated with poly (styrene) nanoparticles and when it is carboxylated.

g. Nanoparticles for gene delivery

Polynucleotide vaccines work by delivering genes encoding relevant antigens to host cells where they are expressed, producing the antigenic protein within the vicinity of professional antigen presenting cells to initiate immune response. Such vaccines produce both humoral and cell-mediated immunity because intracellular production of protein, as opposed to extracellular deposition, stimulates both arms of the immune system. The key ingredient of polynucleotide vaccines, DNA, can be produced cheaply and has much better storage and handling properties than the ingredients of the majority of protein-based vaccines. Hence, polynucleotide vaccines are set to supersede many conventional vaccines particularly for immunotherapy. However, there are several issues related to the delivery of polynucleotides which limit their application. These issues include efficient delivery of the polynucleotide to the target cell population and its localization to the nucleus of these cells, and ensuring that the

integrity of the polynucleotide is maintained during delivery to the target site. Nanoparticles loaded with plasmid DNA could also serve as an efficient sustained release gene delivery system due to their rapid escape from the degradative endo-lysosomal compartment to the cytoplasmic compartment[38]. Hedley *et.al*; reported that following their intracellular uptake and endolysosomal escape, nanoparticles could release DNA at a sustained rate resulting in sustained gene expression. This gene delivery strategy could be applied to facilitate bone healing by using PLGA nanoparticles containing therapeutic genes such as bone morphogenic protein[39].

h. Nanoparticles for drug delivery into the brain

The blood-brain barrier (BBB) is the most important factor limiting the development of new drugs for the central nervous system. The BBB is characterized by relatively impermeable endothelial cells with tight junctions, enzymatic activity and active efflux transport systems. It effectively prevents the passage of water-soluble molecules from the blood circulation into the CNS, and can also reduce the brain concentration of lipid-soluble molecules by the function of enzymes or efflux pumps[40]. Consequently, the BBB only permits selective transport of molecules that are essential for brain function. Strategies for nanoparticle targeting to the brain rely on the presence of and nanoparticle interaction with specific receptor-mediated transport systems in the BBB. For example polysorbate 80/LDL, transferrin receptor binding antibody such as lactoferrin, cell penetrating peptides and melanotransferrin have been shown capable of delivery of a self non transportable drug into the brain via the chimeric construct that can undergo receptor-mediated transcytosis. It has been reported poly (butylcyanoacrylate) nanoparticles was able to deliver hexapeptide

dalargin, doxorubicin and other agents into the brain which is significant because of the great difficulty for drugs to cross the BBB[41].

Oral nanoparticulate systems are believed to be one of the most effective drug delivery system for the poorly water soluble drug as well as the drug which undergoes first pass metabolism. The delivery systems are effective in targeting the cells, reducing the dose thus reducing the dose related toxicities[42].

Oral delivery of nanoparticles are mainly done by the translocation of nanoparticles via lymphatic system and lymph targeting of nanoparticulate systems can permit : (*i*) oral delivery of labile molecules protected by the carrier; (*ii*) oral delivery of poorly soluble molecules following their nanosolubilization in nanoparticulates system; (*iii*) improved bioavailability of drugs with poor absorption characteristics, due both to the large specific surface of nanoparticulates system and to their increased residence time; (*iv*) oral delivery of vaccine antigens to gut-associated lymphoid tissue; (*v*) translocation of antineoplastic drugs for treatment of lymphomas; (*vi*) delivery of diagnostics for the lymphatic system; (*vii*) sustained/controlled drug release, particularly important for toxic drugs (e.g., antineoplastic drugs); (*viii*) reduction of drug-related GI mucosa irritation; and (*ix*) avoidance of the hepatic first-pass effect[43].

1.3. HYPOLIPIDAEMICS:

These are the drugs which lowers the levels of lipid and lipoproteins in the blood. The hypolipidaemic drugs have attracted considerable attention because of their potential to prevent the cardiovascular diseases by retarding the accelerated atherosclerosis in hypolipidaemic individuals.

1.3.1. Classification of hypolipidaemics

- HMG Co.A Reductase inhibitors (Statins): Atorvastatin, Simvastatin, Lovastatin
- Bile acid sequestrants (Resins): Cholestyramine, Cholestipol
- Activated lipoprotein lipase (Fibric acid derivatives): Clofibrate, Fenofibrate, Benzofibrate
- Inhibit lipolysis and triglyceride synthesis: Nicotinic acid
- Others: Ezetimide, Gugulipid

1.3.2. Mechanism of action of statins

Dyslipidemia and hypercholesterolemia are controlled by the liver. Hepatocytes take up from the circulation 50% of total LDL cholesterol. An increase in the activity of LDL receptor in the hepatocyte could be an efficient method to reduce the plasma LDL cholesterol level.

Inhibition of HMG CoA reductase

Statins target the hepatocytes and inhibit the HMG CoA reductase, the enzyme that is responsible for converting HMG CoA to mevalonic acid, a cholesterol precursor. The statins do more than just compete with the normal substrate in the enzymes active site. They alter the conformation of the enzyme when they bind with the enzyme active site.

This prevents HMG CoA reductase from attaining a functional structure. The change in conformation at the active site makes these drugs very effective and specific.

Binding of statins to the HMG CoA reductase is reversible, and their affinity for the enzyme is in the nanomolar range, as compared to the natural substrate which has micromolar affinity.

The inhibition of HMG CoA reductase determines the reduction of intracellular cholesterol, inducing the activation of protease which slices the sterol regulatory element binding proteins (SREBPs) from the endoplastic reticulum. SREBPs are translocated at the level of nucleus, where they increase the gene expression for LDL receptor. The reduction of cholesterol in the hepatocytes leads to the increase of hepatic LDL receptors, which determines the reduction of circulating LDL and its precursors. All statins reduce LDL cholesterol non-linearly, dose dependant and after administration of single daily dose. Efficacy on triglyceride reduction parallels the LDL cholesterol reduction [44].

1.3.3. Adverse effects of statins [45]

Statins are generally well tolerated. The most important adverse effects are liver and muscle toxicity. Myopathy can happen if inhibitors of cytochrome P450 or other inhibitors of statin metabolism are administered together with statins, determining the increase of their blood concentration. Such are the Azole antifungals.

1.4. AIM AND OBJECTIVE:

Aim of the present work is to prepare and evaluate oral nanoparticles for a model drug (Atorvastatin calcium) to improve the bioavailability. Based on this aim the following objective has been undertaken:

- Identification of drug as per existing standard.

- Determining the compatibility of drug-excipients.
- Preparation of nanoparticles by different methods.
- Characterisation of nanoparticles in terms of particle size, zeta potential, drug loading, entrapment efficiency etc.
- In-vitro drug release and in-vivo pharmacokinetic studies in animal.

1.5. PLAN OF WORK:

i. Pre-formulation studies of drug and polymer in terms of

- Identification and physicochemical characterization of drug
- Drug-excipients compatibility study by FT-IR, DSC, PXRD etc.

ii. Preparation of nanoparticles by a suitable method.

iii. Characterization of the prepared nanoparticles in terms of

- Particle Size
- Zeta potential
- Drug loading capacity
- Drug Entrapment Efficiency

iv. *In-vitro* drug release study.

v. Release kinetic study of the optimised formulation

vi. Stability study of the optimised formulation

vii. Surface morphology study of the optimised formulation

viii. *In-vivo* pharmacokinetic studies of the optimised formulation in animal model.

Chapter 2

Review of Literature

2. REVIEW OF LITERATURE

- **Suganeswari M. *et.al;* prepared nanoparticles Containing Atorvastatin calcium and Amlodipine besylate[46].**

  The main aim of the study was to prepare, characterize and evaluate nanoparticles containing Hypolipidaemic drug (Atorvastatin calcium) Antihypertensive agent (Amlodipine besylate) loaded by nanoprecipitation method using tribloere polymeric stabilizer (Pluronic F68).Through the study, it was shown that nanoparticles using PLGA polymers were formulated using nanoprecipitation technique and were characterized for size, drug loading, and *in-vitro* release. Side effect of Atorvastatin was reduced 60% by combining with Amlodipine. The biodegradable nanoparticles are found to be in the range of 50-100nm, stable and they produced excellent solubility and dissolution profile.

- **Arunkumar N. *et.al;* prepared a nanosuspension of Atorvastatin calcium for enhanced solubility and dissolution[47].**

  Poorly soluble drugs are often a challenging task for formulators in the industry as it may cause poor dissolution and hence low oral bioavailability. An attempt was made in the study to prepare nanosuspensions of a poorly soluble drug (Atorvastatin calcium) in order to enhance its dissolution and oral bioavailability. Nanosuspensions were prepared by anti-solvent precipitation followed by sonication technique. They were characterized by thermal gravimetric analysis (TGA), differential scanning calorimetry (DSC), powder x-ray diffraction (PXRD), solubility, dissolution and *in vivo* bioavailability studies. The absence of Atorvastatin peaks in PXRD profiles of

nanosuspensions suggests the transformation of crystalline drug into an amorphous form. TGA examination suggested that the drug was converted into anhydrous form from the original tri-hydrate form. DSC curves also compliment the result obtained by TGA and PXRD. The effect of particle size was found to be significant on the saturation solubility of the drug. The *in vitro* drug release studies showed a significant increase in the dissolution rate of nanosuspensions as compared with pure drug. Bioavailability studies have shown nearly 3 fold increase in the AUC for the nanosuspensions as opposed to the pure drug.

- **Ramani V. *et.al;* prepared nanoparticles of HMG-CoA reductase inhibitor (Simvastatin)** [48]**.**

  Simvastatin is a poorly soluble lipid lowering agent. Its water solubility is very low, approximately 30 µg/mL and poorly absorbed from the gastrointestinal (GI) tract.

  The work was an attempt to overcome the poor solubility and dissolution rate of simvastatin by using Nanosuspension technology. PVP and Tween 80 with Soybean Lecithin were used at different ratios as the surfactants. The formulations were done by Emulsion-solvent evaporation method followed by freezedrying. The formulated nanoparticles were subjected to characterization studies like Particle size analysis, X-ray diffraction studies, Differential Scanning Colorimetry, Scanning electron microscopy and UV analysis. The dissolution test of tablets containing the nanometric drug flakes revealed that, within 30 minutes, 89.76% (w/w) of the simvastatin in the tablet was dissolved in comparison to 45.97% (w/w) conventional tablets.

- **Junise V. *et.al;* prepared chitosan nanoparticles loaded with isoniazid for the treatment of Tuberculosis[49].**

  The objective of the study was to load first line antitubercular drug, isoniazid in chitosan nanoparticles in order to enhance bioavailability and to reduce dose frequency. Chitosan was dissolved in acetic acid aqueous solution at various concentrations; drug was dispersed in chitosan solution kept over magnetic stirrer at room temperature for a period of 30 minute. The tripolyphosphate aqueous solution with various concentrations added drop wise to the above solution, followed by sonication for 5 min. The resulting chitosan nanoparticles suspension was centrifuged at 16,000 rpm for 30 min. After freeze drying the nanoparticles were collected. Though the study it was found that formulation No: 2 having optimum nanonised particles, positive zeta potential, good encapsulation efficiency and good release profile which followed first order release kinetics.

- **Bathool A. *et.al;* prepared Atorvastatin calcium loaded chitosan nanoparticles for sustain drug delivery[50].**

  The aim of the study was to formulate and characterize Atorvastatin calcium loaded chitosan nanoparticles prepared by solvent evaporation method for sustained release. Low oral bioavailability of Atorvastatin calcium (14%) due to an extensive high first-pass effect makes it as prime target for oral sustained drug delivery. Weighed amount of drug and polymer were dissolved in suitable organic solvent DMSO and 2% acetic acid as an organic phase. This solution was added drop wise to aqueous solution of Lutrol F68 and

homogenized at 25000rpm followed by magnetic stirring for 4hrs. Nanoparticles were evaluated for its particle size, scanning electron microscopy (SEM), Fourier-Transform infrared spectroscopy (FTIR), percentage yield, drug entrapment and for *in vitro* release kinetics. Among the four different ratios, 1:4 ratio showed high drug loading and encapsulation efficiency. SEM studies shows that prepared nanoparticles were spherical in shape with a smooth surface. Particle size of prepared nanoparticles was found to be in range between 142 nm to 221 nm. FTIR and DSC shows drug to polymer compatibility ruling out any interactions. *In vitro* release study showed that the drug release was sustained up to 7 days.

- **Fonseca C. *et.al;* prepared paclitaxel-loaded PLGA nanoparticles**[51]**.**

The main objective of the study was to develop a polymeric drug delivery system for paclitaxel, intended to be intravenously administered, capable of improving the therapeutic index of the drug and devoid of the adverse effects of Cremophor EL. To achieve this goal paclitaxel (Ptx)-loaded poly (lactic-co-glycolic acid) (PLGA) nanoparticles (Ptx- PLGA-Nps) were prepared by the interfacial deposition method. The influence of different experimental parameters on the incorporation efficiency of paclitaxel in the nanoparticles was evaluated. The results demonstrate that the incorporation efficiency of paclitaxel in nanoparticles was mostly affected by the method of preparation of the organic phase and also by the organic phase/aqueous phase ratio. The data indicate that the methodology of preparation allowed the formation of spherical nanometric (200 nm), homogeneous and negatively charged particles which were suitable for intravenous administration. The release behaviour of

paclitaxel from the developed nanoparticulate system exhibited a biphasic pattern characterised by an initial fast release during the first 24 h, followed by a slower and continuous release. The *in vitro* anti-tumoral activity of Ptx-PLGA- nanoparticulate system developed in the work was assessed using a human small cell lung cancer cell line (NCI-H69 SCLC) and compared to the *in vitro* anti-tumoral activity of the commercial formulation Taxol. The influence of Cremophor EL on cell viability was also investigated. Exposure of NCI-H69 cells to 25 mg/ml Taxol resulted in a steep decrease in cell viability. The results demonstrate that incorporation of Ptx in nanoparticles strongly enhances the cytotoxic effect of the drug as compared to Taxol.

- **Anilkumar J. *et.al;* prepared biodegradable polylactic-coglycolic acid (PLGA) nanoparticles of simvastatin**[52].

  The objective of the work was to formulate nanoparticles for simvastatin drug. Simvastatin is a lipid lowering agent, undergoes extensive first pass extraction in the liver, the availability of the drug to the general circulation is low (< 5%). Nanoparticles were prepared by precipitation-solvent deposition method using 3^2 full factorial design, Pluronic F-68 as polymeric stabilizer. From the preliminary trials, the constraints for independent variables X1 (amount of PLGA) and X2 (amount of Pleuronic F-68) have been fixed. The prepared formulations were further evaluated for % encapsulation efficiency, particle size, polydispersity index, *in vitro* drug release pattern and drug excipient interactions. Drug: polymer ratio and concentration of stabilizer were found to influence the particle size and entrapment efficiency of simvastatin loaded PLGA nanoparticles. *In vitro* drug release study of selected factorial

formulations (PS1, PS4, PS7) showed, 84.56%, 89.65% and 73.46 % release respectively in 24hrs. The formulation batch PS3 having lowest particle size 122 nm. The release was found to follow first order release kinetics with fickian diffusion mechanism for all batches. These results indicate that simvastatin loaded PLGA nanoparticles could be effective in sustaining drug release for a prolonged period.

- **Jong-Ho Kim *et.al;* prepared cisplatin-loaded glycol chitosan nanoparticles**[53].

  In this study to make a tumor targeting nano-sized drug delivery system, biocompatible and biodegradable glycol chitosan was modified with hydrophobic cholanic acid. The resulting hydrophobically modified glycol chitosans (HGCs) that formed nano-sized self-aggregates in an aqueous medium was investigated as an anticancer drug carrier in cancer treatment. Insoluble anticancer drug, cisplatin (CDDP), was easily encapsulated into the hydrophobic cores of HGC nanoparticles by a dialysis method, wherein the drug loading efficiency was about 80%. The CDDP encapsulated HGC (CDDP-HGC) nanoparticles were well-dispersed in aqueous media and they formed a nanoparticles structure with a mean diameter about 300–500 nm. As a nano-sized drug carrier, the CDDP-HGC nanoparticles released the drug in a sustained manner for a week and they were also less cytotoxic than was free CDDP, probably because of sustained release of CDDP from the HGC nanoparticles. The tumor targeting ability of CDDP-HGC nanoparticles was confirmed by in vivo live animal imaging with near-infrared fluorescence Cy5.5-labeled CDDP-HGC nanoparticles. It was observed that CDDP-HGC

nanoparticles were successfully accumulated by tumor tissues in tumor-bearing mice, because of the prolonged circulation and enhanced permeability and retention (EPR) effect of CDDP-HGC nanoparticles in tumor-bearing mice. As expected, the CDDP-HGC nanoparticles showed higher antitumor efficacy and lower toxicity compared to free CDDP, as shown by changes in tumor volumes, body weights, and survival rates, as well as by immunohistological TUNEL assay data. Collectively, the results indicate that HGC nanoparticles are a promising carrier for the anticancer drug CDDP.

- **Sarma M.; formulated and developed the solid lipid nanoparticles of atorvastatin Calcium**[54].

  Solid lipid nanoparticles (SLN) are a colloidal carrier system for controlled drug delivery. Atorvastatin calcium is a lipophilic antihyperlipidemic drug has very poor oral bioavailability (<15%) due to first pass effect and high intestinal clearance. SLN system of Atorvastatin calcium was investigated for improvement of release, pharmacokinetics and pharmacodynamic activity. The SLN were prepared by solvent injection technique and characterised for entrapment efficiency, zeta potential, and drug delivery characterisation.

  Through the study, it was found that the optimized Solid Lipid Nanoparticles was a suspension of nanosized homogeneous particles with significantly higher entrapment efficiency (>70%). The pharmacokinetic parameters of optimized SLNs in rat, obtained using Graph-pad software revealed 2.74 folds increase in bioavailability as compared to Atorvastatin calcium tablet (marketed formulation). This investigation demonstrated the SLN for improved oral delivery and it was deduced that the solid lipid & surfactant

were the principal formulation factor responsible for the improvement in characteristics, pharmacokinetics and pharmacodynamic activity of SLNs.

- **Fanara D. *et.al;* prepared and characterised the nanocrystal for solubility and dissolution improvement of nifedipine[55].**

  Poorly water-soluble drugs such as nifedipine offer challenging problems in drug formulation as poor solubility is generally associated to poor dissolution characteristics and thus to poor oral bioavailability.

  In order to enhance these characteristics, nifedipine nanoparticles were prepared using high pressure homogenization. The homogenization procedure was first been optimized in regard to particle size and size distribution. Nanoparticles were characterized in terms of size, morphology and redispersion characteristics following water-removal. Saturation solubility and dissolution characteristics were investigated and compared to the un-milled commercial nifedipine to verify the theoretical hypothesis on the benefit of increased surface area. Crystalline state evaluation before and following particle size reduction was also conducted through differential scanning calorimetry (DSC) and powder X-ray diffraction (PXRD) to denote eventual transformation to amorphous state during the homogenization process.

  Through this study, it has been shown that initial crystalline state is maintained following particle size reduction and that the dissolution characteristics of nifedipine nanoparticles were significantly increased in regards to the commercial product.

- **Dustgania A. *et.al;* prepared Chitosan Nanoparticles Loaded by Dexamethasone Sodium Phosphate[56].**

  The aim of the investigation was to describe the synthesis and characterization of novel biodegradable nanoparticles based on chitosan for encapsulation of dexamethasone sodium phosphate. To achieve this objective, ionic gelation method were used. Drug containing nanoparticles were prepared with different amounts of drug. The mean size and size distribution of nanoparticles were measured by dynamic laser light scattering. The mean particle size, varied in the range of 250-350 nm. Values of loading capacity and loading efficiency varied between 33.7%-72.2% and 44.5%-76.0% for prepared nanoparticles.

- **Debnath S. *et.al;* prepared and evaluate chitosan nanoparticles containing cytarabine[57].**

  The activity of Cytarabine was decreased by its rapid deamination to the biologically inactive metabolite uracil-arabinoside. This rapid deamination was the reason for the research for effective formulation of Cytarabine that cannot be deaminated and exhibit better pharmacokinetic parameters. Protection of Cytarabine from fast degradation and elimination was investigated by encapsulating the drug into chitosan nanoparticles. Cytarabine loaded nanoparticles prepared by ionotropic gelation were characterised by SEM and was found to be in the range of 200nm. The mechanism by which drug was being released was non-Fickian (anomalous) solute diffusion mechanism. The *in vivo* biodistribution study shown that the nanoparticles have better distribution of drug compared to free drug in different organs like kidney, lungs and spleen.

Chapter 3

Materials and Methods

3. MATERIALS AND METHOD

3.1. MATERIALS

3.1.1. Chemicals and Reagents

The drug Atorvastatin calcium was obtained as gift sample from Ozone Pharmaceutical, Amingaon, Guwahati. Acetone and Acetic acid was purchased from Merck specialities pvt. Ltd, Shivsagar estate, Mumbai. Chitosan was purchased from Balaji drugs, Mumbai and Pluronic F68 was purchased from Himedia Laboratories pvt. Ltd, Mumbai. All other chemicals were of reagent grade and used as received.

3.1.1.1. Drug Profile:

Model drug candidate: Atorvastatin calcium

Proprietary name: Lipitor

Chemical name: (3*R*, 5*R*)-7-[2-(4-fluorophenyl)-3-phenyl-4-(phenylcarbamoyl)-5-propan-2-ylpyrrol-1-yl]-3, 5-dihydroxyheptanoic acid, calcium salt (2:1) trihydrate.

Molecular formula: $(C_{33}H_{34}\ FN_2O_5)2Ca{\bullet}3H_2O$

Molecular weight: 1209.42

Chemical structure:

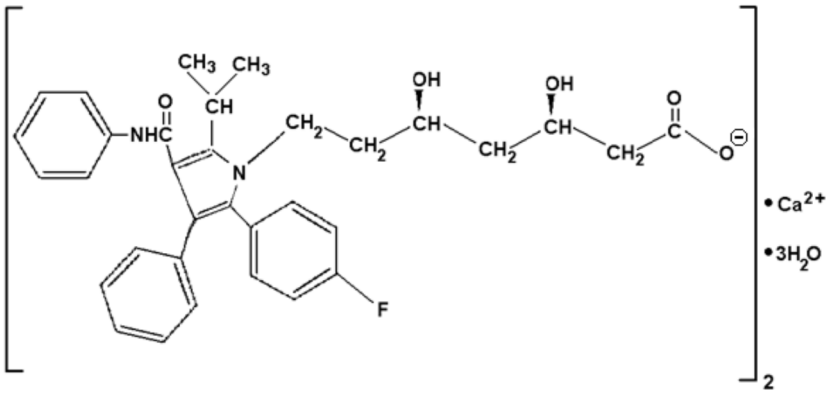

Fig 1: Chemical Structure of Atorvastatin calcium

Atorvastatin calcium is a white to off-white crystalline powder that is insoluble in aqueous solutions of pH 4 and below. Atorvastatin calcium is very slightly soluble in distilled water, pH 7.4 phosphate buffer, and acetonitrile, slightly soluble in ethanol, and freely soluble in methanol, acetone, and DMSO. MP 160 to 170^0C.

Pharmacodynamics

Atorvastatin as well as some of its metabolites are pharmacologically active in humans. The liver is the primary site of action and the principal site of cholesterol synthesis and LDL clearance. Drug dosage rather than systemic drug concentration correlates better with LDL-C reduction. Individualization of drug dosage should be based on therapeutic response.

Pharmacokinetics and Drug Metabolism [58]

Absorption

Atorvastatin is rapidly absorbed after oral administration; maximum plasma concentrations occur within 1 to 2 hours. Extent of absorption increases in proportion to Atorvastatin dose. The absolute bioavailability of Atorvastatin is approximately 14% and the systemic availability of HMG-CoA reductase inhibitory activity is approximately 30%. The low systemic availability is attributed to presystemic clearance in gastrointestinal mucosa and/or hepatic first-pass metabolism. Although food decreases the rate and extent of drug absorption by approximately 25% and 9%, respectively, as assessed by C_{max} and AUC, LDL-C reduction is similar whether Atorvastatin is given with or without food. Plasma Atorvastatin concentrations are lower (approximately 30% for C_{max} and AUC) following evening drug administration compared with morning. However, LDL-C reduction is the same regardless of the time of day of drug administration.

Distribution

Mean volume of distribution of Atorvastatin is approximately 381 litres. Atorvastatin is ≥98% bound to plasma proteins. A blood/plasma ratio of approximately 0.25 indicates poor drug penetration into red blood cells. Based on observations in rats, Atorvastatin is likely to be secreted in human milk.

Metabolism

Atorvastatin is extensively metabolized to ortho- and parahydroxylated derivatives and various beta-oxidation products. *In vitro* inhibition of HMG-CoA reductase by ortho- and parahydroxylated metabolites is equivalent to that of Atorvastatin.

Approximately 70% of circulating inhibitory activity for HMG-CoA reductase is attributed to active metabolites. *In vitro* studies suggest the importance of Atorvastatin metabolism by cytochrome P450 3A4, consistent with increased plasma concentrations of atorvastatin in humans following coadministration with erythromycin, a known inhibitor of this isozyme. In animals, the ortho-hydroxy metabolite undergoes further glucuronidation.

Excretion

Atorvastatin and its metabolites are eliminated primarily in bile following hepatic and/or extra-hepatic metabolism; however, the drug does not appear to undergo enterohepatic recirculation. Mean plasma elimination half-life of Atorvastatin in humans is approximately 14 hours, but the half-life of inhibitory activity for HMG-CoA reductase is 20 to 30 hours due to the contribution of active metabolites. Less than 2% of a dose of Atorvastatin is recovered in urine following oral administration.

Medical uses

The primary uses of Atorvastatin are for the treatment of Dyslipidemia and the prevention of cardiovascular disease. It is recommended to be used only after other measures such as diet, exercise, and weight reduction have not improved cholesterol levels.

Contraindications

- Active liver disease: cholestasis, hepatic encephalopathy, hepatitis, and jaundice
- Unexplained elevations in AST or ALT levels

- Pregnancy
- Breastfeeding

Precaution must be taken when treating with Atorvastatin, because rarely it may lead to rhabdomyolysis,[59] it may be very serious leading to acute renal failure due tomyoglobinuria. If rhabdomyolysis is suspected or diagnosed, Atorvastatin therapy should be discontinued immediately. However, trials show that Atorvastatin may be protective of kidney function. Also Atorvastatin should be discontinued if a patient has markedly elevated CPK levels or if a sympathy is suspected or diagnosed. The likelihood of developing a myopathy is increased by the co-administration of cyclosporine, fibric acid derivatives, erythromycin, niacin, and azole antifungals[60].

Atorvastatin is absolutely contraindicated in pregnancy, it is likely to cause harm to fetal development because of the importance of cholesterol and various products in the cholesterol biosynthesis pathway for fetal development, including steroid synthesis and cell membrane production. It is not recommended that nursing mothers take Atorvastatin due to the possibility of adverse reactions in nursing infants, since experiments with rats indicate that Atorvastatin is likely to be secreted into human breast milk.

Adverse effects

As stated earlier, myopathy with elevation of creatinine kinase(CK)[61] and rhabdomyolysis are the most serious, although rare <1%. Headache is the most common side effect, occurring in more than 10% of patients. Side effects that occur in 1–10% of patients taking Atorvastatin include:

- Weakness

- Insomnia and dizziness
- Chest pain and peripheral edema
- Rash
- Abdominal pain, constipation, diarrhoea, dyspepsia, flatulence, nausea
- Urinary tract infection
- Arthralgia, myalgia, back pain, arthritis
- Sinusitis, pharyngitis, bronchitis, rhinitis
- Infection, flu-like syndrome, allergic reaction

Atorvastatin and other statins are associated with anecdotal reports of memory loss by consumers, which have been seen in clinical practice in a tiny percentage of users, particularly women. Evidence is conflicting with anecdotal reports contrasting with a well-established association of high cholesterol with dementia. However, it is known that cholesterol synthesis is necessary for normal neuron functioning. According to Pfizer, the manufacturer of Lipitor, clinical trials "do not establish a causal link between Lipitor and memory loss[62].

Elevation of alanine transaminase (ALT) and aspartate transaminase (AST) has been described in a few cases.

Drug and food interactions

Interactions with clofibrate, fenofibrate, gemfibrozil, which are fibrates used in accessory therapy in many forms of hypercholesterolemia, usually in combination with statins, increase the risk of myopathy and rhabdomyolysis.

Co-administration of Atorvastatin with one of CYP3A4 inhibitors like itraconazole, telithromycin and voriconazole, may increase serum concentrations of Atorvastatin, which may lead to adverse reactions. This is less likely to happen with other CYP3A4 inhibitors like diltiazem, erythromycin, fluconazole, ketoconazole, clarithromycin, cyclosporine, protease inhibitors or verapamil and only rarely with other CYP3A4 inhibitors like amiodarone and aprepitant[59]. Often bosentan, fosphenytoin, and phenytoin, which are CYP3A4 inducers, can decrease the plasma concentrations of Atorvastatin. But only rarely barbiturates, carbamazepine, efavirenz, nevirapine, oxacarbazepine, rifampin and rifamycin, which are CYP3A4 inducers, can decrease the plasma concentrations of atorvastatin. Oral contraceptives increased AUC values for norethindrone and ethinyl estradiol, these increases should be considered when selecting an oral contraceptive for a woman taking atorvastatin.

Antacids can rarely decrease the plasma concentrations of atorvastatin but do not affect the LDL-C-lowering efficacy.

Niacin also is proved to increase the risk of myopathy or rhabdomyolysis[59].

Statins may also alter the concentrations of other drugs, such as warfarin or digoxin, leading to alterations in effect or a requirement for clinical monitoring[59].

Vitamin D supplementation lowers atorvastatin and active metabolite concentrations yet has synergistic effects on cholesterol concentrations. Grapefruit juice components are known inhibitors of intestinal CYP3A4. Co-administration of grapefruit juice with atorvastatin may cause an increase in C_{max} and AUC, which can lead to adverse reactions or overdose toxicity[63].

3.1.1.2. Excipients and Reagents Profile:

3.1.1.2.1. Chitosan: [64]

Nonproprietary Names: BP: Chitosan hydrochloride

PhEur: Chitosani hydrochloridum.

Synonyms: 2-Amino-2-deoxy-(1,4)-b-D-glucopyranan; deacetylated chitin; deacetylchitin; b-1,4-poly-D-glucosamine; poly-D-glucosamine; poly-(1,4-b-D-glucopyranosamine.

Chemical Name: Poly-b-(1,4)-2-Amino-2-deoxy-D-glucose

Chemistry: Chitosan occurs as odorless, white or creamy-white powder or flakes. Fiber formation is quite common during precipitation and the chitosan may look 'cottonlike'.

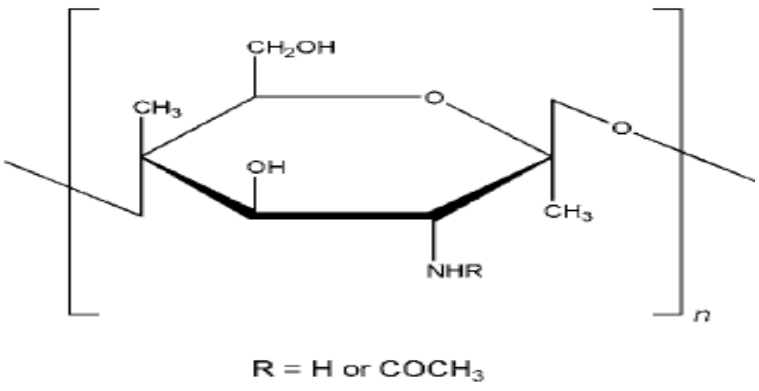

Fig 2: Structural Formula of Chitosan

Typical Properties: Chitosan is a cationic polyamine with a high charge density at pH <6.5; and so adheres to negatively charged surfaces and chelates metal ions. It is a linear polyelectrolyte with reactive hydroxyl and amino groups (available for chemical reaction and salt formation). The properties of chitosan relate to its polyelectrolyte and polymeric carbohydrate character.

Acidity/alkalinity: pH = 4.0–6.0 (1% w/v aqueous solution

Density: The density of chitosan is 1.35–1.40 g/cm3.

Glass transition temperature: The glass transition temperature of chitosan is 203^0 C.

Moisture content: Chitosan adsorbs moisture from the atmosphere, the amount of water adsorbed depending upon the initial moisture content and the temperature and relative humidity of the surrounding air.

Particle size distribution: The particle size is <30 mm.

Solubility: It is sparingly soluble in water; practically insoluble in ethanol (95%), other organic solvents, and neutral or alkali solutions at pH above approximately 6.5. Chitosan dissolves readily in dilute and concentrated solutions of most organic acids and to some extent in mineral inorganic acids.

Viscosity (dynamic): It has a wide range of viscosity types is commercially available. Owing to its high molecular weight and linear, unbranched structure, chitosan is an excellent viscosity-enhancing agent in an acidic environment. It acts as a pseudo-plastic material, exhibiting a decrease in viscosity with increasing rates of shear. The viscosity of chitosan solutions increases with increasing chitosan concentration, decreasing temperature, and increasing degree of deacetylation.

Safety: Chitosan is being investigated widely for use as an excipient in oral and other pharmaceutical formulations. It is also used in cosmetics. Chitosan is generally regarded as a nontoxic and nonirritant material.

Functional Category: Chitosan is used as coating agent; disintegrant; film-forming agent; mucoadhesive; tablet binder; viscosity-increasing agent.

Applications in Pharmaceutical Formulation or Technology: Chitosan is used in cosmetics and is under investigation for use in a number of pharmaceutical formulations. The suitability and performance of chitosan as a component of

pharmaceutical formulations for drug delivery applications has been investigated in numerous studies. These include controlled drug delivery applications, use as a component of mucoadhesive dosage forms, rapid release dosage forms, improved peptide delivery, colonic drug delivery systems,and use for gene delivery.

Incompatibilities: Chitosan is incompatible with strong oxidizing agents.

Stability and Storage Conditions: Chitosan powder is a stable material at room temperature, although it is hygroscopic after drying. Chitosan should be stored in a tightly closed container in a cool, dry place.

3.1.1.2.2. Acetone: [65]

Acetone is the organic compound with the formula $OC(CH_3)_2$. This colorless, mobile, flammable liquid is the simplest example of the ketones. Owing to the fact that acetone is miscible with water, and virtually all organic solvents, it serves as an important solvent in its own right, typically the solvent of choice for cleaning purposes in the laboratory. More than 3 billion kilograms are produced annually; mainly as a precursor to polymers.Familiar household uses of acetone are as the active ingredient in nail polish remover and as paint thinner and sanitary cleaner/ nail polish remover base. It is a common building block in organic chemistry. In addition to being manufactured, acetone also occurs naturally, even being biosynthesized in small amounts in the human body.

Chemical Formula	CH_3COCH_3
Other/Generic Names	Dimethylketone;2-propanone;
Appearance	Clear water white liquid
Physical State	Liquid

Molecular Weight	58.08
Odour	Sweetish
Density at 20°C, 68°F	6.63 lb/US gal
Dielectric Constant 25°C	21.45
Specific Gravity (25°C/25°F)	Not over 0.7880
Vapor Density (Air = 1.0)	2
Vapor Pressure at 20°C, 68°F	181.7 mmHg (3.51 psi)
Viscosity at 15°C, 59°F	0.3371 cP
Water Solubility (miscibility)	Soluble in all proportions in water

3.1.1.2.3. Acetic acid: [66]

Acetic acid is the simplest carboxylic acid next to formic acid in which a single hydrogen atom is attached to the carboxyl group. If a methyl group is attached to the carboxyl group, the compound is acetic acid. Acetic acid is a clear, corrosive, flammable liquid; melting point 16.6 C, boiling point 118 C. Pure acetic acid freezes in ice-like crystal form. So pure acetic acid is called glacial acetic acid, which contains 99.5 -100.5 % w/w. It is the two-carbon carboxylic acid, and a systematic name is ethanoic acid. It is completely miscible with water, ethyl alcohol and ether, but is insoluble in carbon disulfide.

Formula	CH_3COOH
Mol wt.	60.05
Synonyms	Ethylic acid; Methanecarboxylic acid; vinegar; Vinegar acid; Acetic acid, glacial; Ethanoic acid

Physical state	clear liquid
Melting point	16.6^0 C
Boiling point	117 - 118^0C
Specific gravity	1.05
Solubility	Soluble in water

3.1.1.2.4. Pluronic F68: [67]

Synonyms: Lutrol ; Mondan ; Pluronic ; Poloxalkol ; Supronic ; Synperonic

Nonproprietary names:

BP : Poloxamers 188

PhEur : Poloxamera 188

USPNF : Poloxamer 188

Empirical Formula and Molecular weight: The poloxamers polyols are a series of closely related block copolymers of ethylene oxide and propylene oxide conforming to the general formula $HO(C_2H_4O)_n(C_3H_60)_m(C_2H_4O)_nH$ and molecular weight is 510.

Structural Formula:

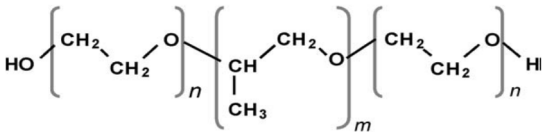

Fig 3: Structure of Pluronic F68

Functional category: Dispersing agents; emulsifying and co-emulsifying agents; solubilising agents; tablet lubricant; wetting agents.

Applications in Pharmaceutical Formulations: Poloxamers are non ionic polyoxyethylene-polypropylene copolymers used primarily in pharmaceutical formulations as emulsifying or solubilising agents. The polyoxyethylene segment is hydrophobic while the polypropylene segment is hydrophobic. All of the polomersare chemically similar in composition, differing only in the relative amounts of propylene and ethylene oxides added during manufacture. Their physical and surface active properties vary over a wide range and a number of different types are commercially available. Poloxamers are used as emulsifying agents in intravenous fat emulsions and as solubilising and stabilising agents to maintain the clarity of elixirs and syrups. Poloxamers may also be used as wetting agents, in ointments, suppository bases and gels; and as tablet binders and coatings. More recently, poloxamers have found use in drug delivery systems.

Descriptions: Poloxamers generally occur as white, waxy, free flowing prilled granules or as cast solids. They are practically colourless and tasteless[68].

3.1.1.2.5. Distilled water: [69]

Empirical formula is H_2O and Molecular weight is 18.02.

Typical properties:

Boiling point	: 100^0c
Critical pressure	: 22.1MPa (218.3 atm)

Critical temperature	: 374.28^{0}C
Dielectric constant	: D25 = 78.54
Dipole moment	: 1.76 in benzene at 258^{0}C
Melting point	: 08^{0}C
Refractive index	: 1.3330
Solubility	: Miscible with most polar solvents
Specific gravity	: 0.9971 at 258^{0}C
Vapour pressure	: 3.17 kPa at 258^{0}C
Viscosity(dynamic)	: 0.89mPas at 258^{0}C

3.1.2. Instruments:

SL.No.	Instruments	Company Name and Address
1.	Digital Weighing Balance	Denver instrument, U.S.A
2.	UV Spectrophotometer	Shimadzu (Model no.UV 1800), Japan
3.	FTIR	Bruker Alpha (Model no. 10059736), Germany
4.	Brookfield Viscometer	DV-E Viscometer, U.S.A
5.	Lyophiliser	Instind freeze dryer, India
6.	Homogeniser	IKA T25 Digital Ultra Turrax, Germany
7.	Centrifuge	REMI-8C centrifuge, India
8.	Melting Point Apparatus	Digital Melting point apparatus, India
9.	DSC	Parkin Almer, U.S.A
10.	Zetasizer Nano S 90	Malvern, U.SA.
11.	Zetasizer Nano ZS 90	Malvern, U.SA.
12.	HPLC	Waters 2489, Ireland
13.	SEM	Carl Zeiss, Germany
14.	Programmable Environment Chamber	REMI, 372 LAG
15.	Digital pH Meter	335, Systronics

3.2. Methods:

3.2.1. Preformulation studies:

3.2.1.1. Organoleptic Properties:

The Organoleptic properties of the drug sample were evaluated visually.

3.2.1.2. Characterisation of drug:

3.2.1.2.1. Melting point determination:

The melting point of the pure drug was determined by using the melting point apparatus (MAC, Digital Melting Point apparatus, Macro Scientific Works) and compared with the reported value from literature.

3.2.1.2.2. Fourier Transform Infrared Spectroscopy (FTIR):

IR spectroscopy is one of the important analytical techniques for chemical identification. The spectra of Atorvastatin calcium was recorded in the range of 4000cm^{-1}-400cm^{-1}(resolution 2cm^{-1}) using FTIR Bruker Alpha. The recorded spectrum was compared with recorded one in the literature. The FTIR spectrums of pure Atorvastatin calcium and reference Atorvastatin calcium were shown in fig. 4 to 5.

3.2.1.3. Analysis of Atorvastatin calcium:

3.2.1.3.1. Preparation of standard curve of Atorvastatin calcium in acetone: water (1:9):

A stock solution of Atorvastatin calcium (100µg/ml) was prepared by dissolving 10 mg of drug in 10ml acetone in 100ml volumetric flask and volume was made upto the

mark with distilled water. From the stock solution eight serial dilute solutions were prepared. The λmax for quantitative analysis of Atorvastatin calcium was determined after scanning the appropriate dilute solution between 200-400nm using Shimadzu, UV-1800, UV spectrophotometer and it was found to be 264nm (Fig 6). The absorbance of the dilute solutions was measured at 264nm against the blank. The absorbance was plotted against the concentration and linear relationship was obtained. The concentration of Atorvastatin calcium in the sample was calculated from regression equations. The data are presented in Table-5 and standard curve is presented in Fig 7.

3.2.1.3.2. Preparation of standard curve of Atorvastatin calcium in acetone: phosphate buffer pH 6.8 (1:9):

A stock solution of Atorvastatin calcium (100µg/ml) was prepared by dissolving 10 mg of drug in 10ml acetone in 100ml volumetric flask and volume was made upto the mark with phosphate buffer pH 6.8. From the stock solution eight serial dilute solutions were prepared. The λmax for quantitative analysis of Atorvastatin calcium was determined after scanning the appropriate dilute solution between 200-400nm using Shimadzu, UV-1800, UV spectrophotometer and it was found to be 264nm (Fig 8) . The absorbance of the dilute solutions was measured at 264nm against the blank. The absorbance was plotted against the concentration and linear relationship was obtained. The concentration of Atorvastatin calcium in the sample was calculated from regression equations. The data are presented in Table-6 and standard curve is presented in Fig 9.

3.2.1.3.3. Preparation of standard curve of Atorvastatin calcium in acetone: 0.1N HCl (1:9):

A stock solution of Atorvastatin calcium (100µg/ml) was prepared by dissolving 10 mg of drug in 10ml acetone in 100ml volumetric flask and volume was made upto the mark with 0.1N HCl. From the stock solution eight serial dilute solutions were prepared. The λmax for quantitative analysis of Atorvastatin calcium was determined after scanning the appropriate dilute solution between 200-400nm using Shimadzu, UV-1800, UV spectrophotometer and it was found to be 264nm (Fig 10). The absorbance of the dilute solutions was measured at 264nm against the blank. The absorbance was plotted against the concentration and linear relationship was obtained. The concentration of Atorvastatin calcium in the sample was calculated from regression equations. The data are presented in Table-7 and standard curve is presented in Fig 11.

3.2.1.4. Solubility study of drug: [70]

50mg Atorvastatin calcium of was weighed and solubility of this sample was checked in distilled water, methanol, phosphate buffer pH 6.8, 0.1N HCl, acetone and DMSO. The solubility data of Atorvastatin calcium is presented in Table-8.

3.2.1.5. Saturation Solubility study of drug: [71]

Weighed amount of Atorvastatin calcium (pure drug) equivalent to 10 mg of the drug was introduced into each one of 25 ml stoppered conical flasks containing 10 ml distilled water, phosphate buffer pH 6.8 and 0.1N HCl. The sealed flasks were agitated on a rotary shaker for 24 hrs at 37° C and equilibrated for 2 days. An aliquot was passed through 0.45 µm membrane filter and the filtrate was suitably diluted and

analyzed for drug content on a UV Spectrophotometer. The saturation solubility data of Atorvastatin calcium is presented in Table-9.

3.2.1.6. Drug excipient compatibility study:

3.2.1.6.1. FTIR study:

This was carried out to find out the compatibility between the drug Atorvastatin calcium and the polymer Chitosan and Pluronic F68. Samples were prepared for drug Atorvastatin calcium, polymer Chitosan, Pluronic F68 and physical mixture (1:1) of drug and polymer. The sample were kept onto the sample holder and scanned from 4000cm^{-1} to 400cm^{-1} (resolution 2cm^{-1}) in Bruker Alpha FTIR spectrophotometer. The spectra obtained were compared and interpreted for the functional group peaks. The FTIR spectrums are shown in Fig 12 to 16 and interpretation is presented in Table-10.

3.2.1.6.2. Differential scanning calorimetry (DSC) study: [72]

Differential scanning calorimetry (DSC) of the bulk drug Atorvastatin calcium was performed using DSC instrument (Parkin Almer, U.S.A) for measurement of the heat loss or gain resulting from physical or chemical changes within a sample as a function of temperature. About 6-7 mg of the individual components or drug-excipients combinations were weighed in aluminium DSC pans and hermetically sealed capsules were prepared with aluminium lids. An initial ramp was used to jump the temperature to 40ºC and then a constant heating rate of 10 ºC/min was used up to 300 ºC under nitrogen atmosphere. The DSC thermogram of drug and physical mixture of drug-polymer are shown in Fig 17 to 19.

3.2.1.7. Viscosity determination:

Viscosity of a solution of 0.5%w/v chitosan in 50 ml glacial acetic acid was measured by Brookfield viscometer (DV-E Viscometer) using spindle No. 25 at 1, 5, 10, 50 rpm at ambient temperature. The viscosity data are shown in Table-11 and Fig 20.

3.2.1.8. Formulation of the Atorvastatin calcium nanoparticle: [73]

Nanoparticles of Atorvastatin calcium were prepared by solvent evaporation technique using chitosan as a coating material and Atorvastatin calcium as a core material as per the composition given in Table-1. Drug and polymer in different ratios were weighed and were dissolved in a suitable organic solvent, acetone and 4% acetic acid forming an organic phase. This organic solution was then added dropwise to aqueous solution of Pluronic F68 and homogenised at 24000 rpm using IKA T25 digital Ultra Turrax, Germany, followed by magnetic stirring for 4hrs. The formed nanoparticles were then recovered by centrifugation (REMI cooling centrifuge, Vasai) for 20 min followed by washing with petroleum ether and lyophilized.

Table 1: Composition of Atorvastatin calcium nanoparticles

Formulations	Atorvastatin calcium in mg	Chitosan in mg	Pluronic F68 in mg	Acetone in ml	4% Acetic acid in ml	Distilled water in ml
F1	10	10	10	10	20	50
F2	10	20	10	10	40	50
F3	10	30	10	10	60	50
F4	10	40	10	10	80	50
F5	10	50	10	10	100	50

F1: Formulation code for no.1 formulation, F2: Formulation code for no.2 formulation, F3: Formulation code for no.3 formulation, F4: Formulation code for no.4 formulation, F5: Formulation code for no.5 formulation.

3.2.1.9. Evaluation of the Prepared Atorvastatin calcium nanoparticles:

The obtained Atorvastatin calcium nanoparticle formulations F1, F2, F3, F4 and F5 were evaluated for percentage yield, drug loading, percentage entrapment efficiency, particle size, polydispersity index, in vitro release rate studies.

3.2.1.9.1. Percentage Yield: [74]

The lyophilised nanoparticles from each formulation were weighed and the respective percentage yield was calculated using the following formula-

$$\text{Percentage Yield} = \frac{\text{Weight of nanoparticles obtained}}{\text{Weight of drug, polymer and pluronic F68 used}} \times 100$$

The percentage yield of the nanoparticles of each formulation is presented in Table-12 and Fig 21.

3.2.1.9.2. Drug Loading: [75]

Accurately weighed equivalent 10 mg of each Atorvastatin calcium loaded nanoparticle formulations were extracted with 20ml Acetone, stirred at 500rpm at room temperature and dispersion was centrifused and filtered by 0.2 µm membrane filters. The filtered solution was taken in a 100ml volumetric flask and the volume was made upto the mark with the help of distilled water. The diluted solution was

further diluted and analysed for the content of Atorvastatin calcium by spectrophotometric determination at 264nm taking distilled water as blank. The drug concentration was calculated from the standard curve of Atorvastatin calcium in distilled water and after that the drug loading was calculated using following equation. The obtained drug loading data are presented in Table-13 and Fig 22.

$$\% \text{ Drug Loading} = \frac{\text{Weight of dug in nanoparticles}}{\text{Weight of nanoparticles taken}} \times 100$$

3.2.1.9.3. Entrapment Efficiency: [75]

The entrapment efficiency was calculated using the following equation-

$$\% \text{ Entrapment Efficiency} = \frac{\text{Weight of drug in nanoparticles}}{\text{Weight of drug used in the formulation}} \times 100$$

The entrapment efficiency of nanoparticle formulations is presented in Table-14 and Fig 23.

3.2.1.9.4. Particle size and Polydispersity index: [76]

In order to analyze particle size, each formulations of drug loaded lyophilised nanoparticles were dispersed in deionised water, centrifused for 5 minutes at 5000

rpm and filtered using 0.2 µm membrane filter. Particle size was determined by using Malvern Zetasizer Nano S90 at a temperature of 25^0C at a measuring angle of 90^0 to the incident beam. The obtained data of particle size analysis are given in Table-15 and Fig 24 to 28.

The Polydispersity index was determined by using Malvern Zetasizer Nano S90 and obtained data of Polydispersity index is given in Table-15 and Fig 24 to 28.

3.2.1.9.5. Zeta potential study: [76]

The zeta potential of Atorvastatin calcium nanoparticles were measured by a laser doppler anemometer coupled with Zetasizer Nano ZS 90 (Malvern Instruments Ltd. UK). A potential of ± 150 mV was set in the instrument. Disposable cuvette of 0.75 ml capacity was used for measurement. The Zeta potential data of Atorvastatin calcium nanoparticles is shown in Table-16 and Fig 29.

3.2.1.9.6. *In vitro* drug release studies: [74]

The *in vitro* drug release studies of Atorvastatin calcium nanoparticles were carried out at $37^0 \pm 2^0$C in 0.1N HCl as well as Phosphate buffer pH 6.8(dissolution medium) for a period of 48 hours using dialysis bag technique. Nanoparticles equivalent to 10mg from each formulation was placed in each one of cellulose dialysis bag (cut-off 5kDa, Himedia, India), and to this a little amount of dissolution medium was added, which was sealed at both ends. The dialysis bag was dipped into the receptor compartment containing 100ml of dissolution medium, which was stirred continuously at about 100 rpm maintained at 37^0C. The receptor compartment was closed to prevent evaporation of dissolution medium. Samples were withdrawn at regular time intervals and the same volume was replaced with fresh dissolution

medium. The samples were measured by UV spectrophotometer at a wavelength 264nm against the blank. The drug release data of different formulations in 0.1N HCl as well as Phosphate buffer pH 6.8 are given in Table-17 to18 and Fig 30 to 31 respectively.

3.2.1.9.7. Selection of Optimised formulation:

The optimised formulation was selected from the nanoparticle formulations considering the % yield, % drug loading, % entrapment efficiency, particle size/ polydispersity index, zeta potential study as well as the *in vitro* drug release study.

The optimised formulation was further evaluated for the release kinetic study, stability study, surface morphology study, DSC study, FTIR study and *in vivo* pharmacokinetic study.

3.2.1.9.8. Release Kinetics: [77]

The *in vitro* release data obtained from optimised formulation (F5) in both the dissolution medium (0.1N HCl as well as Phosphate buffer pH 6.8) was fitted to various kinetic models. Data obtained from drug release studies was analysed according to the equations given in the Table-2. The release rate kinetics is presented in Fig 32 to 39.

Table 2: Different models of release mechanism

Model	Equation
Zero-order	$Q_t = Q_o - K_o t$
First-order	$\ln Q_t = \ln Q_o - K_1 t$
Higuchi matrix	$Q_t = K_H t^{1/2}$
Korsmeyer-Peppas	$\text{Log}(Q_t/Q_o) = \text{Log}K + n\text{Log}t$

Where,

Q_t: Cumulative amount of drug released at any specific time (t).

Q_o: Amount of drug remaining in the formulation

K_o: Rate constant of Zero-order

K_1: Rate constant of First-order

K_H: Rate constant of Higuchi-matrix model

K: Release rate constant which considers structural and geometric characteristics of the nanoparticles.

n: The diffusion exponent; indicative of the mechanism of drug release.

The 'n' value could be used to characterise different release mechanisms as mentioned in Table-3.

Table 3: Different release mechanism of 'n' value

'n'	Mechanism
0.5	**Fickian diffusion(Higuchi matrix)**
0.5<n<1	**Anomalous transport (non-fickian diffusion)** drug release is both diffusion-controlled and swelling-controlled.
1	**Case-II transport(Zero-order)**
n>1	**Super case-II transport**

3.2.1.9.9. Stability Studies: [78]

Accurately weighed equivalent 10 mg of Atorvastatin calcium loaded optimised nanoparticle formulation (F5) was dispersed in 100ml distilled water and it was stored at elevated temperature and relative humidity(25 ± 2^0C/ 60% ± 5% RH, 40 ± 2^0C/ 75% ± 5% RH) in a stability analysis chamber over a period of 3 months. Freshly prepared nanoparticle of 10mg was dispersed in 100ml distilled water and it was stored at 5 ± 3^0C used as control. Samples were kept for 90 days for stability analysis and within 90 days, drug loading of nanoparticle formulation F5 was checked and compared with those of the control formulation. The results of stability study are tabulated in Table-19.

3.2.1.9.10. Surface Morphology: [79]

The shape and surface characteristics of optimised nanoparticles formulation (F5) was visualized using SEM, Zeiss, Germany. The nanoparticles were first dried under vacuum. Nanoparticles were then glued to aluminium sample holders and gold coated

under argon atmosphere. The coated nanoparticles were finally characterised for surface morphology under suitable magnification. The SEM results are shown in Fig 40 to 41.

3.2.1.9.11. DSC analysis: [72]

The DSC analysis of optimised nanoparticle formulation (F5) was done using the DSC instrument (Parkin Almer, U.S.A) for measurement of the heat loss or gain resulting from physical or chemical changes within a sample as a function of temperature. About 6-7 mg of nanoparticles of optimised formulation was weighed in aluminium DSC pans and hermetically sealed capsules were prepared with aluminium lids. An initial ramp was used to jump the temperature to 40ºC and then a constant heating rate of 10 ºC/min was used up to 300 ºC under nitrogen atmosphere. The obtained DSC thermogram of nanoparticles was interpreted with the DSC thermogram of drug, polymer and physical mixture of drug and polymer. The DSC thermogram is shown in Fig 42.

3.2.1.9.12. FTIR Analysis:

This was carried out to find out the drug polymer interaction in the optimised nanoparticle formulation (F5). Samples of nanoparticles of optimised formulation was kept onto the sample holder and scanned from 4000cm^{-1} to 400cm^{-1} (resolution 2cm^{-1}) in Bruker Alpha FTIR spectrophotometer. The spectra obtained was compared with those of the drug, chitosan and pluronic F68 and interpreted for the functional group peaks. The FTIR spectrum of nanoparticles is shown in Fig 43.

3.2.1.9.13. *In-vivo* Pharmacokinetic studies: [80, 81, 82]

The ultimate test of success of a formulation depends on its *in vivo* performance and for the assertion of the same, *in vivo* studies was conducted in a suitable animal model. Approval to carry out *in vivo* study was obtained from Girijananda Chowdhury Institute of Pharmaceutical Science, Institutional Animal Ethics Committee and their guidelines were followed for the studies (1372/c/10/CPCSEA). The animals used for *in vivo* experiments were male rabbits weighing about 600gm-1000gm obtained from Animal House of Girijananda Chowdhury Institute of Pharmaceutical Science, Guwahati, Assam. The animals were kept under standard laboratory conditions at a temperature of 25 ± 2°C and relative humidity (55 ± 5%). The animals (4) were divided into two groups of 3 animals in each group. The animals were housed in animal cages, two per cage, with free access to standard laboratory feed and water. One marketed tablet with label claim of 10 mg (Atorva®) was taken, crushed in mortar, and mixed with 100 ml of double distilled water (0.1 mg/ml). Each rabbit of Group- I was given marketed formulation dose (2.4mg/kg) according to their weight using oral feeding needle. Same dose of nanoparticle suspension was prepared in double distilled water and administered to Group – II of rabbit. The blood sampling was carried out for around 24 hours (0.5 hr, 1hr, 2hr, 4hr, 8hr and 24hr) and 1ml blood sample was withdrawn from the marginal ear vein of the rabbit at regular time interval in centrifuge tubes. Tubes were stored at room temperature, 25 ± 2°C and relative humidity (55 ± 5%) for 30 minutes. The clotted blood was then centrifuged at 5000 rpm for 30 min. The serum was separated and stored at -21 °C until drug analysis was carried out using HPLC method. The collected serum was extracted with acetonitrile: ammonium-acetate (45:55, 5ml) by precipitating protein for analysis and

centrifuged at 5000 rpm for 30 min. After that serum samples were estimated by using HPLC method.

The HPLC conditions:

Instrument: HPLC (Waters 2489)

Reagents: Ammonium-acetate, Acetonitrile (HPLC grade), Glacial Acetic acid

Standard: Atorvastatin calcium standard

Column: 3.9 x 150 mm, Nova-pack® C184 µm (Ireland)

Detection: 264 nm wave length

Flow rate: 1.5ml/ min

Injection volume: 20µl

Column temperature: 25^0c

Run time: 6 min

Internal standard: Amlodipine Bisylate

Mobile phase preparation:

Ammonium acetate 0.05 M solution was prepared by dissolving accurately about 1.93 gms of CH_3COONH_4 in a 50 ml of glass double distilled water and then adding 0.25 ml of glacial acetic acid and diluting to 500 ml with glass double distilled water. Mobile phase was prepared by mixing 275ml of 0.05 M ammonium acetate solution with 225 ml of acetonitrile and its pH was found to be 6.09. The mobile phase consisting of acetonitrile and 0.05 M ammonium acetate solution in the ratio of 45:55 (v/v) with an apparent pH 6.09 was selected as the optimum composition of mobile phase, because it was found that this solvent system resolved both the components ideally. This mobile phase was ultrasonicated for 20min, and then it was filtered through 0.45µm membrane filter paper.

Standard stock solution preparation:

100µg/ml solution of both Atorvastatin calcium standard and Amlodipine bisylate standard were prepared by dissolving 10mg of each one into each 100ml volumetric flask. The volume was made upto the mark with the mobile phase after dissolving the drug.

Calibration curve preparation:

4ml of blank serum was taken in each one of 5 no.s of 10ml volumetric flask and into each one of them 4ml of Amlodipine bisylate standard solution (internal standard) was added. 5 various concentrations (10, 20, 30, 40 and 50 µg/ml) of Atorvastatin calcium was prepared by dissolving 1ml, 2ml, 3ml, 4ml and 5ml of standard Atorvastatin calcium solution into the above respective volumetric flask. The rest of the volume was made up with mobile phase. The samples were injected into HPLC column after the base line correction with the mobile phase at 264nm. After that the calibration curve was plotted against peak area versus concentration. The HPLC spectrum and calibration curve are presented in Fig 44 to 46.

Method validation:

The developed analytical method was subjected to validation with respect to various parameters such as linearity, limit of quantification (LOQ), limit of detection (LOD), accuracy and precision as per the ICH guidelines. [83]

Linearity:

Linearity was established by least square regression analysis of the calibration curve. The linearity was determined over the concentration range of 10-50 µg/ml for both Atorvastatin calcium and Amlodipine bisylate in triplicate. Peak areas of Atorvastatin calcium and Amlodipine bisylate were plotted versus their respective concentrations and linear regression analysis was performed on the resultant curves. Correlation

coefficients (n = 3) were compared among the three determination. The constructed calibration curves are shown in Fig. 47 to 48.

LOQ and LOD:

The LOQ was determined as the lowest amount of analyte that was reproducibly quantified above the baseline noise following triplicate injections. LOD was determined on the basis of signal to noise ratios and was determined using analytical response of three times of Amlodipine bisylate, the background noise. Both LOQ and LOD were calculated on the peak area using the following equations:

$$\mathbf{LOQ = 10 \times N/B, \quad LOD = 3 \times N/B}$$

Where, N is the standard deviation of the peak areas (triplicate injections) of the drug, B is the slope of the corresponding calibration curve.

Accuracy:

Accuracy of the method was determined by interpolation of peak areas of three replicate samples (n = 3) of stock solutions containing 20 µg/ml of Atorvastatin calcium and 10 µg/ml of Amlodipine bisylate, from the calibration curve that had been previously prepared. The accuracy data for the assay of each component of interest are summarized in Table-23.

Precision:

Intraday precision was estimated by assaying the stock solution containing 20 µg/ml of Atorvastatin calcium and 10 µg/ml of Amlodipine bisylate, three times (results averaged for statistical evaluation) in the same analytical run. The statistical validation data for intraday precision are summarized in Table-24.

Interday precision was evaluated by analyzing the stock solution containing 20 µg/ml of Atorvastatin calcium and 10 µg/ml of Amlodipine bisylate, three levels analyzed

on three consecutive days (results averaged for statistical evaluation) in the same analytical runs. The statistical validation data for interday precision are summarized in Table-25.

Evaluation of drug in the blood serum:

Depending on the method validation data the optimised condition was selected for the determination of drug in the blood sample.

1ml of serum from each centrifuge tube were taken out with the help of micropipette and transferred to each one of 10ml volumetric flask. 4ml of Amlodipine bisylate standard solution (internal standard) was added to each one of volumetric flask and rest of the volume was made up with the help of mobile phase. The samples were injected into the HPLC column according to their time interval. The presence of drug in the sample was calculated with help of calibration curve.

Pharmacokinetic parameter evaluation:

The pharmacokinetic data were evaluated from the drug concentration in blood vs time release profile and using different formula for pharmacokinetic calculation.

Data for presence of drug in plasma at different time interval is presented in Table-26, comparison of *in vivo* drug release and *in vivo* pharmacokinetic data are presented in Fig 49 and Table-27 respectively.

Chapter 4

Results and Discussion

4. RESULTS AND DISCUSSION

4.1. Results of the visual observation of the pure drug were found as follows:

Colour: White

Odour: Characteristic

Taste: Bitter

4.2. Characterisation of drug:

4.2.1. Melting point determination:

The melting point of the pure drug sample of Atorvastatin calcium was found to be 164^0c. As the melting point of API was within the reported ranges specified in literature (160-170^0c), it revealed that API was in its pure and pharmacologically active form.

4.2.2.Fourier Transform Infrared Spectroscopy (FTIR):

FTIR spectroscopy was performed to identify the supplied pure drug. The spectrum of the pure drug was compared with the reference spectrum of Atorvastatin calcium as shown in Fig 4 and Fig 5 respectively and in the Table 4.

Table 4: IR interpretation of Atorvastatin calcium

Sl no.	Functional group	IR Absorption bands (cm^{-1})	
		Reference drug	Sample drug
1.	O-H	3360	3362
2.	N-H	3230	3236
3.	CH_3	2970	2971
4.	C-H (aromatic)	2824	2824
5.	C=O	1640	1649
6.	C-N	1570	1578
7.	C-C	1430	1432

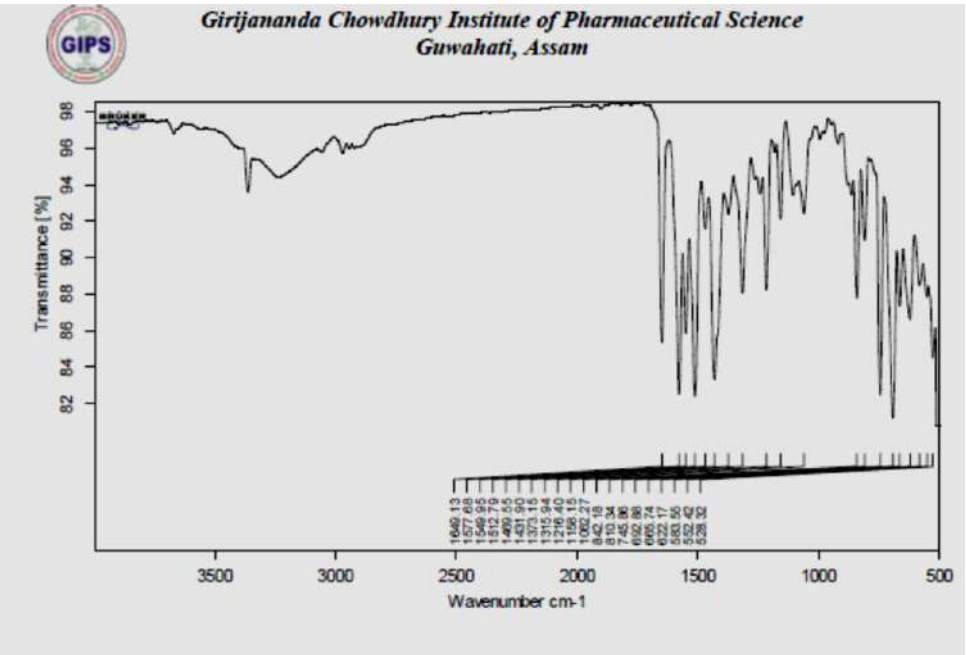

Fig 4: IR spectrum of pure Atorvastatin Calcium

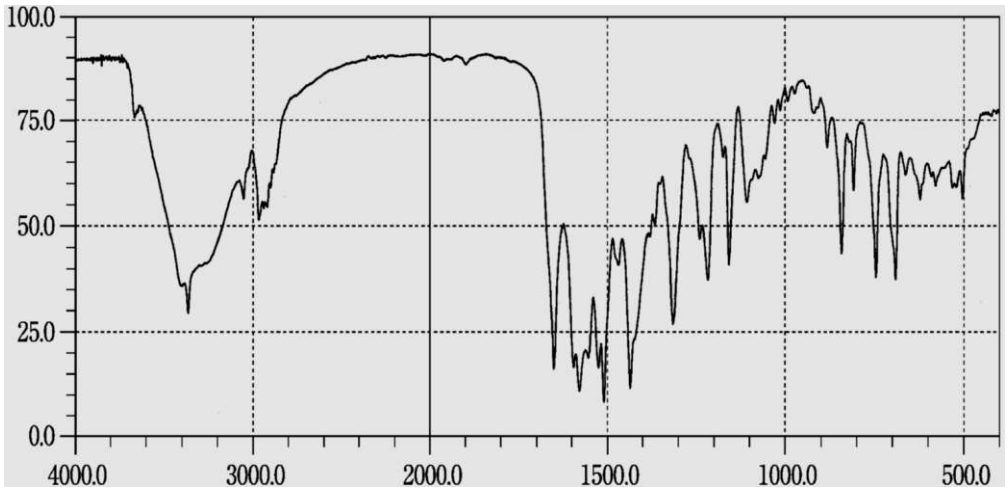

Fig 5: IR spectrum of reference Atorvastatin Calcium

As the IR spectrum of supplied Atorvastatin calcium matches with the IR spectrum of reference Atorvastatin calcium, it can be concluded that the supplied drug sample was pure Atorvastatin calcium.

4.3. Analysis of Atorvastatin calcium:

4.3.1. Preparation of calibration curve of Atorvastatin calcium in acetone: water (1:9):

After scanning the appropriate dilute solution in the range of 200-400nm the λ_{max} was found to be 264nm. The UV spectrum and calibration curve of Atorvastatin calcium in the above mentioned solvent system were presented in Fig 6 and Fig 7 respectively. The data of the calibration curve was presented in Table 5. The linearity of the curve was found between concentration ranges of 0.2-4µg/ml.

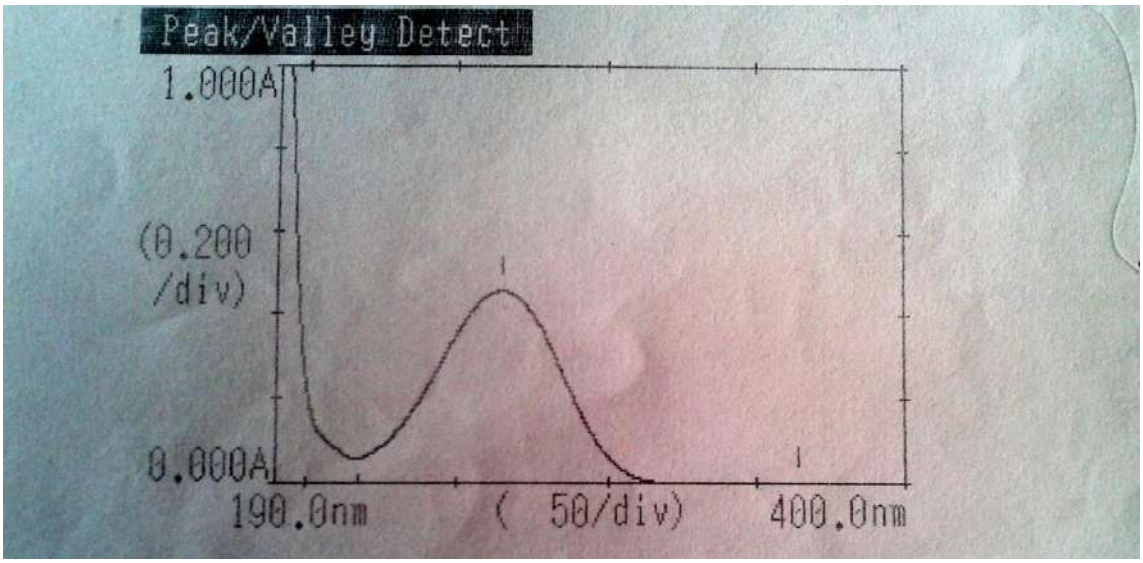

Fig 6: UV spectra of Atorvastatin calcium in acetone: water (1:9), (λ_{max}=264 nm)

Table 5: Data for calibration curve of Atorvastatin Calcium in acetone: water (1:9) at λ_{max}264nm

Concentration(µg/ml)	Absorbance
0	0
0.2	0.0354
0.4	0.0855
0.6	0.1337
0.8	0.1988
1	0.2358
2	0.4595
4	0.9102
Regression equation, R^2=0.999	

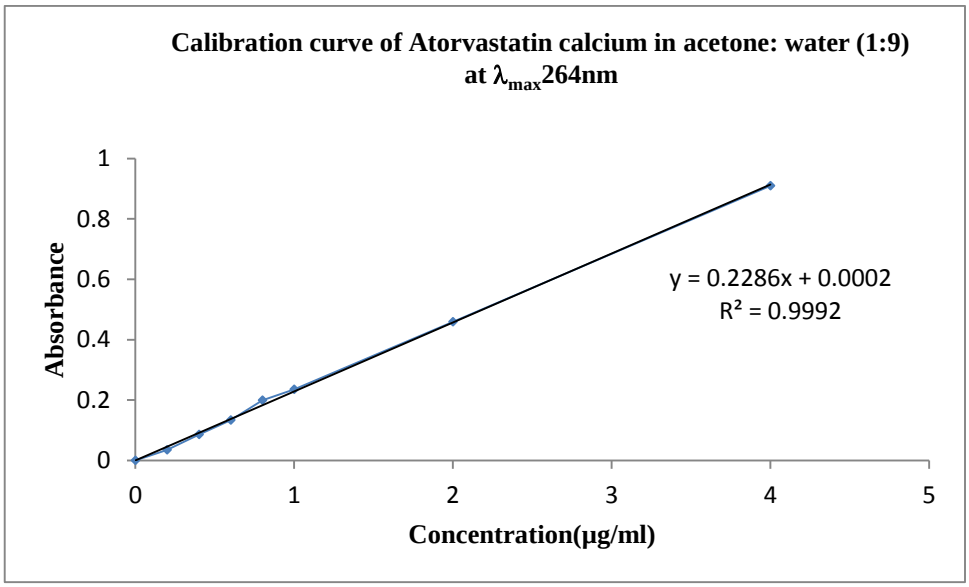

Fig 7: Calibration curve of Atorvastatin calcium in acetone: water (1:9) at λ_{max} 264nm

4.3.2. Preparation of calibration curve of Atorvastatin calcium in acetone: phosphate buffer pH 6.8 (1:9):

After scanning the appropriate dilute solution in the range of 200-400nm the λ_{max} was found to be 264nm. The UV spectrum and calibration curve of Atorvastatin calcium in the above mentioned solvent system were presented in Fig 8 and Fig 9 respectively. The data of the calibration curve was presented in Table 6. The linearity of the curve was found between concentration ranges of 0.2-4µg/ml.

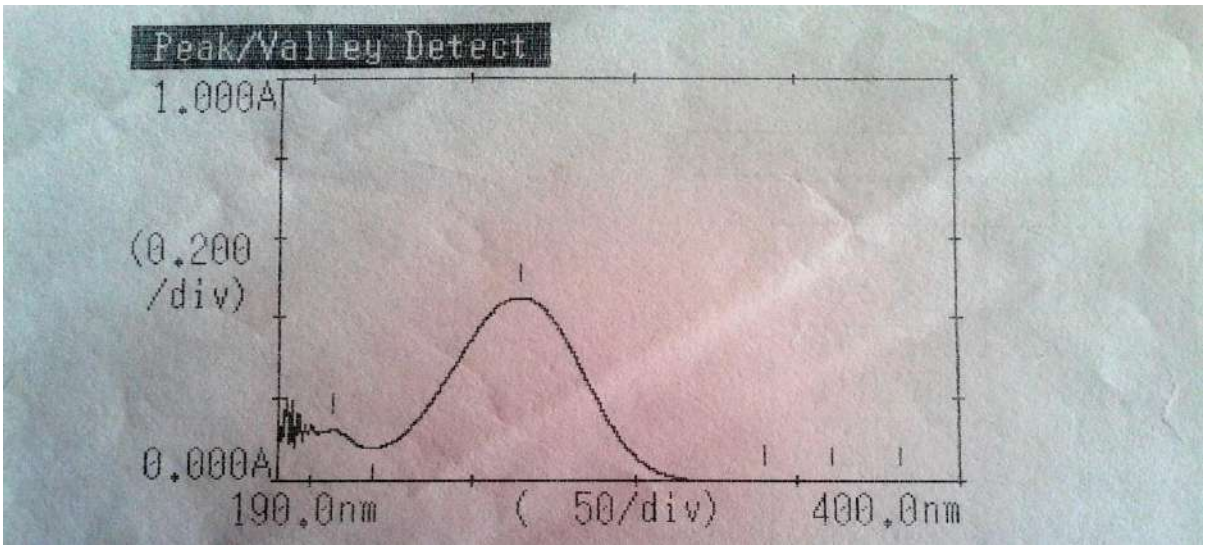

Fig 8: UV spectra of Atorvastatin calcium in acetone: phosphate buffer pH 6.8 (1:9), (λ_{max}=264 nm)

Table 6: Data for calibration curve of Atorvastatin Calcium in acetone: phosphate buffer pH 6.8 (1:9) at λ_{max} 264nm

Concentration(µg/ml)	Absorbance
0	0
0.2	0.0356
0.4	0.0834
0.6	0.1468
0.8	0.1994
1	0.2494
2	0.4475
4	0.913
Regression equation, R^2= 0.998	

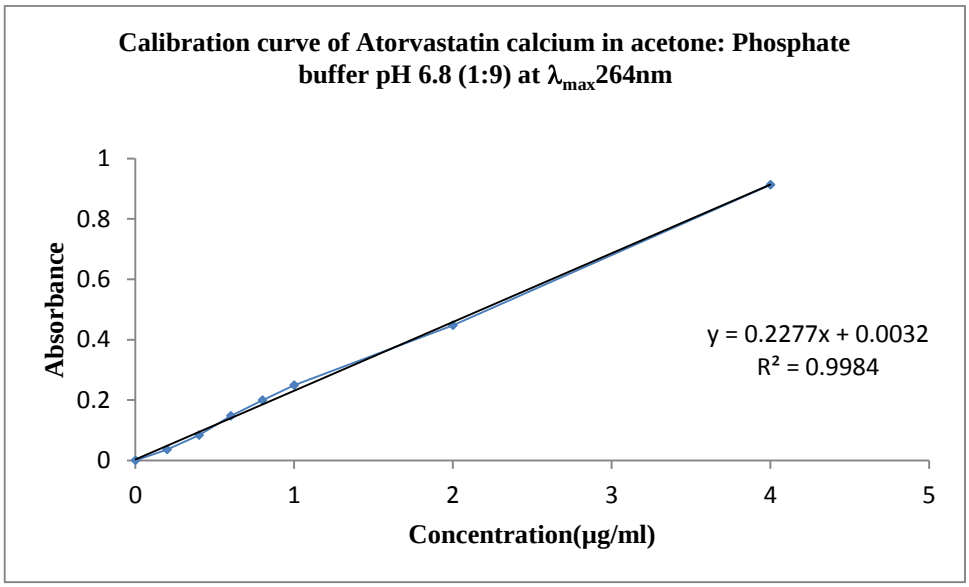

Fig 9: Calibration curve of Atorvastatin calcium in acetone: phosphate buffer pH 6.8(1:9) at λ_{max} 264nm

4.3.3. Preparation of calibration curve of Atorvastatin calcium in acetone: 0.1N HCl (1:9):

After scanning the appropriate dilute solution in the range of 200-400nm the λ_{max} was found to be 264nm. The UV spectrum and calibration curve of Atorvastatin calcium in the above mentioned solvent system were presented in Fig 10 and Fig 11 respectively. The data of the calibration curve was presented in Table 7. The linearity of the curve was found between concentration ranges of 0.2-4µg/ml.

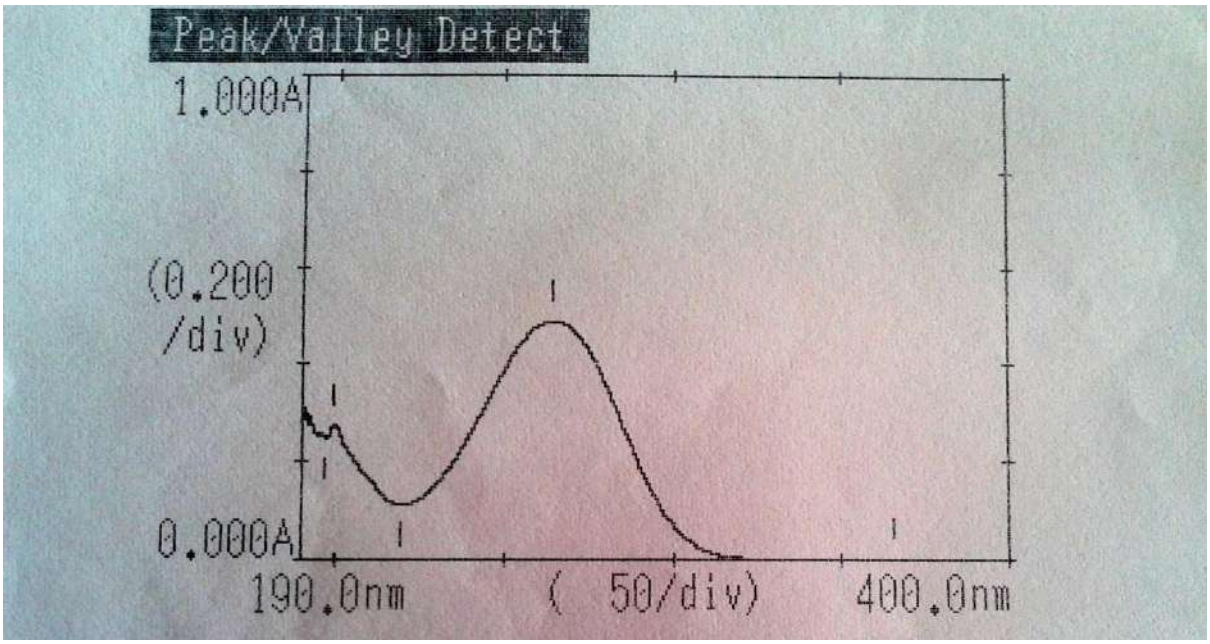

Fig 10: UV spectra of Atorvastatin calcium in acetone: 0.1N HCl (1:9), (λ_{max}=264 nm)

Table 7: Data for standard calibration curve of Atorvastatin Calcium in acetone: 0.1N HCl (1:9) at λ_{max} 264nm

Concentration(µg/ml)	Absorbance
0	0
0.2	0.0433
0.4	0.0744
0.6	0.1224
0.8	0.1757
1	0.2114
2	0.4685
4	0.9357
Regression equation R^2= 0.999	

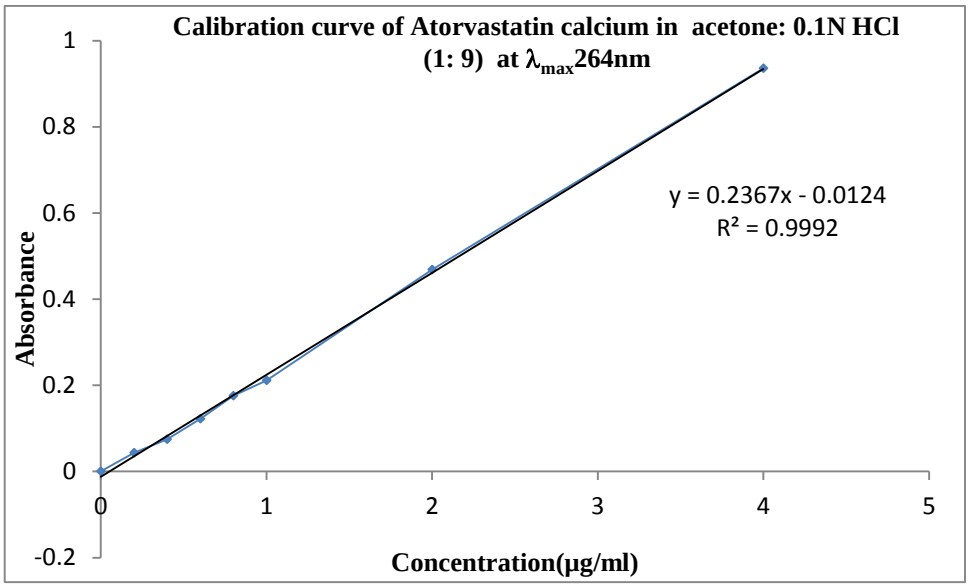

Fig 11: Calibration curve of Atorvastatin calcium in acetone: 0.1N HCl (1:9) at λ_{max} 264nm

4.4. Solubility study of drug:

Results of qualitative solubility study of the Atorvastatin calcium in different solvents were presented in Table 8:

Table 8: Solubility of Atorvastatin calcium

Sample no.	Solvents	Solubility
1.	Distilled water	Slightly soluble
2.	Phosphate buffer pH 6.8	Slightly soluble
3.	0.1N HCl	Slightly soluble
4.	Acetone	Freely soluble
5.	DMSO	Freely soluble
6.	Methanol	Freely soluble

4.5. Saturation Solubility study of drug:

The saturation solubility study of the drug in different solvents was performed and its solubility were summarised in Table 9.

Table 9: Saturation solubility of Atorvastatin calcium

Sample no.	Solvents	Absorbance at 264nm	Saturation solubility in µg/ml
1.	Distilled water	0.0547	239.9
2.	Phosphate buffer pH 6.8	0.0779	329.9
3.	0.1N HCl (pH, 1.2)	0.0025	61.4

From the above data it can be conclude that Atorvastatin is more soluble in phosphate buffer pH 6.8 than the simulated gastric fluid, pH 1.2.

4.6. Drug excipient compatibility study:

4.6.1. FTIR study:

FT-IR spectroscopy study was carried out separately to find out, the compatibility between the drug Atorvastatin calcium and the polymers Chitosan and Pluronic F68 used for the preparation of nanoparticles. The FT-IR was performed for drug, polymer and the physical mixture of drug-polymer.

The spectrum obtained from FT-IR spectroscopy studies at wavelength between 4000 $cm^{-1}$to 400 cm^{-1} are given in Table 10 and Figures 12 to 16.

Table 10: IR interpretation of drug, polymer and 1:1 ratio of physical mixture of drug-polymer

Sl no.	Functional group	IR Absorption bands (cm^{-1})		
		Drug	Drug + Chitosan	Drug +Pluronic F 68
1.	O-H	3362	3351	3320
2.	N-H	3236	3213	3259
3.	CH_3	2971	3013	2970
4.	C-H (aromatic)	2824	2814	2827
5.	C=O	1649	1649	1649
6.	C-N	1578	1577	1578
7.	C-C	1432	1430	1433

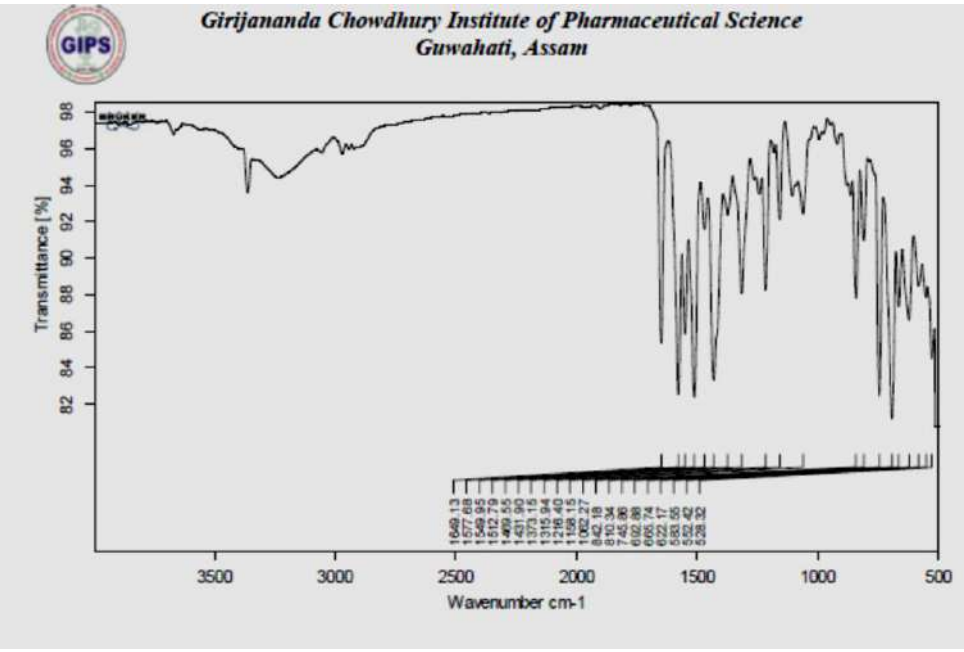

Fig 12: IR spectrum of pure Atorvastatin calcium

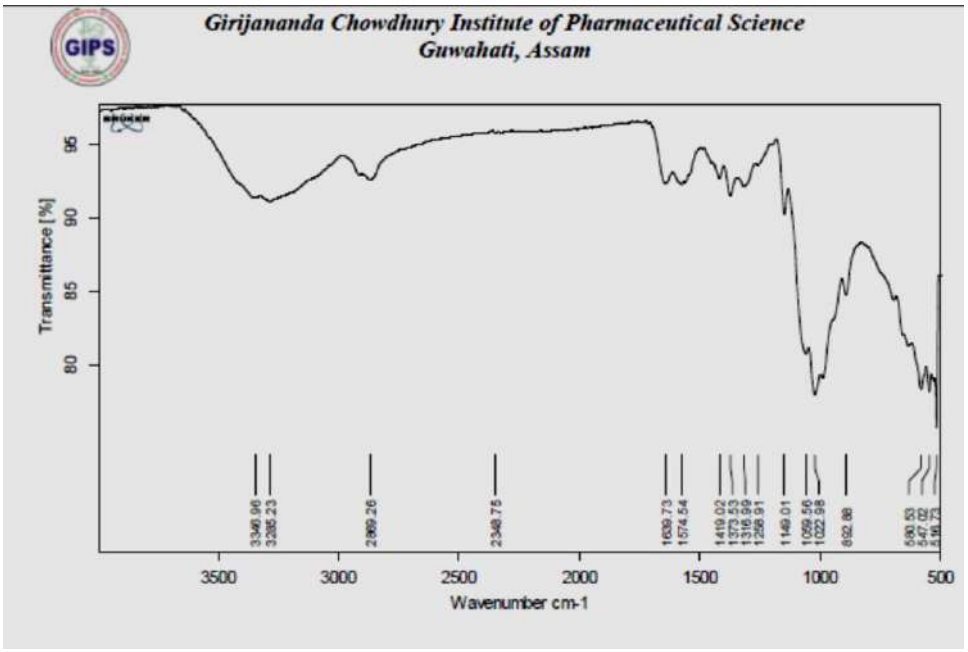

Fig 13: IR spectrum of Chitosan

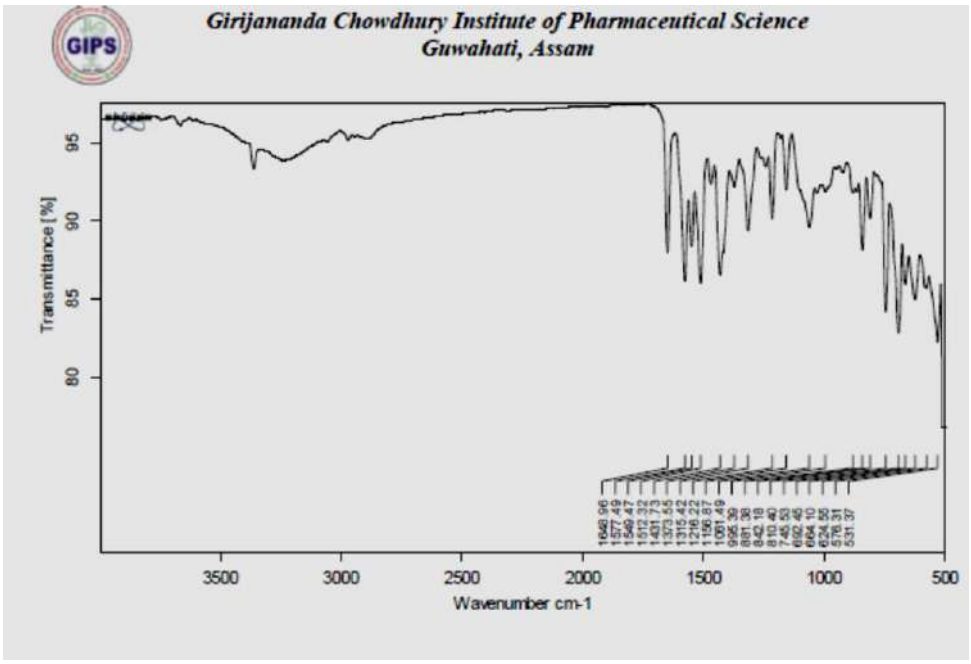

Fig 14: IR spectrum of 1:1 ratio of Atorvastatin calcium –chitosan physical mixture

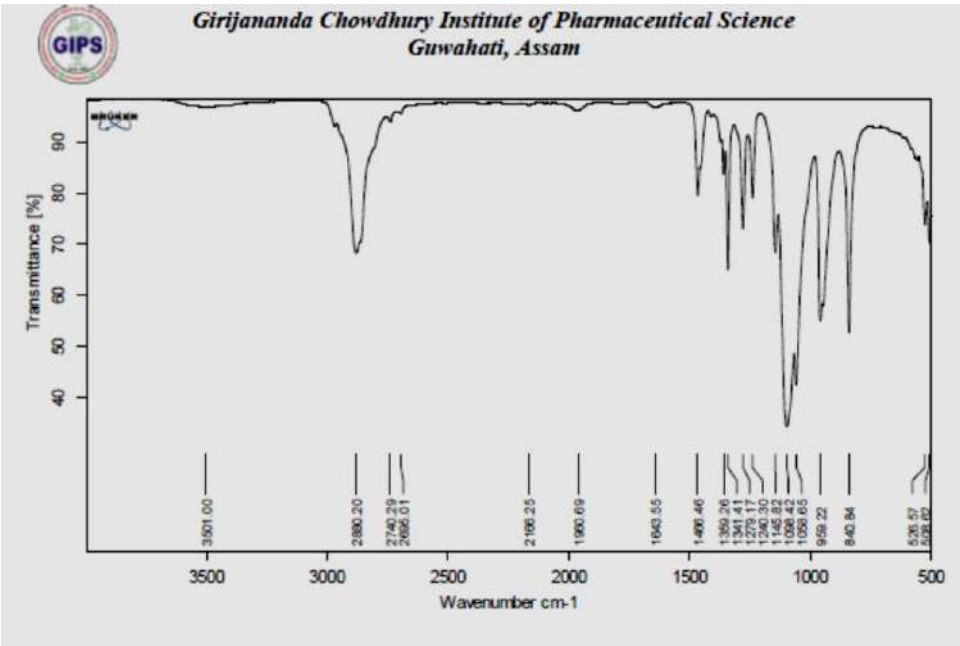

Fig 15: IR spectrum of Pluronic F68

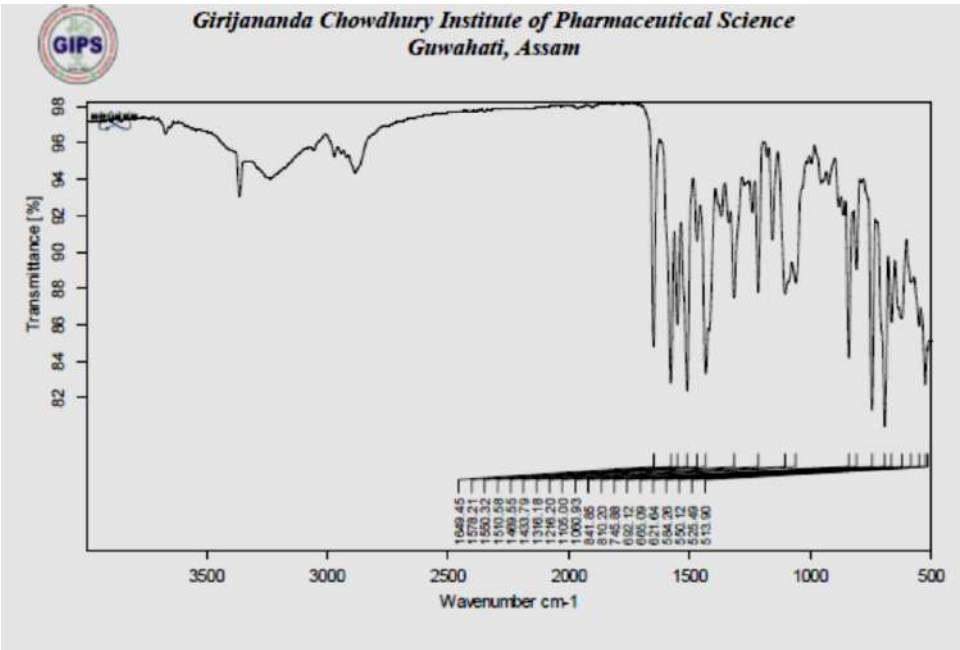

Fig 16: IR spectrum of 1:1 ratio of Atorvastatin Calcium-Pluronic F68 physical mixture

FTIR of Atorvastatin calcium showed the following peaks at 3362, 3236, 2971, 2960.83, 2824, 1649, 1578 and 1432nm due to O-H, N-H, CH_3,C-H(aromatic), C=O, C-N and C-C functional groups. The physical mixture of drug with polymer Chitosan and Pluronic F68 clearly shows the retention of these characteristic peaks of Atorvastatin calcium (Table 10 and Figures 12 to 16), thus revealing no interaction between the selected drug and polymers.

4.6.2. DSC study:

DSC study was carried out separately to find out, the compatibility between the drug Atorvastatin calcium and the polymers Chitosan and Pluronic F68 used for the preparation of nanoparticles. The DSC thermogram was performed for drug and the physical mixture of drug-polymer.

The thermogram obtained from DSC studies at temperature between 20^0c to 260^0c is given in Figures 17 to 19.

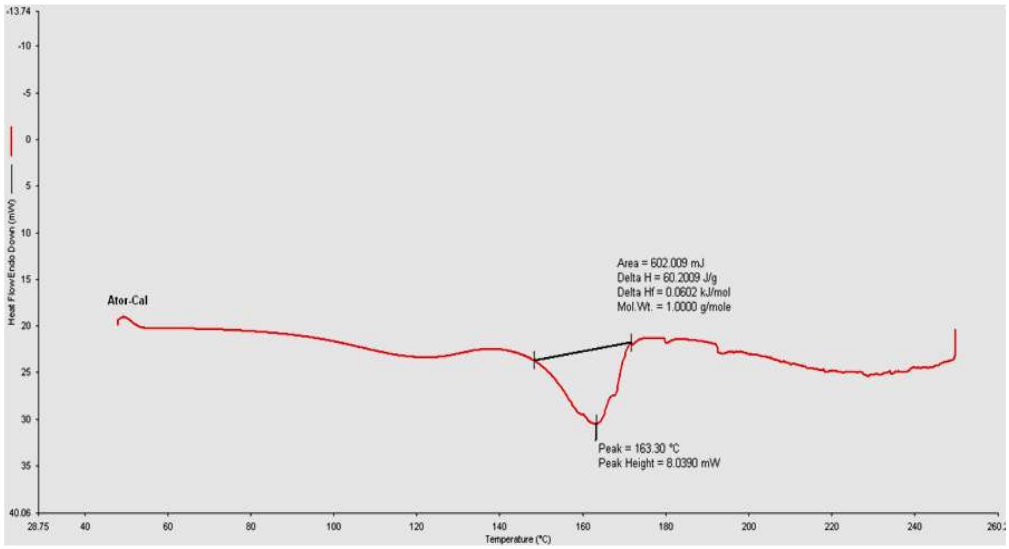

Fig 17: DSC thermogram of the pure Atorvastatin Calcium

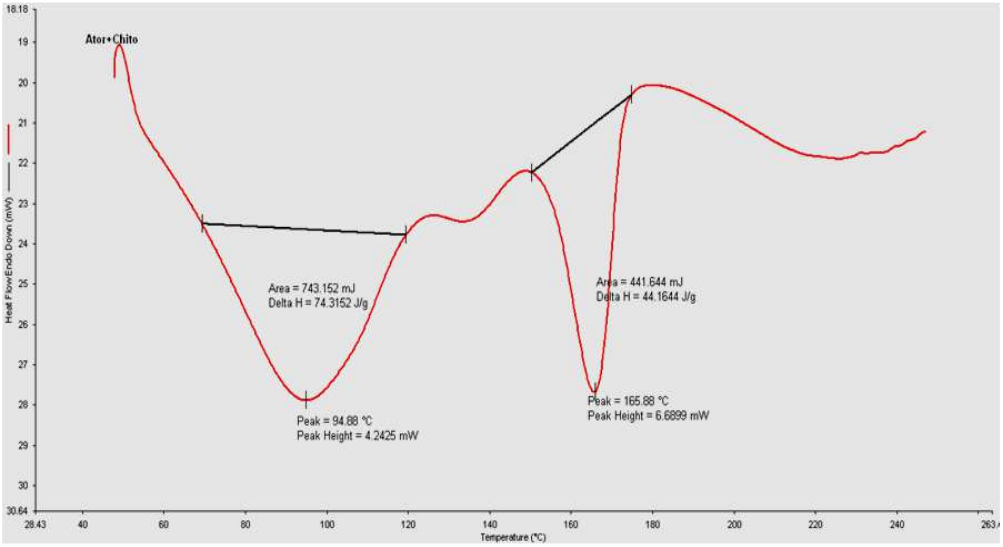

Fig 18: DSC thermogram of 1:1 ratio of pure Atorvastatin calcium and chitosan physical mixture

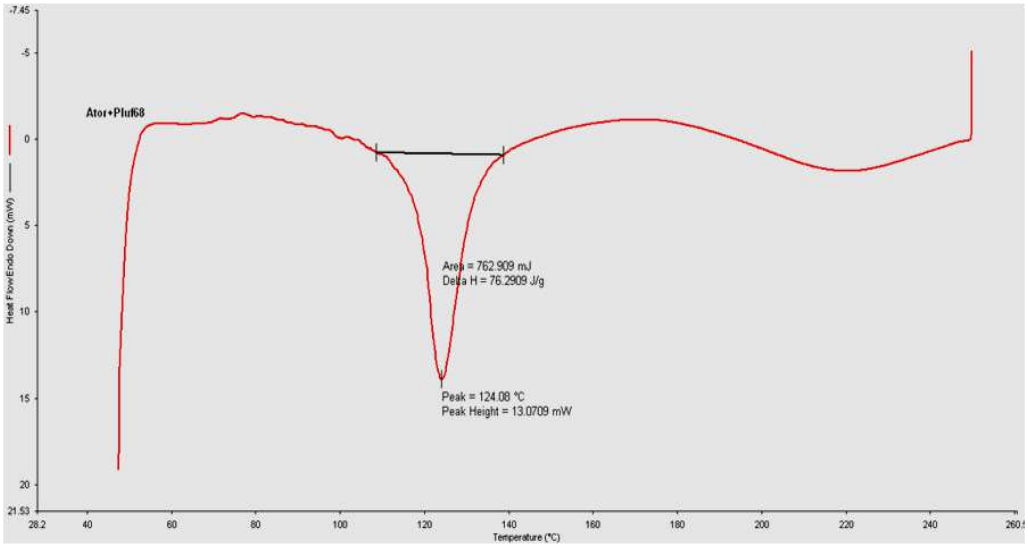

Fig 19: DSC thermogram of 1:1 ratio of pure Atorvastatin Calcium and Pluronic F68

The thermogram of pure Atorvastatin calcium shows a sharp endothermic peak at 163.3 °C (Fig 17), which corresponds to its melting point. The thermogram of Atorvastatin calcium with excipient like Chitosan and Pluronic F68 shows sharp endothermic peak at 165.88^0c and 124.08^0c (Fig 18 &19) respectively, due to the presence of Atorvastatin calcium. Thus, the thermal data did not reveal any interaction between the drug and the excipients.

4.6.3. Viscosity determination:

Table 11: Viscosity of Chitosan solution at different RPM

RPM	Viscosity (0.5% Concentration of Chitosan), cps
1	203500
5	26020
10	2260
50	470

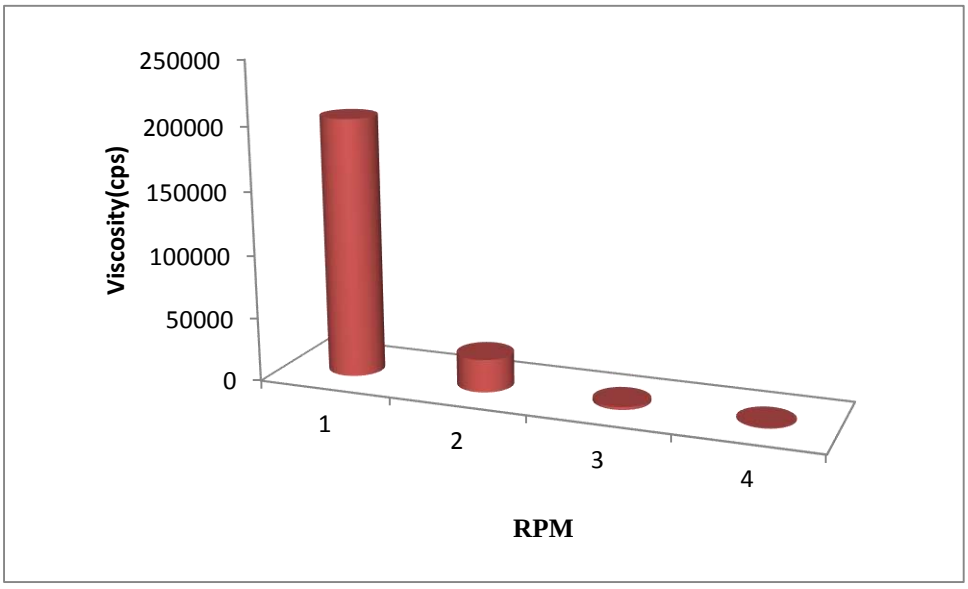

Fig 20: Viscosity of Chitosan solution at different RPM

Viscosity of 0.5% Chitosan at different rpm was determined using 25 no spindle and the viscosity was found to be decreases as the shear rate (rpm) increases.

4.6.4. Evaluation of the Prepared Atorvastatin calcium nanoparticles:

4.6.4.1. Percentage Yield:

Table 12: Nanoparticles yield from different formulations

Formulations	Drug to Polymer ratio (by wt)	Yield (mg ± SD)*	%Yield (% ± SD)*
F_1	1:1	20 ± 0.22	66.66 ± 0.73
F_2	1:2	28 ± 0.28	70 ± 0.70
F_3	1:3	37 ± 0.34	74 ± 0.68
F_4	1:4	48 ± 0.45	80 ± 0.75
F_5	1:5	60 ± 0.48	85.71± 0.68

SD = Standard deviation, *= Average of three determination

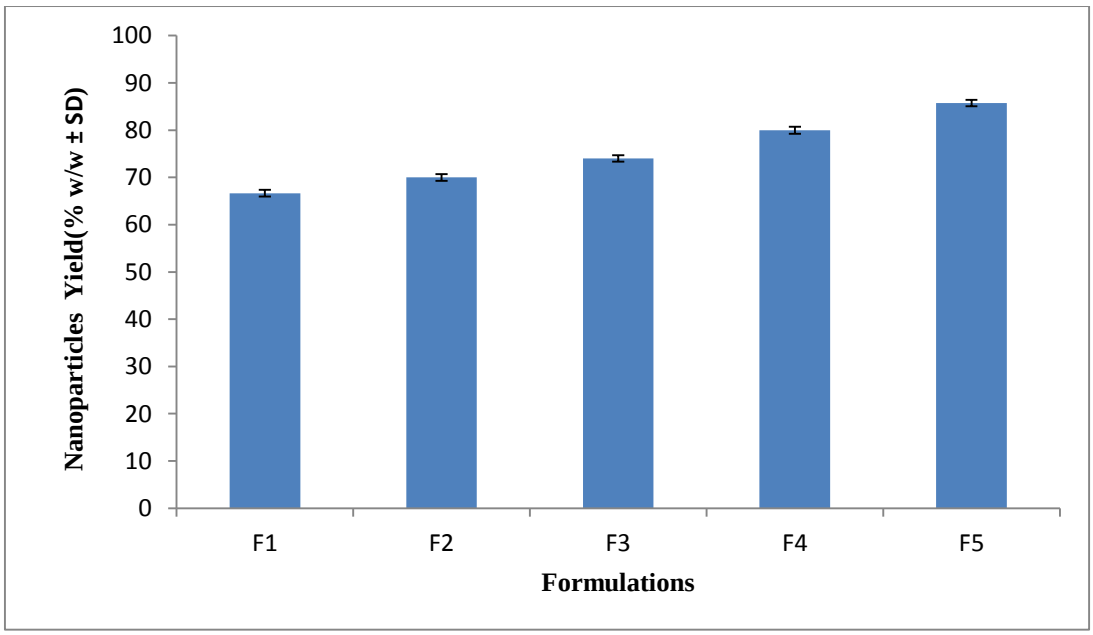

Fig 21: Nanoparticles yield from different formulations

The percentage yield for different formulations is shown in Table-12. The percentage yield ranged between 66.66% to 85.71% w/w depending on the drug polymer ratio.The yield of nanoparticles is found to be increase with increase in polymer concentration.

4.6.4.2. Drug Loading:

Table 13: Drug loading data for different formulations

Formulations	Drug to Polymer ratio (by wt)	Actual drug content (mg ± SD)*	Weight of powdered nanoparticles (mg ± SD)*	% Drug Loading (%± SD)*
F_1	1:1	0.8 ± 0.22	20 ± 0.22	4 ± 1.1
F_2	1:2	2.52 ± 0.28	28 ± 0.28	9 ± 1.0
F_3	1:3	4.81 ± 0.34	37 ± 0.34	13 ± 0.92
F_4	1:4	7.2 ± 0.45	48 ± 0.45	15 ± 0.93
F_5	1:5	9.6 ± 0.48	60 ± 0.48	16 ± 0.80

SD = Standard deviation, *= Average of three determination

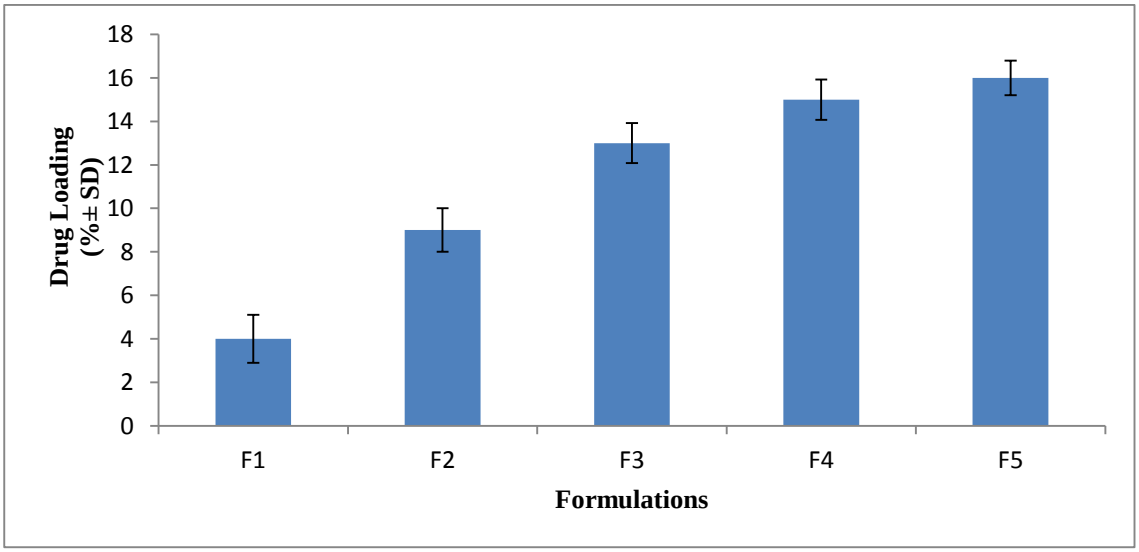

Fig 22: Drug loading data for different formulations

The drug loading for different formulations is shown in Table-13. The prepared nanoparticles showed good drug loading capacity which ranged from 4% to 16% depending on the drug polymer ratio. The drug loading capacity of nanoparticles increased with increase in polymer concentration. The low drug loading values indicate relatively low affinity of the drug with the polymer matrix. Another explanation for poor drug loading is probably solubility and ionization of the drug. Atorvastatin calcium is insoluble in water and has an ionization constant of 4.46. The aqueous Pluronic F68 (surfactant) solution has a pH of about 6. Therefore, when the organic phase is added dropwise into the aqueous surfactant solution, part of the drug is ionized and escapes from the nanoparticles during diffusion of the acetone into the aqueous phase. Increasing the polymer content in the formulation increased drug loading inside the nanoparticles. However, when the polymer content is 5% in the formulation (F5), saturation of the polymer particles occurs with such a high drug loading. The excess drug escapes from the acetone phase into the water. Another possibility for the decreased drug loading at low polymer content in the formulation can be explained by saturation of the cationic sites on the chitosan by anionic drug molecules. Therefore, excess drug is being lost from the particles during its formation process.

4.6.4.3. Entrapment Efficiency:

Table 14: Entrapment Efficiency data for different formulations

Formulations	Drug to Polymer ratio (by wt)	Amounts of drug taken in the formulation(mg)	Amounts of drug present in the formulation(mg ± SD)*	% Entrapment Efficiency (%±SD)*
F_1	1:1	10	0.8 ± 0.22	8 ± 2.2
F_2	1:2	10	2.52 ± 0.28	25.2 ± 2.8
F_3	1:3	10	4.81 ± 0.34	48.1 ± 3.4
F_4	1:4	10	7.2 ± 0.45	72 ± 4.5
F_5	1:5	10	9.6 ± 0.48	96 ± 4.8

SD = Standard deviation, *= Average of three determination

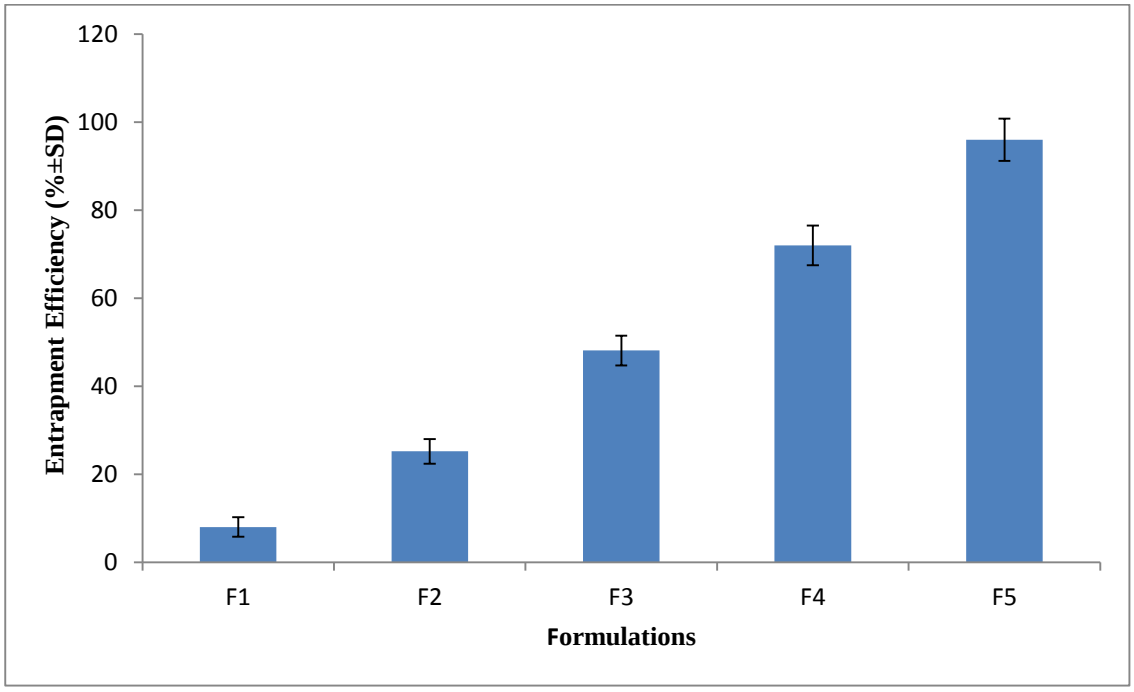

Fig 23: Entrapment Efficiency data for different formulations

The entrapment efficiency for different formulations is shown in Table-14. The prepared nanoparticles showed entrapment efficiency in the range of 8% to 96% depending on the drug polymer ratio. The entrapment efficiency of nanoparticles increased with increase in polymer concentration.The low drug entrapment efficiency values indicate relatively low affinity of the drug with the polymer matrix. Another explanation for poor entrapment efficiency is probably solubility and ionization of the drug. Atorvastatin calcium is insoluble in water and has an ionization constant of 4.46. The aqueous Pluronic F68 (surfactant) solution has a pH of about 6. Therefore, when the organic phase is added dropwise into the aqueous surfactant solution, part of the drug is ionized and escapes from the nanoparticles during diffusion of the acetone into the aqueous phase. Increasing the polymer content in the formulation increased drug entrapment efficiency inside the nanoparticles. However, when the polymer content is 5% in the formulation (F5), saturation of the polymer particles occurs with such high drug entrapment efficiency. The excess drug escapes from the acetone phase into the water. Another possibility for the decreased drug entrapment efficiency at low polymer content in the formulation can be explained by saturation of the cationic sites on the chitosan by anionic drug molecules. Therefore, excess drug is being lost from the particles during its formation process.

4.6.4.4. Particle size and Polydispersity index:

The Particle size and Polydispersity index of prepared nanoparticles was determined by using Malvern Zetasizer S90 and the results are shown in Table-15 and Fig 24 to 28.

Table 15: Particle size and Polydispersity index data for different formulations

Formulations	Drug to Polymer ratio (by wt)	Particle size(nm ± SD)*	Polydispersity index ± SD*
F_1	1:1	219.3 ± 0.016	0.461 ± 0.002
F_2	1:2	298.2 ± 0.023	0.318 ± 0.012
F_3	1:3	477.8 ± 0.019	0.326 ± 0.015
F_4	1:4	678.9 ± 0.021	0.283 ± 0.008
F_5	1:5	820.8 ± 0.024	0.252 ± 0.004

SD = Standard deviation, *= Average of three determination

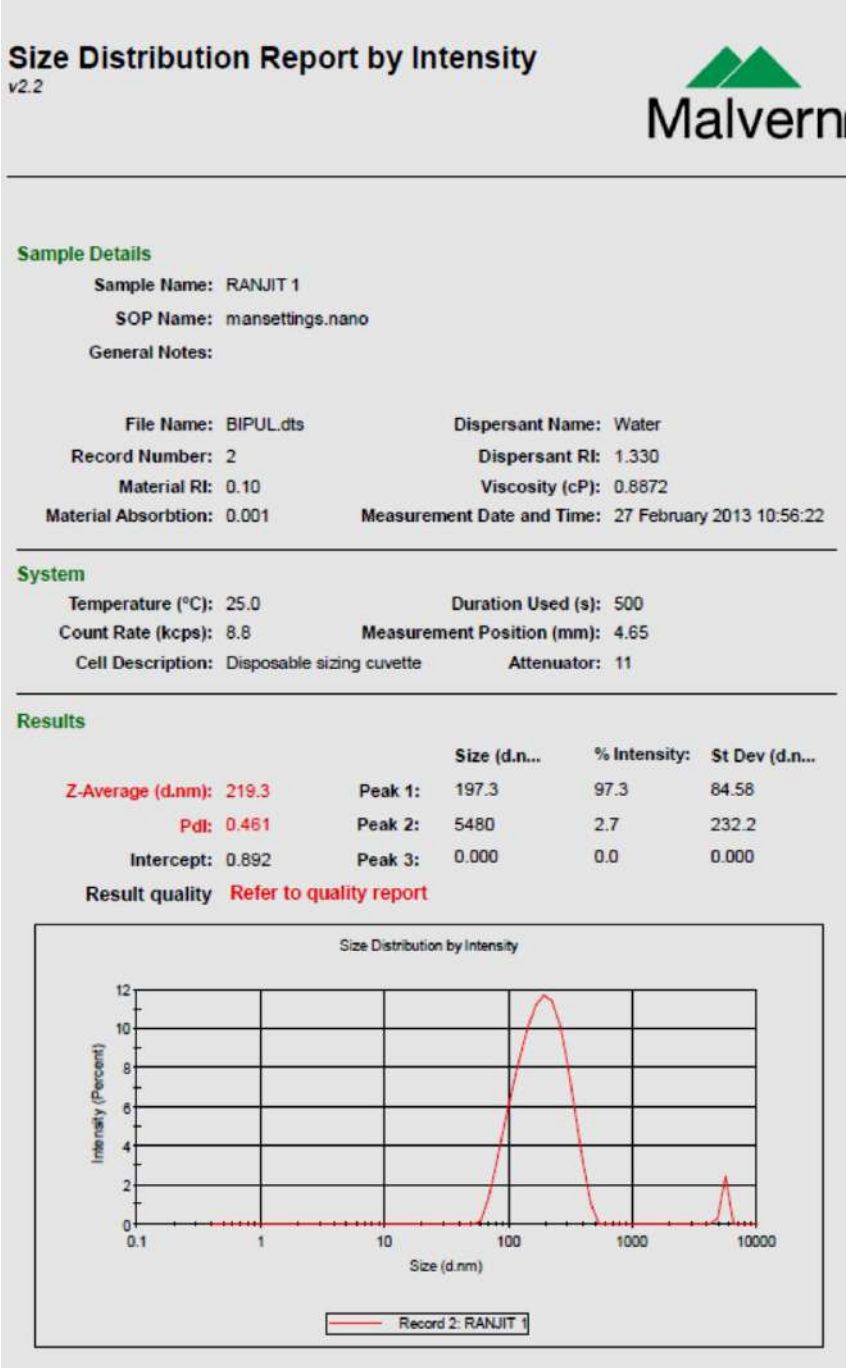

Size Distribution Report by Intensity
v2.2

Malvern

Sample Details

Sample Name:	RANJIT 1		
SOP Name:	mansettings.nano		
General Notes:			
File Name:	BIPUL.dts	Dispersant Name:	Water
Record Number:	2	Dispersant RI:	1.330
Material RI:	0.10	Viscosity (cP):	0.8872
Material Absorbtion:	0.001	Measurement Date and Time:	27 February 2013 10:56:22

System

Temperature (°C):	25.0	Duration Used (s):	500
Count Rate (kcps):	8.8	Measurement Position (mm):	4.65
Cell Description:	Disposable sizing cuvette	Attenuator:	11

Results

			Size (d.n...	% Intensity:	St Dev (d.n...
Z-Average (d.nm):	219.3	Peak 1:	197.3	97.3	84.58
PdI:	0.461	Peak 2:	5480	2.7	232.2
Intercept:	0.892	Peak 3:	0.000	0.0	0.000

Result quality: Refer to quality report

Fig 24: Particle size and Polydispersity index of F1 formulation

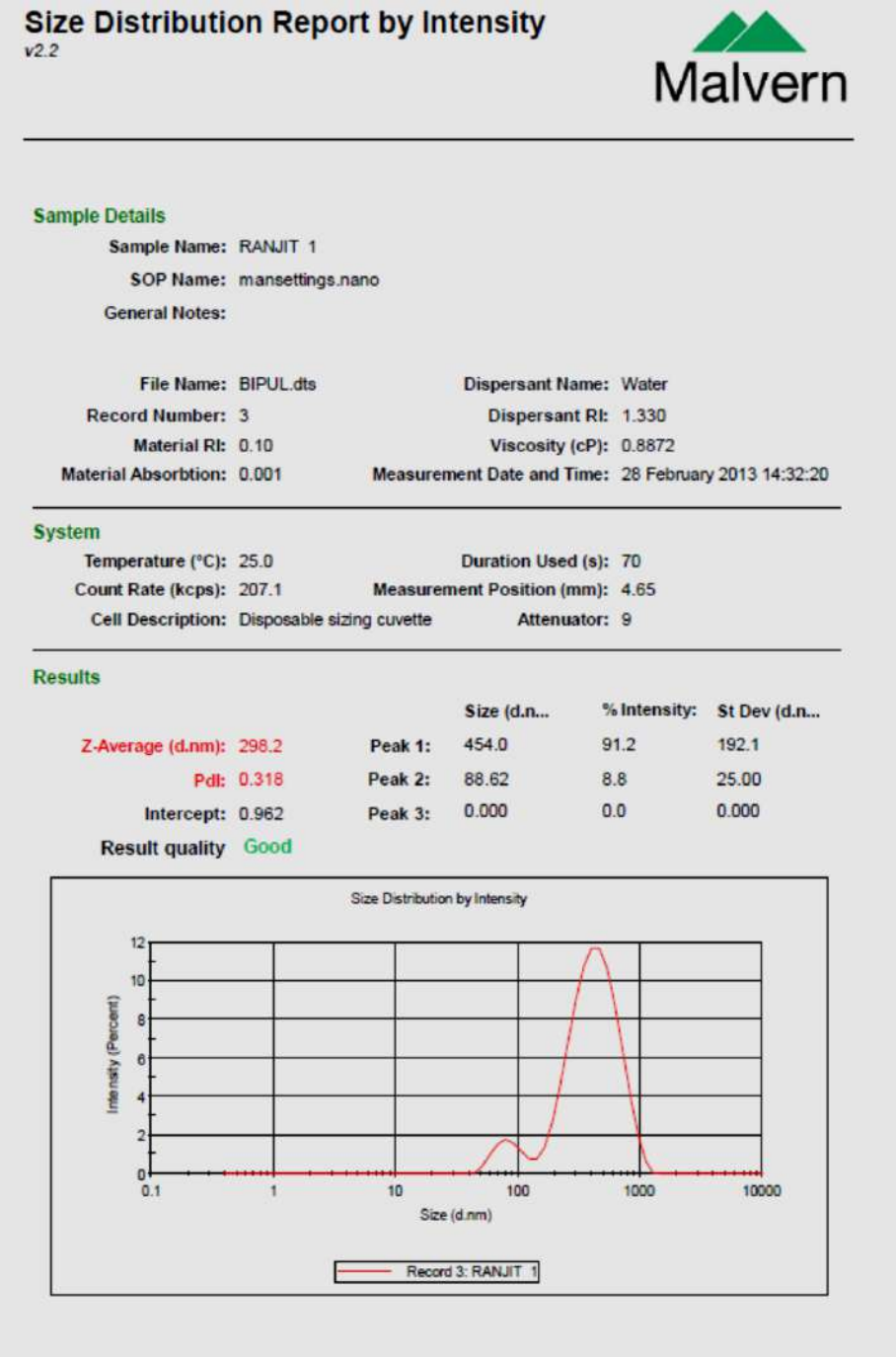

Size Distribution Report by Intensity
v2.2

Malvern

Sample Details

Sample Name: RANJIT 1
SOP Name: mansettings.nano
General Notes:

File Name: BIPUL.dts
Record Number: 3
Material RI: 0.10
Material Absorbtion: 0.001
Dispersant Name: Water
Dispersant RI: 1.330
Viscosity (cP): 0.8872
Measurement Date and Time: 28 February 2013 14:32:20

System

Temperature (°C): 25.0
Count Rate (kcps): 207.1
Cell Description: Disposable sizing cuvette
Duration Used (s): 70
Measurement Position (mm): 4.65
Attenuator: 9

Results

			Size (d.n...	% Intensity:	St Dev (d.n...
Z-Average (d.nm):	298.2	Peak 1:	454.0	91.2	192.1
PdI:	0.318	Peak 2:	88.62	8.8	25.00
Intercept:	0.962	Peak 3:	0.000	0.0	0.000
Result quality	Good				

Fig 25: Particle size and Polydispersity index of F2 formulation

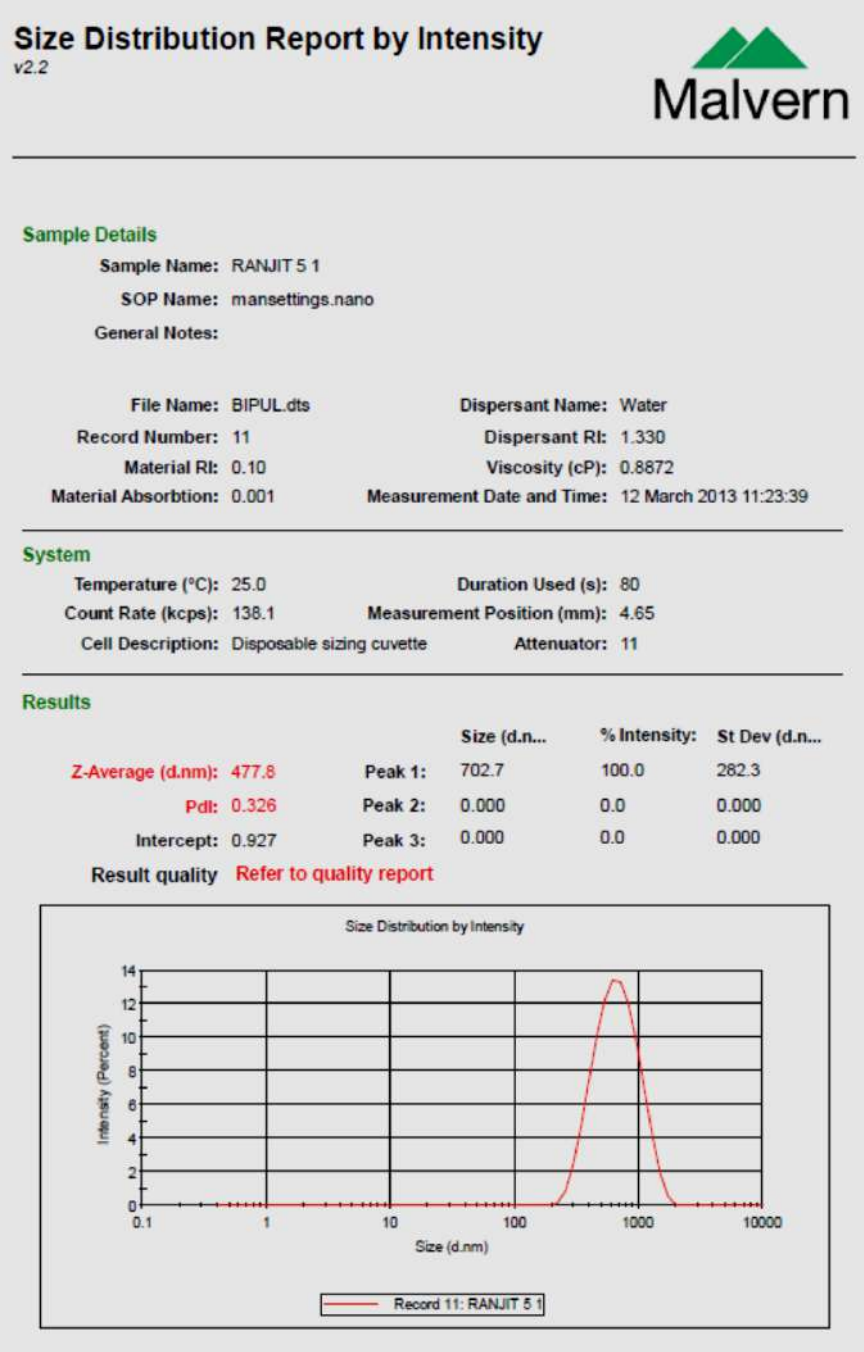

Size Distribution Report by Intensity
v2.2

Malvern

Sample Details

Sample Name: RANJIT 5 1
SOP Name: mansettings.nano
General Notes:

File Name: BIPUL.dts
Record Number: 11
Material RI: 0.10
Material Absorbtion: 0.001
Dispersant Name: Water
Dispersant RI: 1.330
Viscosity (cP): 0.8872
Measurement Date and Time: 12 March 2013 11:23:39

System

Temperature (°C): 25.0
Count Rate (kcps): 138.1
Cell Description: Disposable sizing cuvette
Duration Used (s): 80
Measurement Position (mm): 4.65
Attenuator: 11

Results

		Size (d.n...	% Intensity:	St Dev (d.n...
Z-Average (d.nm): 477.8	Peak 1:	702.7	100.0	282.3
PdI: 0.326	Peak 2:	0.000	0.0	0.000
Intercept: 0.927	Peak 3:	0.000	0.0	0.000

Result quality Refer to quality report

Fig 26: Particle size and Polydispersity index of F3 formulation

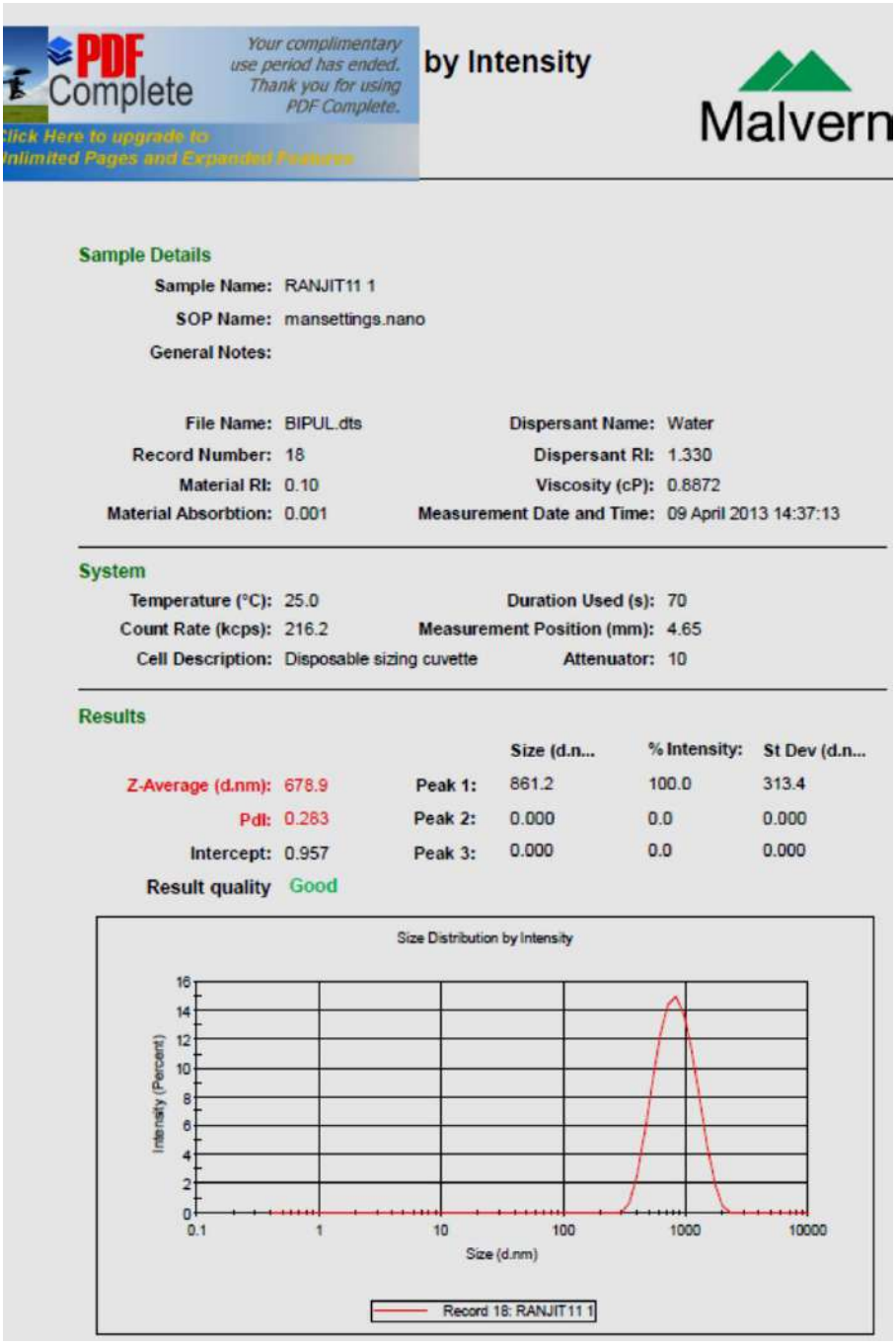

Fig 27: Particle size and Polydispersity index of F4 formulation

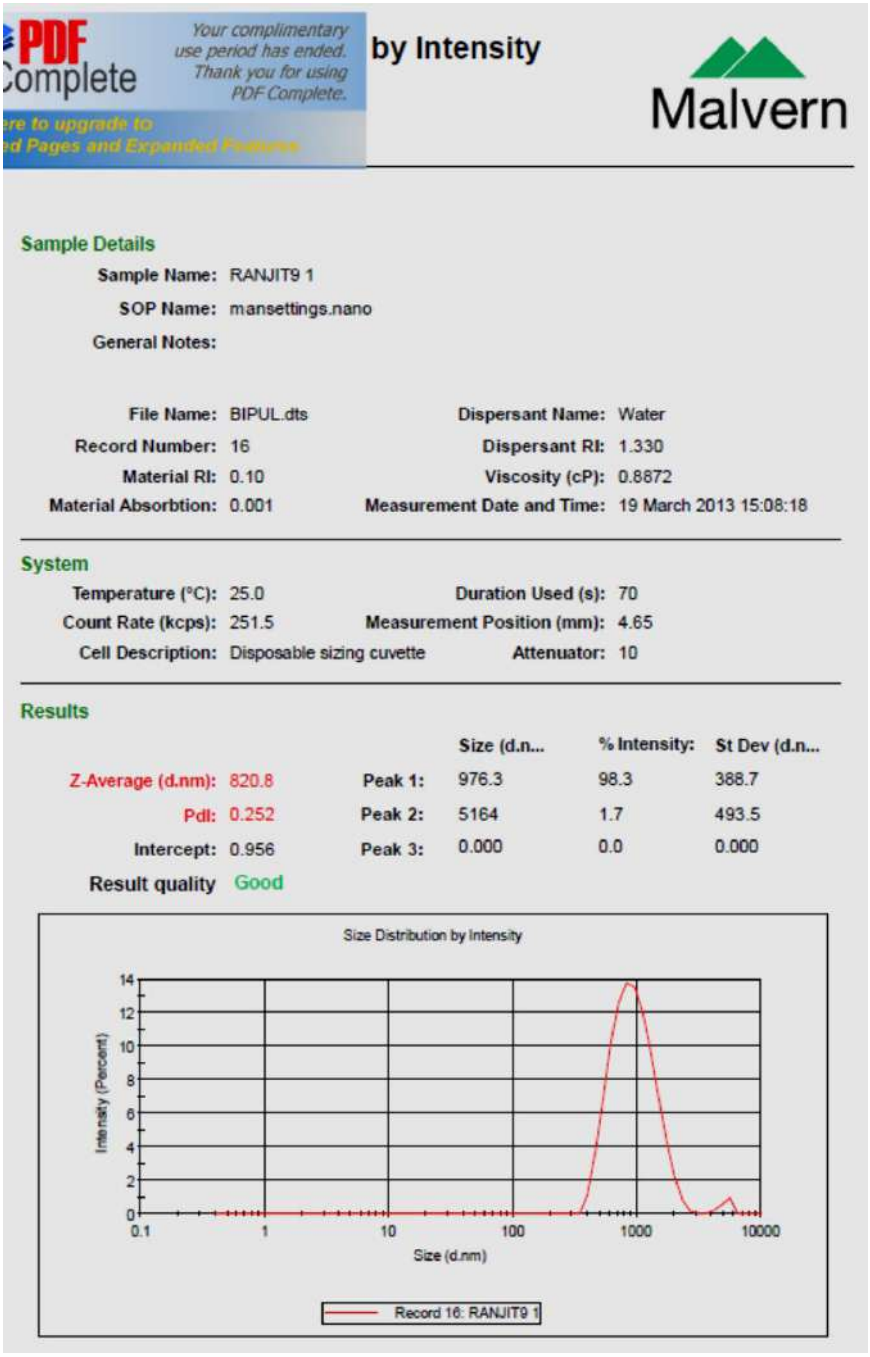

Fig 28: Particle size and Polydispersity index of F5 formulation

The particle size and polydispersity index was determined by Malvern S90. The effect of the drug to polymer ratio on size of the nanoparticles were studied using five different weight ratios of drug and polymer, namely 1:1, 1:2, 1:3, 1:4 and 1:5. Incorporation of the polymer above 5% in the formulation resulted in aggregation and

separation of particles to form white sediment immediately. Therefore, the study was carried out in the range of 1-5% polymer incorporation in the formulation. Particle size data for nanoparticle was shown in Table 15. The mean particle size (Z-average diameter) for the formulations (F1 to F5) varied in the range from 219.3 nm to 820.8 nm and the Polydispersity index of the nanoparticles was found to be in the range of 0.252 to 0.461(Fig 24 to 28). The ability of nanoparticles to alter the biodistribution and pharmacokinetics of drugs has important *in-vivo* therapeutic applications. In this respect the size and polydispersity index of the nanoparticles are of prime importance. Nanoparticles of fewer diameters with hydrophilic surface have longer circulation in blood and nanoparticles with less polydispersity index have greater homogeneity throughout the system and they are more stable in suspension.

4.6.4.5.Zeta potential study:

The zeta potential of prepared nanoparticle formulations was measured by a laser doppler anemometer coupled with Zetasizer Nano ZS 90 (Malvern Instruments Ltd. UK). The Zeta potential data of prepared nanoparticle formulations is shown in Table-16 and Fig 29.

Table 16: Data of Zeta potential study of nanoparticle formulations

Formulations	Drug to Polymer ratio (by wt)	Zeta potential (mV ± SD)*
F_1	1:1	13.03 ± 0.32
F_2	1:2	19.77 ± 0.45
F_3	1:3	23.1 ± 0.58
F_4	1:4	29.16 ± 0.43
F_5	1:5	46.9 ± 0.49

SD = Standard deviation, *= Average of three determination

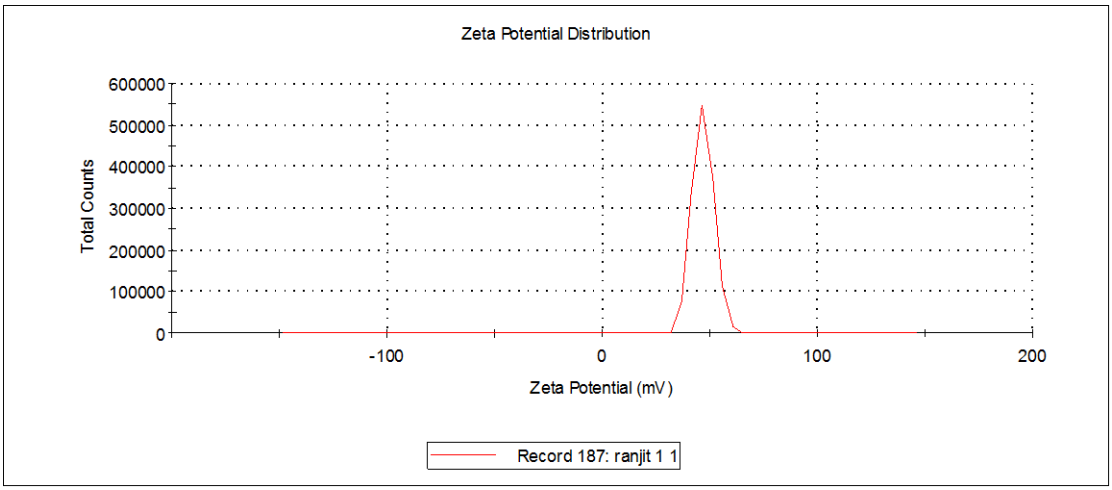

Fig 29: Zeta potential study of F5 formulation

The zeta potential values for nanoparticles were shown in Table-16. The zeta potential remained in the range of positive values for all formulations (+ 13.03 mV to + 46.9mV). The positive surface charge of the nanoparticles was observed due to the presence of the quaternary ammonium groups of Chitosan. The positive surface charge for the nanoparticles could allow for a longer residence time for the particles by ionic interaction. The adsorbed surfactant (Pluronic F68) present onto the nanoparticles surface may shield the particle surface, thus covering with the electrically neutral layers. The relative constancy of zeta potential indicates Atorvastatin calcium was encapsulated within the nanoparticles and a major part of the drug is not present on the nanoparticle surface.

4.6.4.6. *In vitro* drug release studies:

The *in vitro* drug release studies of Atorvastatin calcium nanoparticles were carried out at $37^0 \pm 2^0$C in 0.1N HCl as well as Phosphate buffer pH 6.8 for a period of 48 hours using dialysis bag technique. The drug release data of different formulations in

0.1N HCl as well as Phosphate buffer pH 6.8 are given in Table-17/Fig 30 and Table-18/Fig 31.

Table 17: *In vitro* drug release data for different formulations in 0.1N HCl

Time(hr)	% Cumulative Drug Release (%± SD)*				
	F1	F2	F3	F4	F5
0	0	0	0	0	0
1	20± 0.22	14.26± 0.18	12.58± 0.12	9.41± 0.45	2.48± 0.33
2	23.5± 0.24	17.35± 0.22	15.32± 0.14	12.58± 0.42	6.28± 0.45
3	26.73±0.32	19.32± 0.24	17.73± 0.28	14.28± 0.32	9.24± 0.56
4	35.37± 0.34	30.45± 0.24	24.36± 0.24	18.05± 0.44	12.26± 0.38
5	42.16± 0.26	34.53± 0.28	30.24± 0.34	22.42± 0.23	14.24± 0.44
6	45.61± 0.28	37.46± 0.34	32.78± 0.28	28.68± 0.28	18.34± 0.48
7	60.52± 0.26	45.26± 0.40	38.44± 0.28	34.94± 0.44	22.66± 0.26
8	73.43± 0.44	48.28± 0.38	42.96± 0.32	37.68± 0.22	28.82± 0.34
24	85.24± 0.42	52.15± 0.44	48.48± 0.40	44.66± 0.36	32.96± 0.46
48	95.04± 0.48	64.6± 0.52	58.94± 0.56	52.54± 0.52	44.62± 0.32

SD = Standard deviation, *= Average of three determination

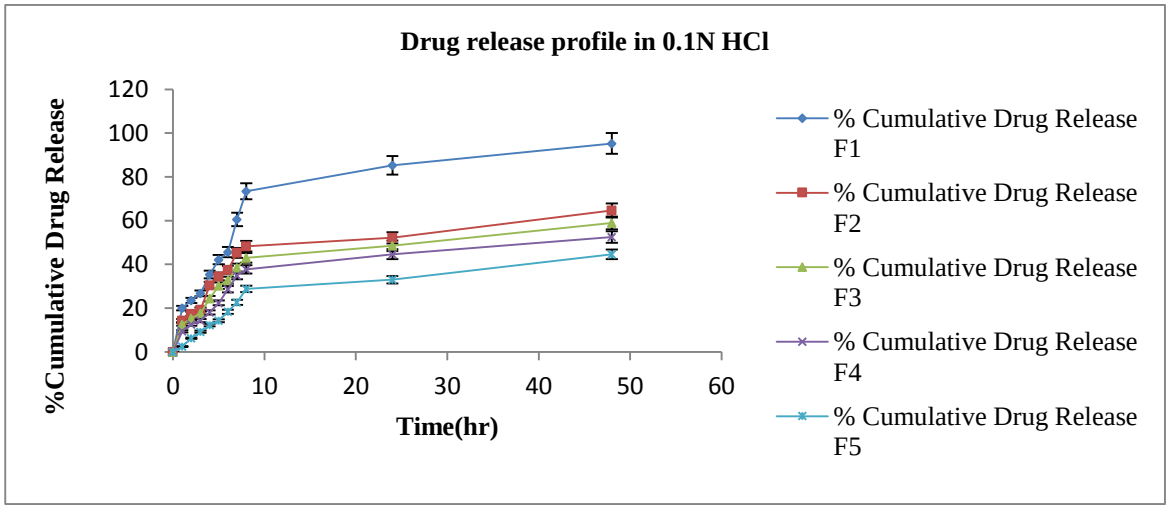

Fig 30: *In vitro* drug release profile for different formulations in 0.1N HCl

Table 18: *In vitro* drug release data for different formulations in Phosphate buffer pH 6.8

Time(hr)	% Cumulative Drug Release (%± SD)*				
	F1	F2	F3	F4	F5
0	0	0	0	0	0
1	40± 0.22	28.06± 0.24	25.8± 0.18	10.1± 0.62	5.08± 0.44
2	50.5± 0.09	44.25± 0.32	35.52± 0.32	18.48± 0.45	11.8± 0.54
3	56.73± 0.42	50.32± 0.14	48.7± 0.16	25.8± 0.54	22.64± 0.62
4	65.27± 0.52	60.85± 0.16	54.31± 0.18	30.05± 0.56	28.6± 0.42
5	72.06± 0.16	69.23± 0.24	60.21± 0.32	38.62± 0.64	34.54± 0.42
6	75.61± 0.28	71.4± 0.52	68.78± 0.44	44.48± 0.62	38.24± 0.46
7	80.62± 0.32	75.46± 0.22	71.75± 0.23	48.64± 0.58	45.36± 0.60
8	83.63± 0.42	78.28± 0.14	75.96± 0.17	56.28± 0.42	52.12± 0.54
24	85.44± 0.26	82.15± 0.26	78.48± 0.36	64.28± 0.44	60.26± 0.28
48	95.24± 0.38	94.6± 0.44	88.54± 0.54	82.1± 0.54	74.12± 0.28

SD = Standard deviation, *= Average of three determination

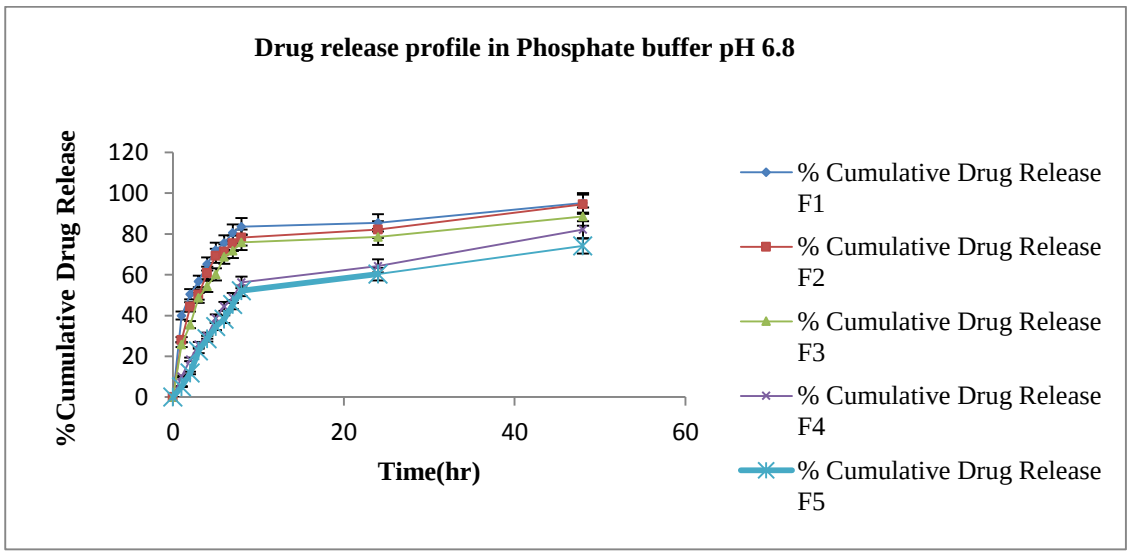

Fig 31: *In vitro* drug release profile for different formulations in Phosphate buffer pH 6.8

The percentage cumulative drug release of Atorvastatin calcium from prepared nanoparticulate formulations was sustained for longer duration as the amount of polymer is increased. It is clearly shown from Fig 30/Fig 31, that drug from the nanoparticleformulations were released in controlled manner which is due to the hydration ability of chitosan, which on coming in contact with dissolution media leads to the formation of gelatinous mass which act as retardant material for the drug to diffuse out. Thus a prolonged release of drug is attained. At the end of second day (48hrs), the percentage cumulative drug release from F1 was found to be95.04 and 95.24%, F2 showed 64.6 and 94.6%, F3 showed 58.94 and 88.54%, F4 showed 52.54 and 82.1%and F5 showed 44.62 and 74.12%in 0.1N HCl and Phosphate buffer pH 6.8 respectively. It was found that F5 formulation was able to sustain the drug release for more period of time compared to other prepared formulations and the drug release was found to be more in case of Phosphate buffer pH 6.8 compared to 0.1N HCl.

4.6.4.7. Selection of Optimised formulation:

Among the different Atorvastatin calcium nanoparticle formulations, the formulation F5 (drug-polymer ratio 1:5) was selected as optimised formulation, after considering its optimum mean particle size/ polydispersity index, better drug loading capacity, entrapment efficiency, optimum zeta potential and also drug release at sustained manner upto 48 hrs. Further studies were carried out on optimised formulation (F5), such asrelease kinetic study, stability study, surface morphology study, DSC study, FTIR study and *in vivo* pharmacokinetic study.

4.6.4.8. Release Kinetics:

The *in vitro* release data obtained from optimised formulation (F5) was fitted to various kinetic models. The release rate kinetic models are shown in Fig 32 to 39.

Table 19: Data for Release kinetic study of optimised formulation in 0.1N HCl

Time (hr)	Square root of time (hr)	Log time (hr)	% Cumulative Drug Release(Q_t) (%± SD)*	Log Q_t ± SD *	Log Q_o ± SD *
1	1	0	2.48± 0.33	0.394 ± 0.33	1.99 ± 0.33
2	1.4142	0.301	6.28± 0.45	0.797 ± 0.45	1.97 ± 0.45
3	1.732	0.4771	9.24± 0.56	0.965 ± 0.56	1.96 ± 0.56
4	2	0.602	12.26± 0.38	1.08 ± 0.38	1.94 ± 0.38
5	2.236	0.6989	14.24± 0.44	1.15 ± 0.44	1.93 ± 0.44
6	2.449	0.7781	18.34± 0.48	1.26 ± 0.48	1.91 ± 0.48
7	2.645	0.845	22.66± 0.26	1.35 ± 0.26	1.88 ± 0.26
8	2.828	0.903	28.82± 0.34	1.46 ± 0.34	1.85 ± 0.34
24	4.898	1.38	32.96± 0.46	1.51 ± 0.46	1.82 ± 0.46
48	6.928	1.681	44.62± 0.32	1.65 ± 0.32	1.74 ± 0.32

SD = Standard deviation, *= Average of three determination

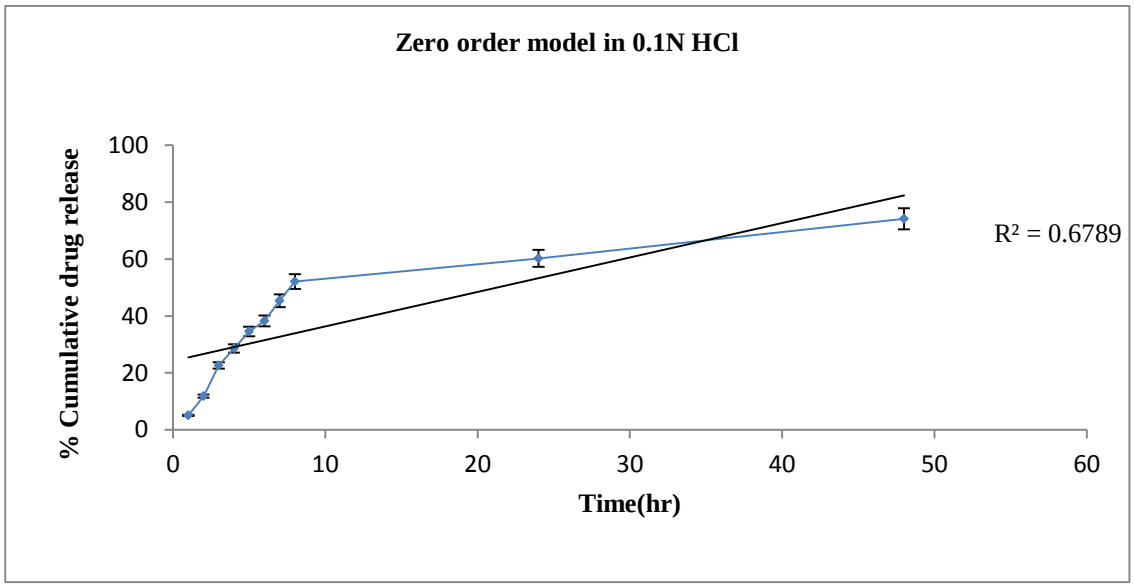

Fig 32: Zero order release kinetic study of optimised formulation in 0.1N HCl

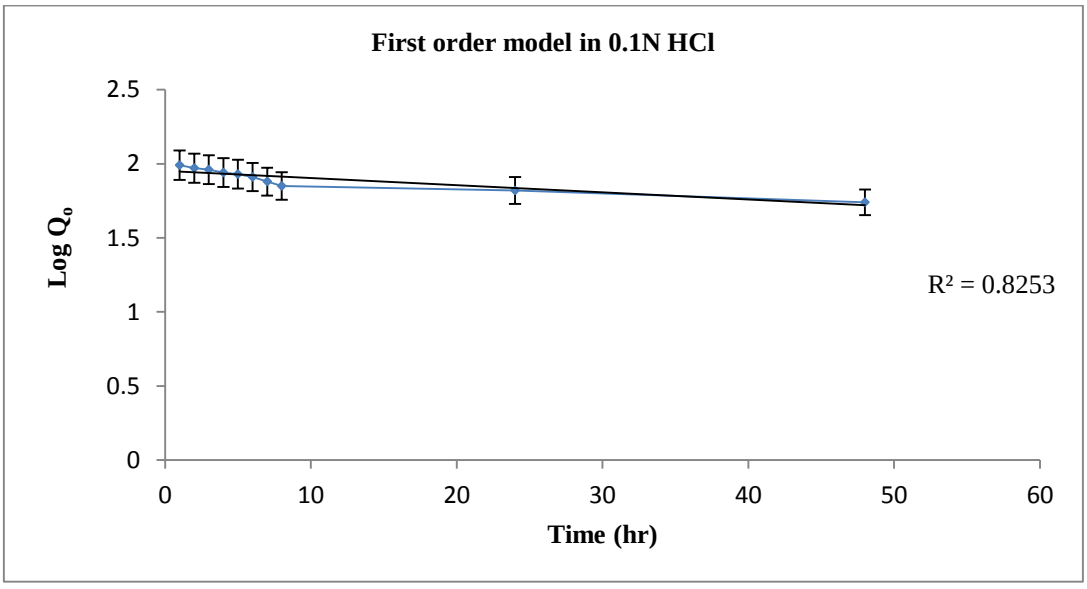

Fig 33: First order release kinetic study of optimised formulation in 0.1N HCl

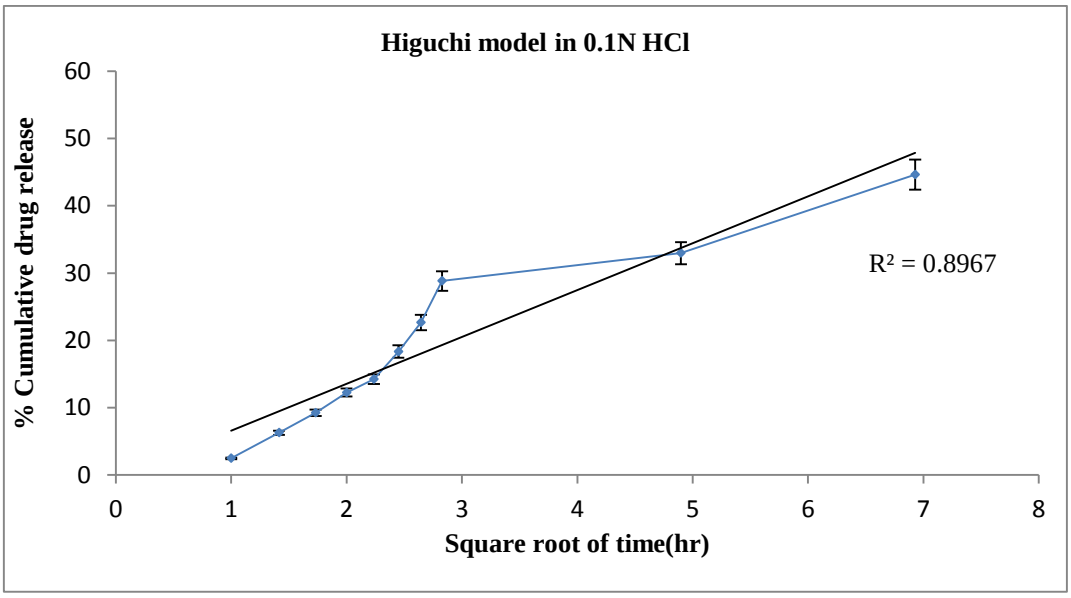

Fig 34: Higuchi release kinetic study of optimised formulation in 0.1N HCl

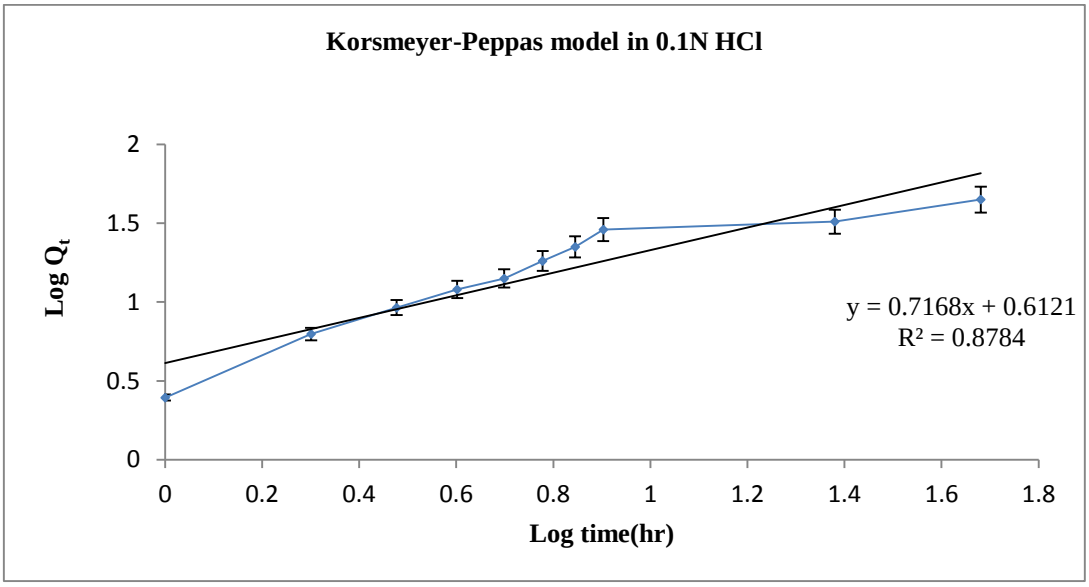

Fig 35: Korsmeyer-Peppas release kinetic study of optimised formulation in 0.1N HCl

Table 20: Data for Release kinetic study of optimised formulation in Phosphate buffer pH 6.8

Time (hr)	Square root of time (hr)	Log time (hr)	% Cumulative Drug Release(Q_t) (%± SD)*	Log Q_t ± SD *	Log Q_o ± SD *
1	1	0	5.08 ± 0.44	0.7058 ± 0.44	1.977 ± 0.44
2	1.4142	0.301	11.8 ± 0.54	1.071 ± 0.54	1.945 ± 0.54
3	1.732	0.4771	22.64 ± 0.62	1.354 ± 0.62	1.888 ± 0.62
4	2	0.602	28.6 ± 0.42	1.456 ± 0.42	1.853 ± 0.42
5	2.236	0.6989	34.54 ± 0.42	1.538 ± 0.42	1.815 ± 0.42
6	2.449	0.7781	38.24 ± 0.46	1.582 ± 0.46	1.790 ± 0.46
7	2.645	0.845	45.36 ± 0.60	1.656 ± 0.60	1.737 ± 0.60
8	2.828	0.903	52.12 ± 0.54	1.717 ± 0.54	1.680 ± 0.54
24	4.898	1.38	60.26 ± 0.28	1.780 ± 0.28	1.599 ± 0.28
48	6.928	1.681	74.12 ± 0.28	1.869 ± 0.28	1.412 ± 0.28

SD = Standard deviation, *= Average of three determination

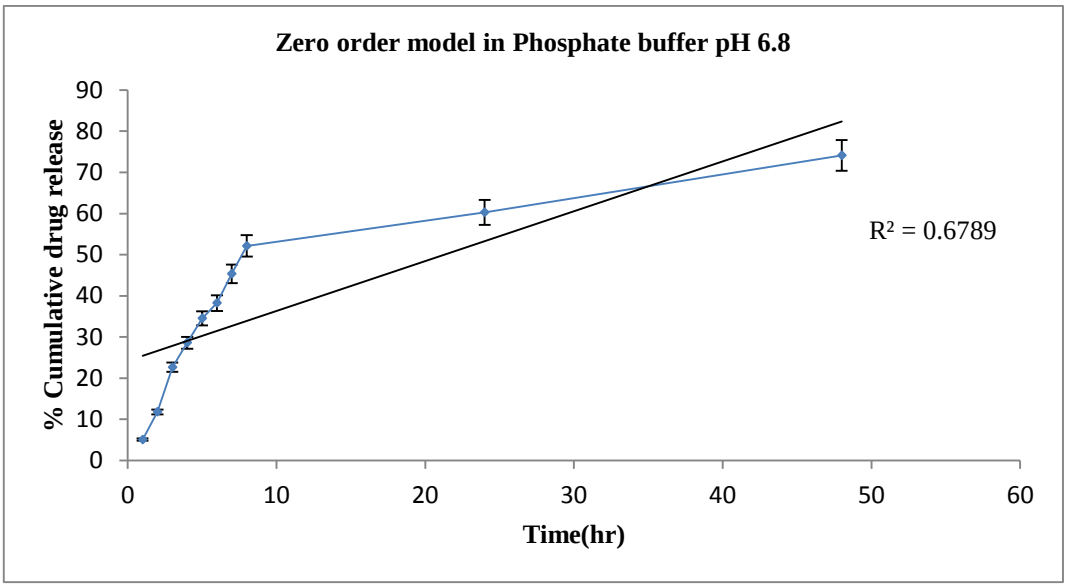

Fig 36: Zero order release kinetic study of optimised formulation in Phosphate buffer pH 6.8

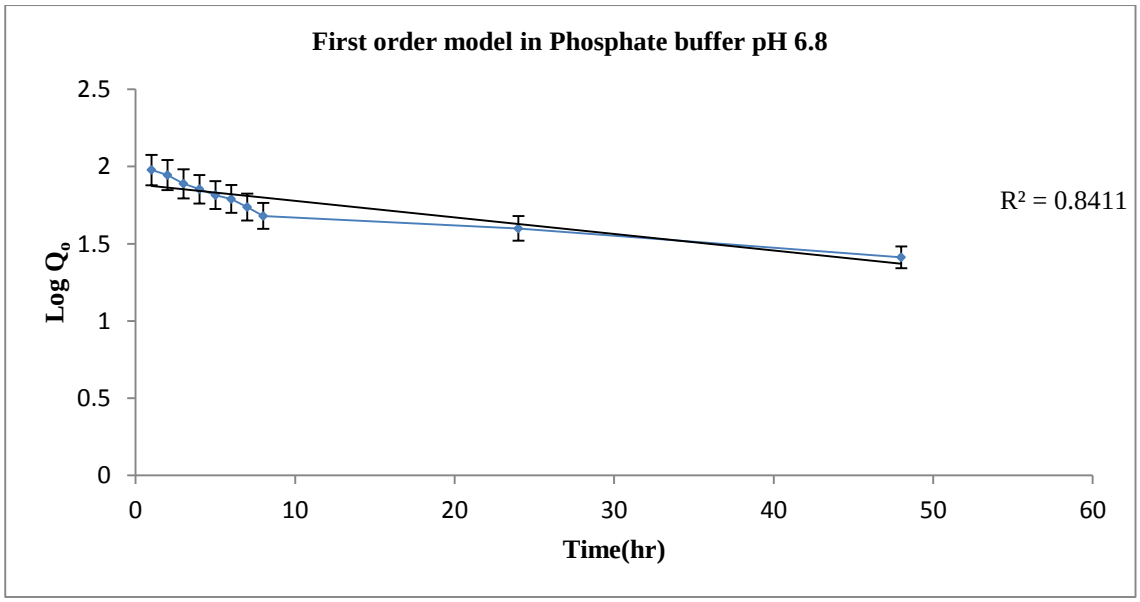

Fig 37: First order release kinetic study of optimised formulation in Phosphate buffer pH 6.8

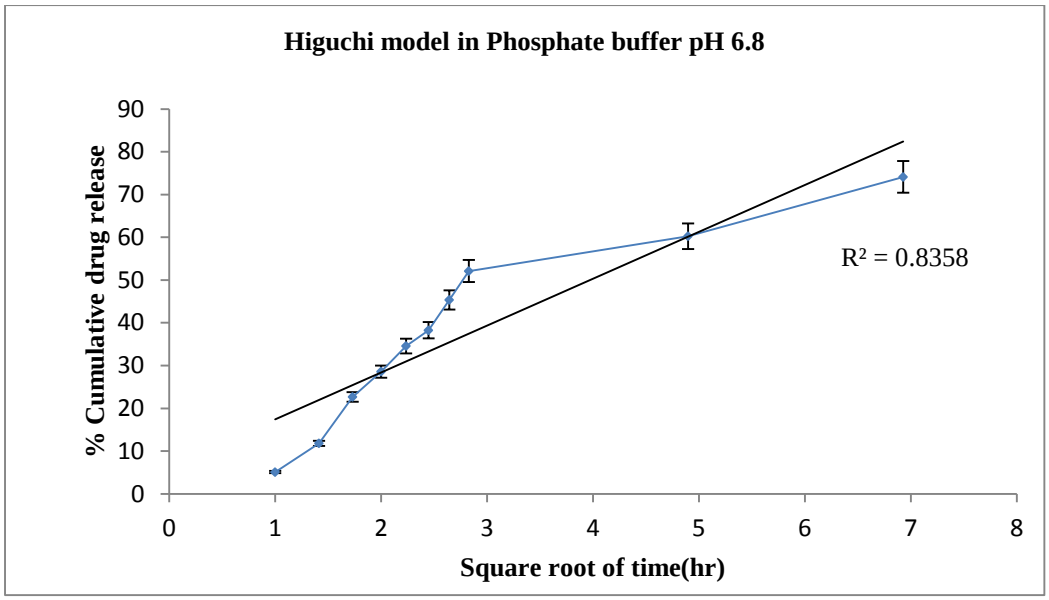

Fig 38: Higuchi release kinetic study of optimised formulation in Phosphate buffer pH 6.8

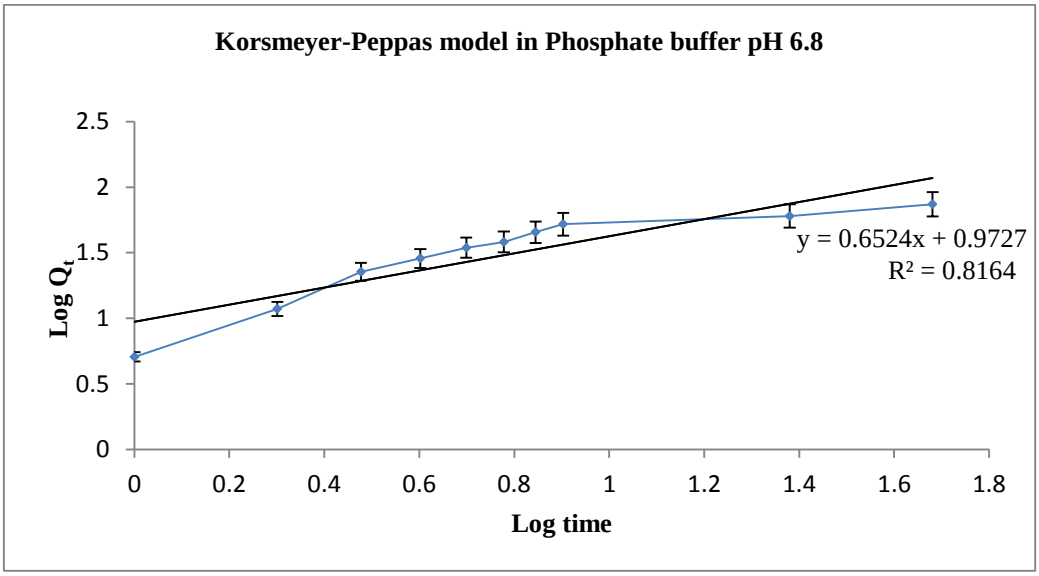

Fig 39: Korsmeyer-Peppas release kinetic study of optimised formulation in Phosphate buffer pH 6.8

The value of resulting regression coefficient for each model is calculated (Fig 32 to 39). The data was also fitted into Korsemeyer-Peppas model in order to obtain the 'n' value to describe the mechanism of drug release. The 'n' value of 0.7168 in 0.1N HCl and 0.6524in Phosphate buffer pH 6.8 indicates that the drug release follows anolamous (non-fickian) diffusion mechanism which signifies that the drug release is both diffusion-controlled and swelling-controlled. From these results, it can be revealed that the release of Atorvastatin calcium from the nanoparticles follows first order and diffusion and swelling mechanism in case of phosphate buffer pH 6.8 whereas it follows the Higuchi model and diffusion and swelling mechanism in case of 0.1 N HCl.

4.6.4.9. Stability study:

The Atorvastatin calcium nanoparticles of optimised formulation (F5) were subjected to stability analysis over a period of 3 months. The obtained results of drug loading in nanoparticles after 15, 30, 60 and 90 days of stability studies are tabulated in Table-21. Drug loading data of freshly prepared formulation stored at 5± 3^0C were considered as control and compared against sample.

Table 21: Data for Stability studyof Optimised formulation

Time(days)	Drug loading(%w/w ± SD)*		
	Control (5 ± 3^0C)	Sample (25 ± 2^0C/ 60% ± 5% RH)	Sample (40 ± 2^0C/ 75% ± 5% RH)
0	16 ± 0.72	16 ± 0.44	16 ± 0.54
15	15.85 ± 0.78	15.82 ± 0.48	15.78 ± 0.54
30	15.85 ± 0.92	15.76 ± 0.72	15.02 ± 0.62
60	15.8 ± 0.62	15.46 ± 0.64	14.92 ± 0.64
90	15.72 ± 0.62	15.06 ± 0.66	14.32 ± 0.72

SD = Standard deviation, *= Average of three determination

From the stability studies data it can be revealed that there was no effective changes in the Atorvastatin calcium content in the formulation stored at 25± 2^0C/ 60%± 5% RH at the end of 90 days. However, the samples kept at 40± 2^0C/ 75%± 5% RH, shows significant reduction in the amount of Atorvastatin calcium at the end of 90 days. This might be due to the degradation of both drug and polymer having a low glass transition temperature and low melting point.

4.6.4.10. Surface Morphology:

The shape and surface characteristics of nanoparticles of optimised formulation (F5) was visualized using SEM, Zeiss, Germany. The SEM results are shown in Fig 40 to 41.

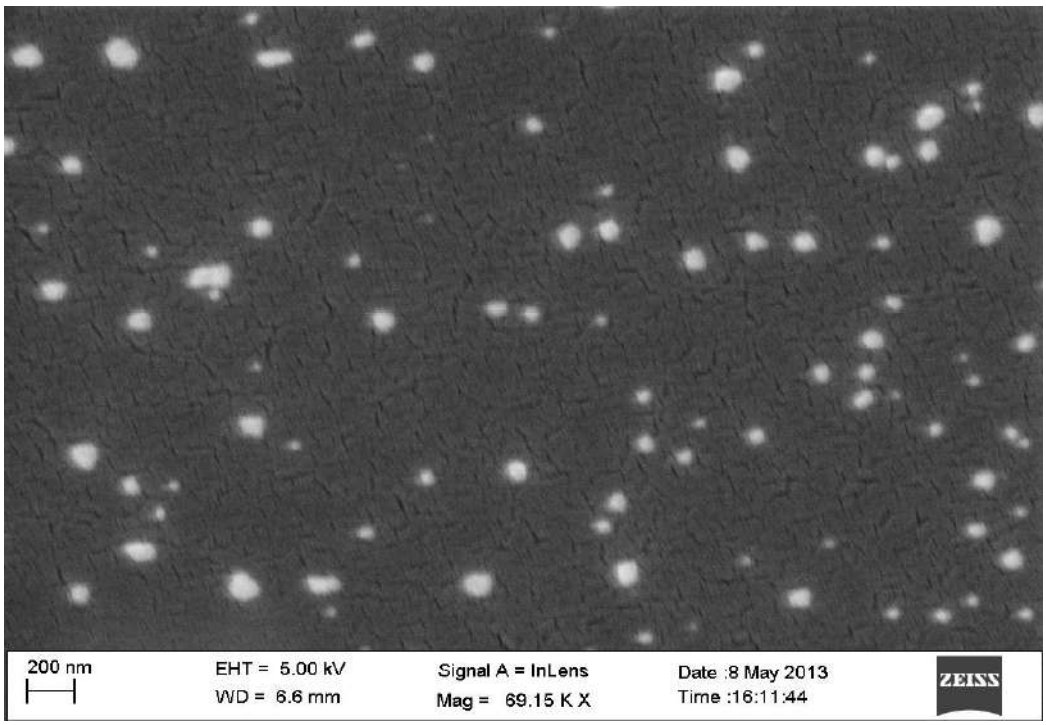

Fig 40: SEM image of optimised formulation

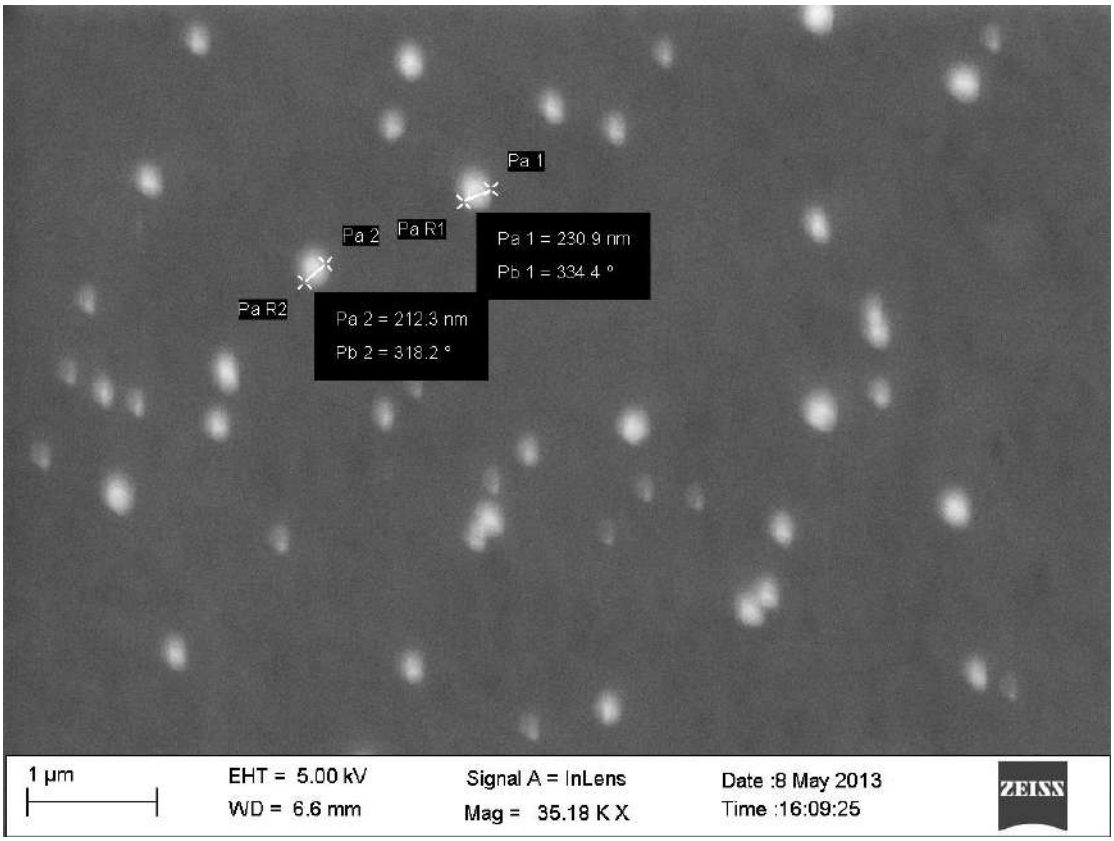

Fig 41: SEM image of optimised formulation

All particles were found to be spherical with a smooth surface and the particle size ranges varies from 212.3nm to 230.9nm (Fig 41). Magnification of a single particle showed the internal cage like structure where the drug molecules are dispersed uniformly throughout the polymer matrix (Fig 40). The drug appears as white spots on the surface. It was observed that when a high energy electron beam were passed to scan the particles in SEM, the polymer burns out leaving the drug particles viewed as a cage like structure.

4.6.4.11. DSC analysis:

The DSC analysis of nanoparticles of optimised formulation (F5) was done using the DSC instrument (Parkin Almer, U.S.A) for measurement of the heat loss or gain resulting from physical or chemical changes within a sample as a function of

temperature. The obtained DSC thermogram of nanoparticles was interpreted with the DSC thermogram of drug, polymer and physical mixture of drug and polymer. The DSC thermogram is shown in Fig 42.

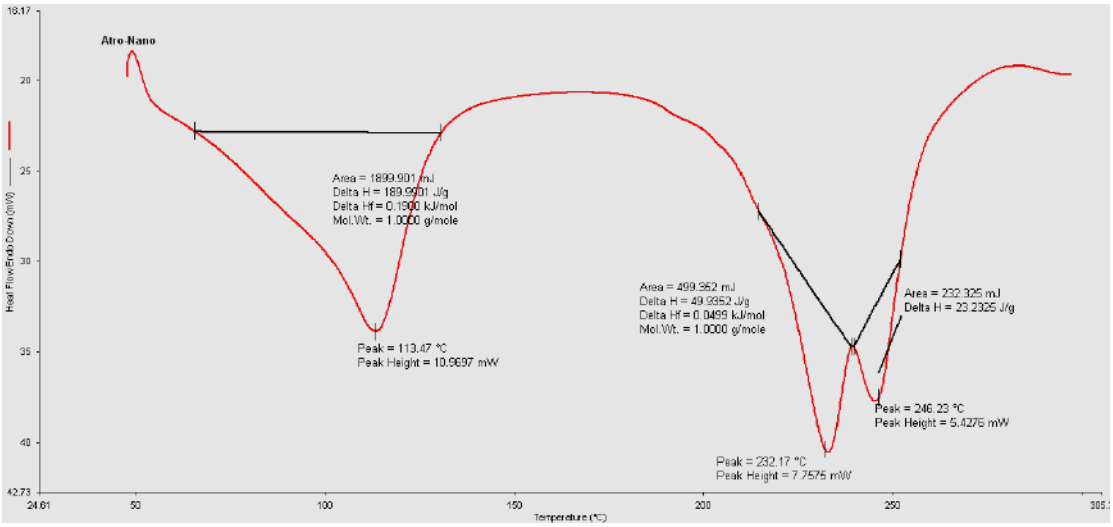

Fig 42: DSC thermogram of optimised formulation

The thermal behaviour of the freeze dried nanoparticles suggested that the polymer inhibited the melting of the drug crystals. The physical mixture of drug and chitosan showed a sharp endothermic peak at 165.88^{0}C and the physical mixture of drug and pluronic F68 showed a sharp endothermic peak at 124.08^{0}C, whereas thedrug showed a sharp endothermic peak at 163.3^{0}C. Freeze dried drug loaded nanoparticle showed a broad endothermic peak at 113.47^{0}C, which represents the effect of adsorbed pluronic F68 as surfactant onto the drug loaded nanoparticles. The slightly shifted sharp endothermic peak of nanoparticles that was observed at232.17^{0}C and at 246.23^{0}C represents that the polymer present in the sample inhibited the melting and crystallization of the drug present on the nanoparticle.

4.6.4.12. FTIR Analysis:

This was carried out to find out the drug polymer interaction in the nanoparticles of optimised formulation (F5).

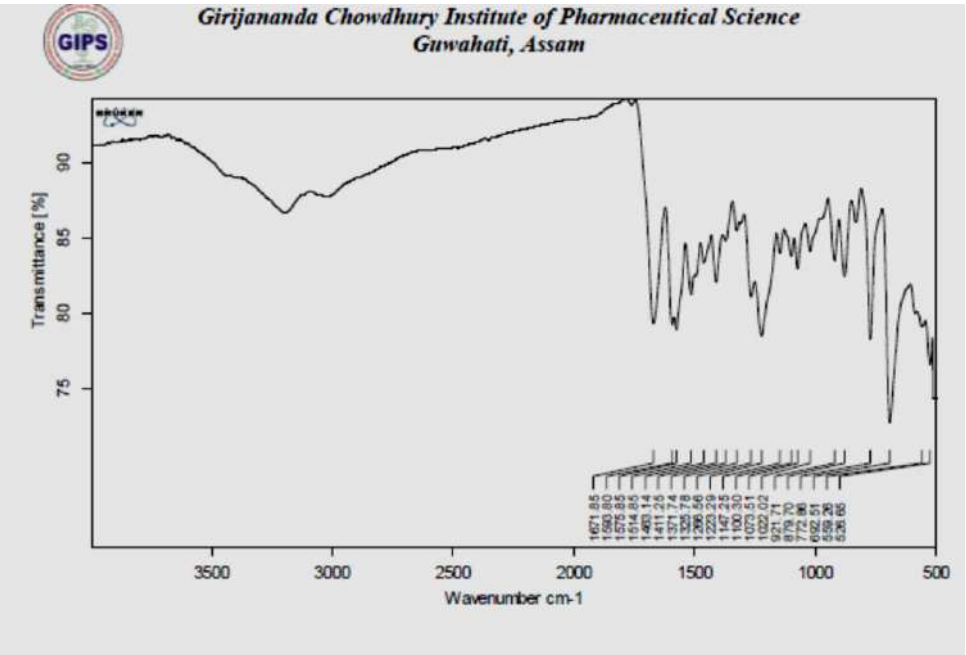

Fig 43: FTIR spectrum of optimised formulation

Pure Atorvastatin calcium has characteristic IR peaks at 3236 cm^{-1} (NH stretch), 1649 cm^{-1}(CO), 1578 cm^{-1} (CN). Chitosan spectrum showed 3295 cm^{-1} (NH stretch), 1649 cm^{-1} (CO), 1574 cm^{-1} (CN). Freeze dried solid sample of Atorvastatin calcium loaded nanoparticle exhibited mainly the Chitosan absorption peaks with few overlapping peaks from the Atorvastatin calcium. It can be concluded that no strong drug polymer interaction occurred inside the nanoparticles.

4.6.4.13. *In-vivo* Pharmacokinetic studies:

The *in vivo* pharmacokinetic study of nanoparticles of optimised formulation (F5) of Atorvastatin calcium was performed in rabbit and the presence of drug in plasma is

calculated with the help of HPLC. The HPLC spectrum and standard curve are presented in Fig 44 to 46 and the data for standard curve are presented in Table-22.

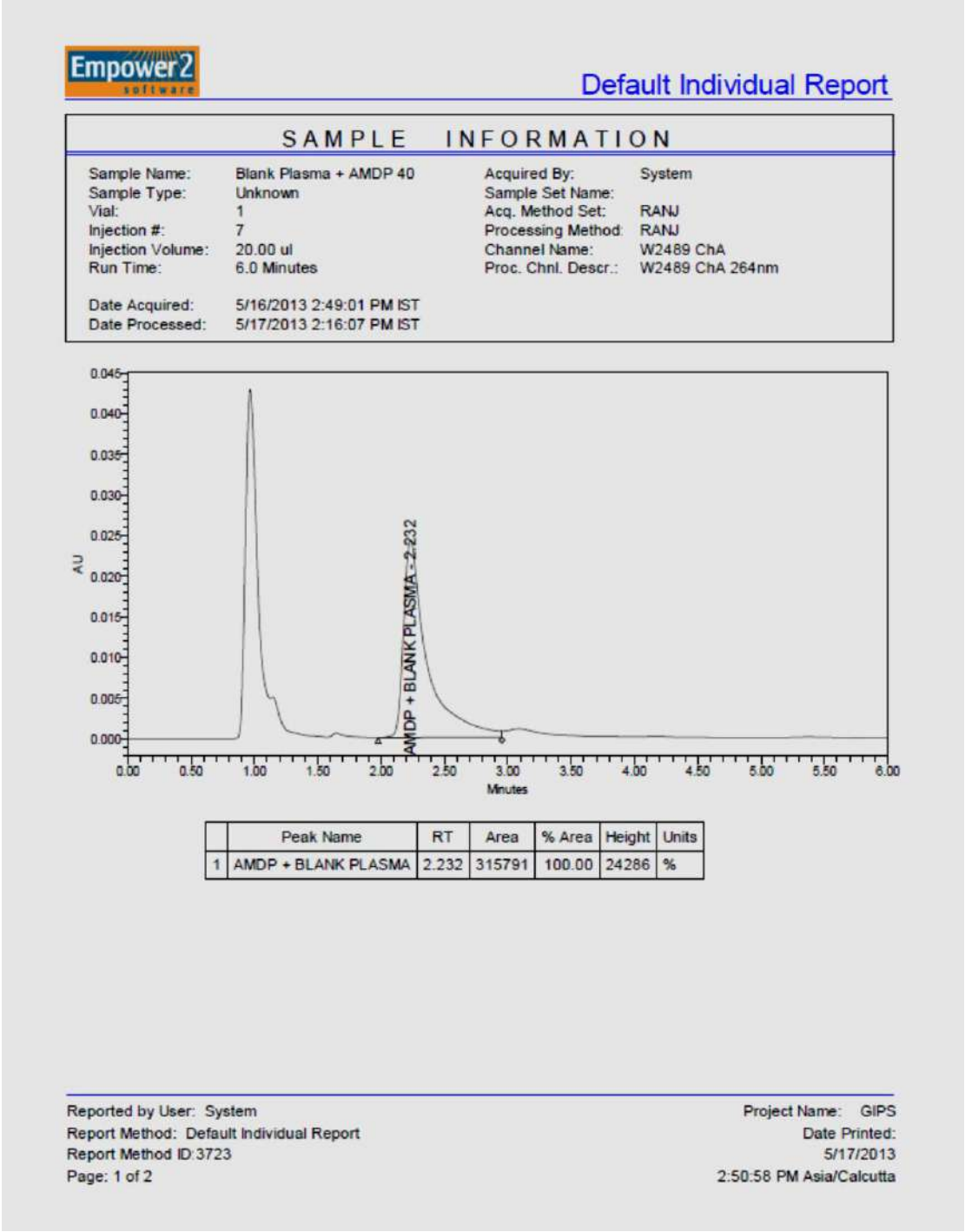

Fig 44: HPLC spectrum of blank plasma and Amlodipine bisylate (internal standard)

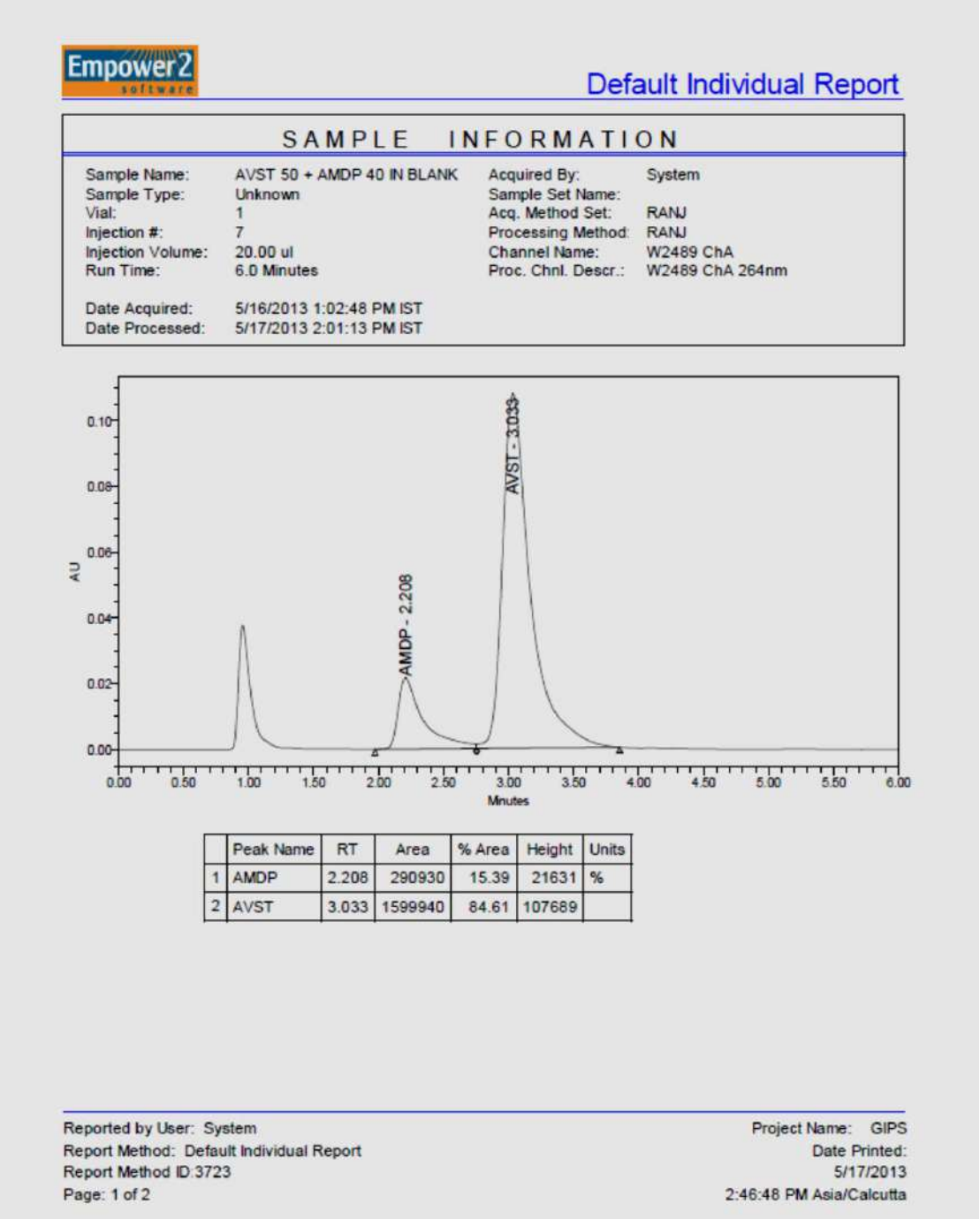

	Peak Name	RT	Area	% Area	Height	Units
1	AMDP	2.208	290930	15.39	21631	%
2	AVST	3.033	1599940	84.61	107689	

Fig 45: HPLC spectrum of blank plasma, Amlodipine bisylate (internal standard) and Atorvastatin calcium

Table 22: Data for standard curve of Atorvastatin calcium in blank plasma

Sl. No.	Concentration of Atorvastatin calcium (µg/ml)	Retention Time (min)	Peak Area
1.	10	3.086	339893
2.	20	3.064	634670
3.	30	3.043	911357
4.	40	3.040	1216861
5.	50	3.033	1599940

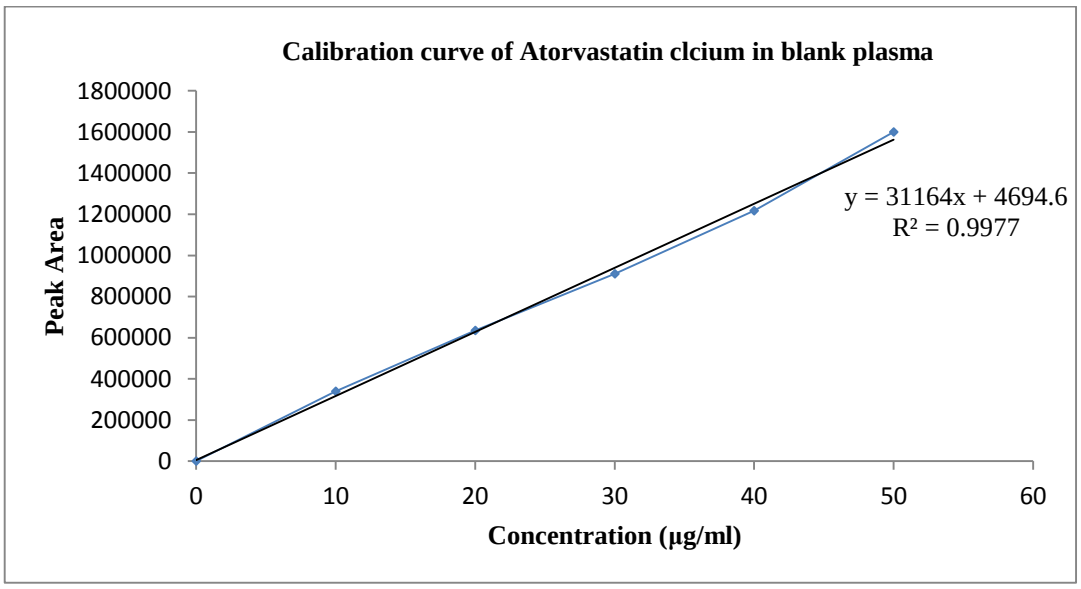

Fig 46: Calibration curve of Atorvastatin clcium in blank plasma

Method validation:

Linearity:

The prepared calibration curves are shown in Fig. 47 to 48.

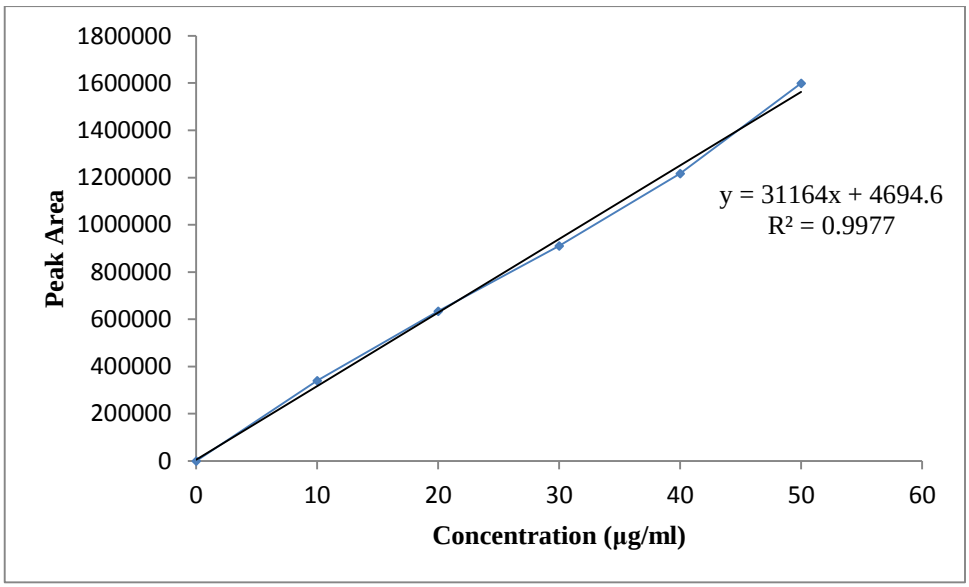

Fig 47: Calibration curve of Atorvastatin calcium at 264 nm by HPLC Method.

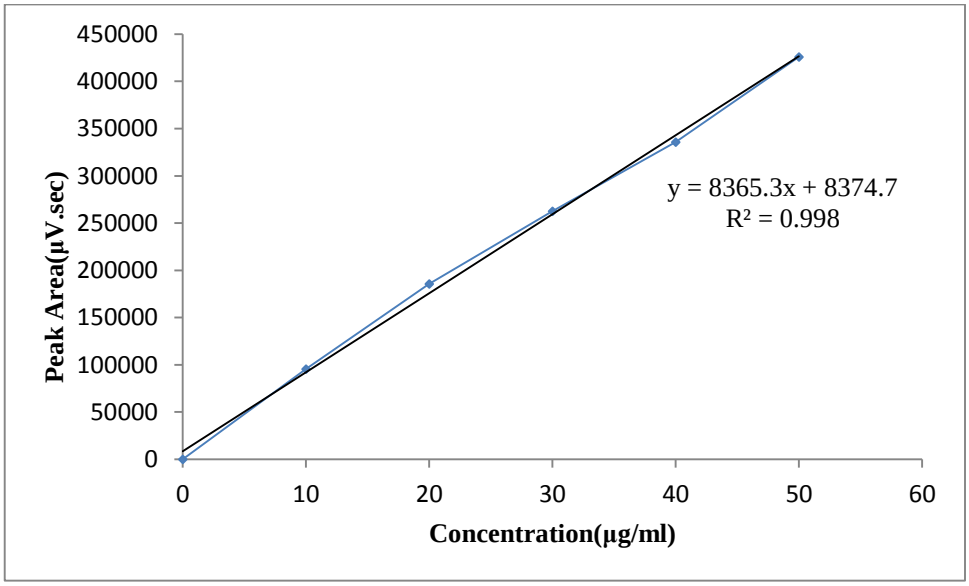

Fig 48: Calibration curve of Amlodipine bisylate at 264 nm by HPLC Method.

The constructed calibration curves were linear over the concentration range of 10-50 µg/ml for both Atorvastatin calcium and Amlodipine bisylate. Peak areas of Atorvastatin calcium and Amlodipine bisylate were plotted versus their respective concentrations and linear regression analysis was performed on the resultant curves. Correlation coefficients (n = 3) were found to be more than 0.99 for both the drugs. Typically, the regression equations were found to be: y = 31164 x + 4694.6 (R^2 = 0.9977) for Atorvastatin calcium and y = 8365.3x + 8374.7 (R^2 = 0.998) for Amlodipine bisylate respectively.

LOQ and LOD:

The LOQ and LOD was determined using the equations

$$\mathbf{LOQ = 10 \times N/B, \quad LOD = 3 \times N/B}$$

Where, N is the standard deviation of the peak areas (triplicate injections) of the drug, B is the slope of the corresponding calibration curve.

The limit of quantification (LOQ) and the limit of detection (LOD) of Atorvastatin calcium were found to be 0.058 µg/ml and 0.0017 µg/ml, and Amlodipine bisylate were0.023 µg/ml and 0.0071 µg/ml respectively.

Accuracy:

Accuracy of the method was determined by interpolation of peak areas of three replicate samples (n = 3) of stock solutions containing 20 µg/ml of Atorvastatin calcium and 10 µg/ml of Amlodipine bisylate, from the calibration curve that had been previously prepared. The accuracy data for the assay of each component of interest are summarized in Table-23.

Table 23: Statistical validation data for accuracy determination

Sl No.	Name of drug and concentration	Interpolated concentration (mean ± SD)*
1.	Atorvastatin calcium (20 µg/ml)	19.54 ± 0.0543
2.	Amlodipine bisylate (10 µg/ml)	9.88 ± 0.0688

SD = Standard deviation, *= Average of three determination

Precision:

The statistical validation data for intraday and interday precision are summarized in Table-24 to 25.

Table 24: Statistical validation data for determination of intraday precision

Sl No.	Name of drug and concentration	Interpolated concentration (mean ± SD) *
1.	Atorvastatin calcium (20 µg/ml)	19.54 ± 0.0543
2.	Amlodipine bisylate (10 µg/ml)	9.88 ± 0.0688

SD = Standard deviation, *= Average of three determination

Table 25: Statistical validation data for determination of interday precision

Sl No.	Name of drug and concentration	Interpolated concentration (mean ± SD) *
1.	Atorvastatin calcium (20 µg/ml)	19.48 ± 0.072
2.	Amlodipine bisylate (10 µg/ml)	9.83 ± 0.0435

SD = Standard deviation, *= Average of three determination

The method validation data represents that the constructed calibration curves were linear over the concentration range of 10-50 µg/ml for both Atorvastatin calcium and Amlodipine bisylate.Correlation coefficients (n = 3) were found to be more than 0.99 for both the drugs. The limit of quantification (LOQ) and the limit of detection (LOD) of Atorvastatin calcium were found to be 0.058 µg/ml and 0.0017 µg/ml, and Amlodipine bisylate were 0.023 µg/ml and 0.0071 µg/ml respectively. The accuracy data represents no significant changes in drug concentration and the precision data represents that there are no any significant changes in drug concentration during the intraday and interday precision study.

Therefore the developed method is selected as validated method for the determination of both the drug in formulation as well as in serum.

Evaluation of drug in the blood serum:

The presence of drug in plasma at different time interval are presented in Table-26 and plasma drug concentration vs time release profile are shown in Fig 49. The *in vivo* pharmacokinetic parameters are shown in Table-27.

Table 26: Data for presence of drug in plasma at different time interval

		Amount of drug in plasma (µg/ml± SD) *	
Sl. No.	**Sampling Time (hr)**	**Marketed formulation(Atorva®)**	**Nanoparticle Optimised formulation**
1.	0.5	40.3± 0.88	101.6± 0.92
2.	1	62.28± 0.68	138.8± 0.96
3.	2	103.3± 0.74	219.78± 0.94
4.	4	86.2± 0.68	168.24± 0.88
5.	8	54.32± 0.78	108.34± 0.76
6.	24	24.28± 0.98	64.38± 0.92

SD = Standard deviation, *= Average of three determination

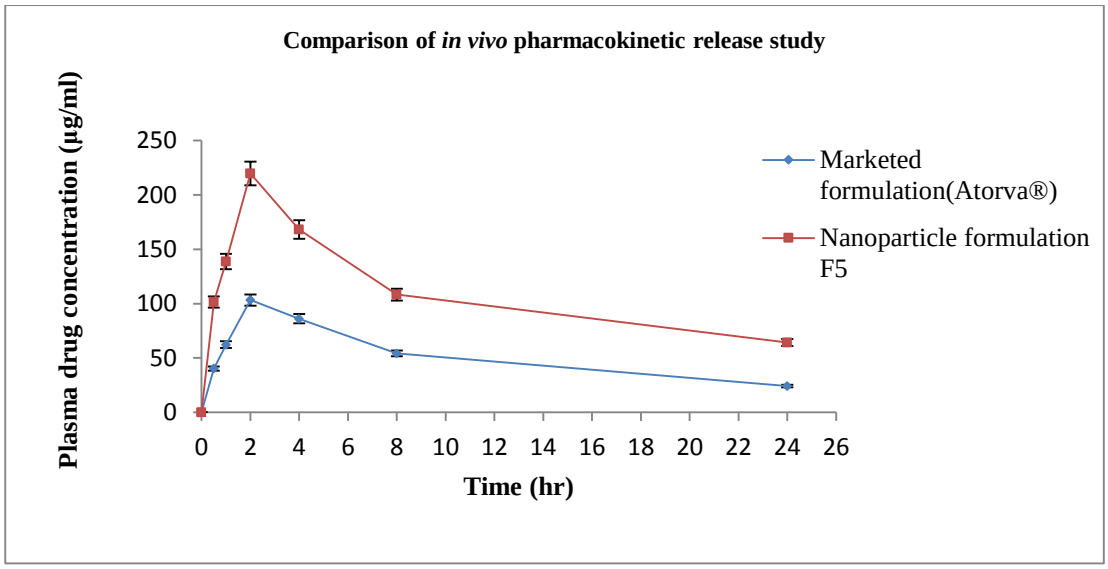

Fig 49: Plasma drug concentration vs Time release profile

Table 27: *In-vivo* pharmacokinetic parameters

Parameters	Units± SD *	Marketed formulation(Atorva®)	Nanoparticle Optimised formulation
C_{max}	µg/ml	103.3± 1.22	219.78± 2.54
T_{max}	Hrs	2± 0.24	2± 0.08
AUC_{0-t}	µg-hr/ml	1232.84± 2.66	2618.98± 2.98

SD = Standard deviation, *= Average of three determination

From the*In vivo* pharmacokinetic study, it can be revealed that the optimised nanoparticle formulation (F5) of Atorvastatin calcium shows better C_{max}, T_{max} and AUC than the marketed formulation(Atorva®) of drug. It was found that the C_{max} in serum for optimised nanoparticle formulation (219.78 µg/ml) represents greater improvement than the marketed formulations (103.3 µg/ml). It was also observed that AUC_{0-t} of optimised nanoparticle formulation was 2618.98 µg-hr/ml andthus the difference were highly significant ascompared to AUC_{0-t} of marketed tablet suspension (Table-27) formulation. The t_{max} of optimised nanoparticle formulation was found to be similarwhen compared to t_{max} of marketed tablet suspension. The difference inC_{max} of optimised nanoparticle formulation was very significant when compared with the marketed tablet suspesion. It was also observed that AUC_{0-t} of optimised nanoparticle formulation was2618.98 µg-hr/ml, thus the difference was very significant as compared to marketed tabletsuspensions.

Furthermore, this result attributed that the presence of surfactants in nanoparticle system might have caused changes in membrane permeability of the GI tract and the inhibition of an apically polarized efflux system, which could lead to enhancement of the oral absorption.

Chapter 5

Conclusion

5. CONCLUSION

Nanoparticulate drug delivery system is a promising approach for the formulation of Atorvastatin calcium nanoparticle. The oral delivery of hydrophobic drugs can be made possible by nanoparticulate drug delivery systems, which have been shown to improve oral bioavailability. Nanoparticulate will continue to enable novel applications in drug delivery and solve problems associated with the delivery of poorly soluble drugs.

From the studies the following can be drawn-

Atorvastatin calcium which was supplied for the study is a standard drug which was evaluated by IR spectroscopy as well as determining the melting point. The saturation solubility revealed that Atorvastatin calcium is more soluble in phosphate buffer, pH 6.8 than simulated gastric fluid, pH 1.2. The drug-excipients compatibility study revealed that drug is compatible with Chitosan and Pluronic F68 which was evaluated by IR spectroscopy and DSC.

Based upon the Preformulation studies, 5 different batches of nanoparticles of Atorvastatin calcium was prepared using the Solvent evaporation method. The prepared nanoparticles were evaluated in terms of % nanoparticle yield, % drug loading, % entrapment efficiency, particle size/ polydispersity index and *in vitro* drug release study. The nanoparticle yield was found to be in the range between 66.66% to 85.71% w/w, drug loading capacity was found to be in the range between 4% to 16%, entrapment efficiency was found to be in the range between 8% to 96%, particle size of Atorvastatin calcium nanoparticles was found to be in the range of 219.3nm to 820.8nm and the Polydispersity index of the nanoparticles was found to be in the range of 0.252 to 0.461. The zeta potential was found to be of positive values for all

the formulations (+ 13.03 mV to + 46.9mV). The relative constancy of zeta potential indicates Atorvastatin calcium was encapsulated within the nanoparticles and a major part of the drug is not present on the nanoparticle surface. At the end of second day (48hrs), the percentage cumulative drug release from F1 was found to be 95.04 and 95.24%, F2 showed 64.6 and 94.6%, F3 showed 58.94 and 88.54%, F4 showed 52.54 and 82.1% and F5 showed 44.62 and 74.12% in 0.1N HCl and Phosphate buffer pH 6.8 respectively. It was found that F5 formulation was able to sustain the drug release for more period of time compared to other prepared formulations and the drug release was found to be more in case of Phosphate buffer pH 6.8 compared to 0.1N HCl.

Among the different Atorvastatin calcium nanoparticle formulations, the formulation F5 (drug-polymer ratio 1:5) was selected as optimised formulation, after considering its optimum mean particle size/ polydispersity index, better drug loading capacity, entrapment efficiency, optimum zeta potential and also drug release at sustained manner upto 48 hrs. Further studies were carried out on optimised formulation (F5), such as release kinetic study, stability study, surface morphology study, DSC study, FTIR study and *in vivo* pharmacokinetic study.

Drug release kinetic studies of optimised formulation show anolamous (non-fickian) diffusion mechanism which signifies that the drug release is both diffusion-controlled and swelling-controlled. Stability studies indicates that there was no effective changes in the Atorvastatin calcium content in the formulation stored at 25 ± 2^0C/ 60% ± 5% RH at the end of 90 days. SEM studies indicate that particles were spherical in shape with a smooth surface and the particle size range was found to be 212.3nm to 230.9nm. DSC study indicates absence of Atorvastatin calcium peaks in the nanoparticle formulation, which indicates that the drug may be dispersed in the form

of amorphous state. FTIR results indicates that freeze dried solid sample of Atorvastatin calcium loaded nanoparticle exhibited mainly the Chitosan absorption peaks with few overlapping peaks from the Atorvastatin calcium which reveals that no strong drug polymer interaction occurred inside the nanoparticles. *In vivo* pharmacokinetic study, revealed that the optimised formulation shows better C_{max}, t_{max} and AUC than the marketed formulation (Atorva®) of drug.

From the study, it is concluded that Atorvastatin calcium loaded chitosan nanoparticles is an effective formulation for the oral drug delivery as it produces sustaining action to increase bioavailability as well as the nano size of the drug promotes the bioavailability which is evaluated through *in vivo* study in rabbit.

Chapter 6

References

6. REFERENCES

1. Yellela SRK., Pharmaceutical Technologies for enhancing oral bioavailability of poorly soluble drugs; Journal of Bioequivalence and Bioavailability, Vol. 2(2), 1-9.

2. Bhadra D, Bhadra S, Jain P, Jain NK., Pegnology: a review of PEG-ylated systems; Pharmazie, 2002; 57: 5-29.

3. Kommareddy S., Tiwari SB., Amiji MM., Long-circulating polymeric nanovectors for tumor-selective gene delivery; Technology in Cancer Research and Treatment, 2005; 4: 615-625.

4. Lee M., Kim SW., Polyethylene glycol-conjugated copolymers for plasmid DNA delivery; Pharmaceutical Research, 2005; 22: 1-10.

5. Vila A., Sanchez A., Tobio M., Calvo P., Alonso MJ., Design of biodegradable particles for protein delivery; Journal of Control Release, 2002; 78: 15-24.

6. Mu L., Feng SS., A novel controlled release formulation for the anticancer drug paclitaxel (Taxol(R)): PLGA nanoparticles containing vitamin E TPGS; Journal of Control Release, 2003; 86: 33-48.

7. Kreuter J., Nanoparticles in Colloidal drug delivery systems, 1994; 219-342.

8. Reverchon E., Adami R., Nanomaterials and supercritical fluids; The Journal of Supercritical Fluids, 2006; 37: 1-22.

9. Kompella UB., Bandi N., Ayalasomayajula SP., Poly (lactic acid) nanoparticles for sustained release of budesonide; Drug Delivery Technology, 2001; 1: 1-7.

10. Ravi MN., Bakowsky U., Lehr CM., Preparation and characterization of cationic PLGA nanospheres as DNA carriers; Biomaterials, 2004; 25: 1771-1777.

11. Li YP., Pei YY., Zhou ZH., Zhang XY., Gu ZH., Ding J., Zhou JJ., Gao XJ., PEGylated polycyanoacrylate nanoparticles as tumor necrosis factor-[alpha] carriers; Journal of Control Release, 2001; 71: 287-296.

12. Zambaux M., Bonneaux F., Gref R., Maincent P., Dellacherie E., Alonso M., Labrude P., Vigneron C., Influence of experimental parameters on the characteristics of poly(lactic acid) nanoparticles prepared by double emulsion method; Journal of Control Release, 1998; 50: 31-40.

13. Niwa T., Takeuchi H., Hino T., Kunou N., Kawashima Y., Preparation of biodegradable nanoparticles of water-soluble and insoluble drugs with D,L lactide/ glycolide copolymer by a novel spontaneous emulsification solvent diffusion method and the drug release behaviour; Journal of Control Release, 1993; 25: 89-98.

14. Boudad H., Legrand P., Lebas G., Cheron M., Duchene D., Ponchel G., Combined hydroxypropyl-[beta]- cyclodextrin and poly(alkylcyanoacrylate) nanoparticles intended for oral administration of saquinavir; International Journal of Pharmaceutics, 2001; 218: 113-124.

15. Calvo P., Remunan-Lopez C., Vila-Jato JL., Alonso MJ., Novel hydrophilic chitosan-polyethylene oxide nanoparticles as protein carriers; Journal of Applied Polymer Science, 1997; 63: 125-132.

16. Sun Y., Mezian M., Pathak P., Qu L., Polymeric nanoparticles from rapid expansion of supercritical fluid solution; Chemistry 2005; 11: 1366-1373.

17. Desai MP., Labhasetwar V., Walter E., Levy RJ., Amidon GL., The mechanism of uptake of biodegradable microparticles in Caco-2 cells is size dependent; Pharmaceutical Research, 1997; 14:1568- 1573.

18. Zauner W., Farrow NA., Haines AM., In vitro uptake of polystyrene microspheres: effect of particle size, cell line and cell density; Journal of Control Release, 2001; 71: 39-51.

19. Redhead HM., Davis SS., Illum L., Drug delivery in poly(lactide-co-glycolide) nanoparticles surface modified with poloxamer 407 and poloxamine 908; Journal of Control Release , 2001;70(3):353-363.

20. Panyam J., Dali MM., Sahoo SK., Ma W., Chakravarthi SS., Amidon GL., Levy RJ., Labhasetwar V., Polymer degradation and in vitro release of a model protein from (poly-lactide-co-glycolide) nano and microparticles; Journal of Control Release, 2003; 92: 173-187.

21. Muller RH., Wallis KH., Surface modification of i.v. injectable biodegradable nanoparticles with poloxamer polymers and poloxamine 908; International Journal of Pharmaceutics, 1993; 89: 25-31.

22. Grislain L., Couvreur P., Lenaerts V., Roland M., Deprez-Decampeneere D., Speiser P., Pharmacokinetics and distribution of a biodegradable drug-carrier; International Journal of Pharmaceutics, 1983; 15: 335-345.

23. Olivier JC., Drug transport to brain with targeted nanoparticles; NeuroRx, 2005; 2: 108-119.

24. Couvreur P., Barratt G., Fattal E., Legrand P., Vauthier C., Nanocapsule technology: a review; Critical Reviews in Therapeutic Drug Carrier Systems, 2002; 19: 99-134.

25. Chen Y., Mohanraj VJ., Parkin JE., Chitosan-dextran sulfate nanoparticles for delivery of an antiangiogenesis peptide; Letters in Peptide Science, 2003; 10: 621-627.

26. Magenheim B., Levy MY., Benita S., A new *in vitro* technique for the evaluation of drug release profile from colloidal carriers - ultrafiltration technique at low pressure; International Journal of Pharmceutics, 1993; 94: 115-123.

27. Verdun C., Brasseur F., Vranckx H., Couvreur P., Roland M., Tissue distribution of doxorubicin associated with polyhexylcyanoacrylate nanoparticles; Cancer Chemotherapy and Pharmacology, 1990; 26: 13-18.

28. Couvreur P., Kante B., Lenaerts V., Scailteur V., Roland M., Speiser P., Tissue distribution of antitumor drugs associated with polyalkylcyanoacrylate nanoparticles; Journal of Pharmceutical Science, 1980; 69: 199-202.

29. Bibby DC., Talmadge JE., Dalal MK., Kurz SG., Chytil KM., Barry SE., Shand DG., Steiert M., Pharmacokinetics and biodistribution of RGD-targeted doxorubicin loaded nanoparticles in tumor-bearing mice; International Journal of Pharmceutics, 2005; 293: 281-290.

30. Chiannilkulchai N., Ammoury N., Caillou B., Devissaguet JP., Couvreur P., Hepatic tissue distribution of doxorubicin-loaded nanoparticles after i.v. administration in reticulosarcoma M 5076 metastasis-bearing mice; Cancer Chemotherapy and Pharmacology, 1990; 26: 122-126.

31. Moghimi SM., Hunter AC., Murray JC., Long-circulating and target-specific nanoparticles: theory to practice; Pharmacological Review, 2001; 53: 283-318.

32. Torchilin V., Trubetskoy V., Which polymer can make nanoparticulate drug carriers long circulating? ; Advanced Drug Delivery Review, 1995; 16: 141-155.

33. Bennis S., Chapey C., Couvreur P., Robert J., Enhanced cytotoxicity of doxorubicin encapsulated in polyisohexylcyanoacrylate nanospheres against multidrug-resistant tumour cells in culture; European Journal of Cancer, 1994; 30A: 89-93.

34. Damge C., Michel C., Aprahamian M., Couvreur P.,Devissaguet JP., Nanocapsules as carriers for oral peptide delivery; Journal of Control Release, 1990; 13: 233-239.

35. Hussain N., Jani PU., Florence AT., Enhanced oral uptake of tomato lectin-conjugated nanoparticles in the rat; Pharmceutical Research, 1997; 14: 613-618.

36. Russell-Jones GJ., Arthur L., Walker H., Vitamin B12- mediated transport of nanoparticles across Caco-2 cells; International Journal of Pharmceutics, 1999; 179: 247-255.

37. Jani P., Halbert GW., Langridge J., Florence AT., The uptake and translocation of latex nanospheres and microspheres after oral administration to rats; Journal of Pharmacy and Pharmacology, 1989; 41: 809-812.

38. Panyam J., Zhou WZ., Prabha S., Sahoo SK., Labhasetwar V., Rapid endo-lysosomal escape of poly(DL-lactide-co-glycolide) nanoparticles: implications for drug and gene delivery; Faseb Journal, 2002; 16: 1217-1226.

39. Hedley M., Curley J., Urban R., Microspheres containing plasmid-encoded antigens elicit cytotoxic T-cell responses; Nature Medicine, 1998; 4: 365-368.

40. Chen Y., Dalwadi G., Benson H., Drug delivery across the blood-brain barrier; Current Drug Delivery, 2004; 1: 361-376.

41. Kreuter J. Influence of the surface properties on nanoparticle-mediated transport of drugs to the brain; Journal of Nanoscience and Nanotechnology, 2004; 4: 484-488.

42. Amidon GL., Lennernas H., Shah VP., A theoretical basis for a biopharmaceutical classification system: The correlation of *in vitro* drug product dissolution and *in vivo* bioavailability; Pharmaceutical Research, 1995; 12: 413-420.

43. Hussain N., Jaitely B., Florence AT., Recent advances in understanding the uptake of microparticulates across the gastrointestinal lymphatics; Advanced Drug Delivery Review, 2001; 50:107.

44. Tripathi VD., Hypolipidaemic Drugs; Text Book of General Pharmacology, 2009; Chapter 45, 612-623.

45. Stancu C., Sima A., Statins: mechanism of action and effects; Journal of cellular and Molecular Medicine, 2001; 4:378-387.

46. Suganeswari M., Shering A., Azhagesh K., Bharathi P., Sathish B., Preparation, Characterization And Evaluation Of Nanoparticles Containing Hypolipidemic Drug And Antihypertensive Drug; International Journal of Pharmaceutical & Biological Archives, 2011; 2(3):949-953.

47. Arunkumar N., Deecaraman M., Rani C., Mohanraj KP., Kumar V., Preparation and solid state characterization of atorvastatin nanosuspensions for enhanced solubility and dissolution, International Journal of Pharmaceutical Technology and Research, 2009; 1(4), 1717-1725.

48. Ramani V., Chauhan S., Joshi J., Ghelani T., Deshmukh G., Seth AK., Patel J., Philips M., Gupta R., Formulation and Evaluation of nanoparticles of HMG -CoA reductase inhibitor; Pharma Science Monitor, 2011; Vol-2 (4), 42-58.

49. Muhammed Rafeeq PE., Junise V., Saraswathi R., krishnan PN., Dilip C., Development and characterization of chitosan nanoparticles loaded with isoniazid for the treatment of Tuberculosis; Research Journal of Pharmaceutical, Biological and Chemical Sciences, 2010; 1(4), 383-390.

50. Bathool A., Vishakante GD., Khan MS., Shivakumar HG., Development and characterization of atorvastatin calcium loaded chitosan nanoparticles for sustain drug delivery; Advanced Material Letters, 2012; **3**(6), 466-470

51. Fonseca C., Simoes S., Gaspar R., Paclitaxel-loaded PLGA nanoparticles: preparation, physicochemical characterization and *in vitro* anti-tumoral activity; Journal of Controlled Release, 2002; 83: 273–286.

52. Anilkumar J., Shinde N., Harinath NM., Formulation and optimization of biodegradable polylactic-coglycolic acid nanoparticles of simvastatin using factorial design; Pelagia Research Library, Der Pharmacia Sinica, 2011; 2 (5):198-209.

53. Kim JH., Kim YS., Park K., Lee S., Nam HY., Min KH., Jo HG., Park JH., Choi K., Jeong SY., Park RW., Kim IS., Kim K., Kwon IC., Antitumor efficacy of cisplatin-loaded glycol chitosan nanoparticles in tumor-bearing mice; Journal of Controlled Release, 2008; 127: 41-49.

54. Sarma M., Formulation and development of solid lipid nanoparticles of Atorvastatin calcium; 2nd international conference and exhibition on pharmaceutical regulatory affairs, 2012.

55. Hecq J., Deleers M., Fanara D., Vranku H., Amighi K., Preparation and characterisation of nanocrystals for solubility and dissolution rate enhancement of nifedipine; International journal of pharmaceutics, 2005;167-177.

56. Dustgania A., Farahania EV., Imanib M., Preparation of Chitosan Nanoparticles Loaded by Dexamethasone Sodium Phosphate; Iranian Journal of Pharmaceutical Sciences, 2008; 111-114.

57. Debnath S., Datta D., Babu MN., Kumar RS., Senthil V., Studies on the preparation and Evaluation of chitosan nanoparticles containing cytarabine; International Journal of Pharmaceutical Science and Nanotechnology,2010; 3: 957-964.

58. Shitara Y., Sugiyama Y., Pharmacokinetic and pharmacodynamic alterations of 3-hydroxy-3-methylglutaryl coenzyme A (HMG-CoA) reductase inhibitors: drug–drug interactions and inter individual differences in transporter and metabolic enzyme functions; Pharmacology and Therapeutics, 2001; 112:71–105.

59. Hermann M., Bogsrud MP., Molden E., Asberg A., Mohebi BU., Ose L., Retterstøl K., Exposure of atorvastatin is unchanged but lactone and acid metabolites are increased several-fold in patients with atorvastatin-induced myopathy; Clinical Pharmacology and Therapeutics, 2006; 4: 532–539.

60. Williams D., Feely J., Pharmacokinetic-pharmacodynamic drug interactions with HMG-CoA reductase inhibitors; Clinical Pharmacokinetics, 2002; 41 (5): 343–370.

61. Lipitor: Prescribing Information, Pfizer. June 2009.

62. Ghirlanda G., Oradei A., Manto A., Lippa S., Uccioli L., Caputo S., Greco AV., Littarru GP., Evidence of plasma CoQ10-lowering effect by HMG-CoA reductase inhibitors: a double-blind, placebo-controlled study; Journal of Clinical Pharmacology, 1993; 33 (3): 226–229.

63. Kane GC., Lipsky JJ., Drug-grapefruit juice interactions; Mayo Clinic Proceedings, 1993; 75 (9): 933–942.

64. Rowe RC., Sheskey PJ., Quinn ME., Handbook of Pharmaceutical excipients; Pharmaceutical Press, 2009; 6: 159-161.

65. Stylianos S., Alan B. L., "Acetone" in Ullmann's Encyclopedia of Industrial Chemistry, Wiley-VCH, Weinheim, 2005.

66. Backup Data Report for Acetic Acid, prepared under NIOSH Contract No. 210-76-0123, available as "Ten NIOSH Analytical Methods," Order No. PB 275-834 from NTIS, Springfield, VA 22161.

67. Rowc RC., Paul JS., Owen SC., Book of Pharmaceutical Excipients,1998; 44-53,726-731,1417-1427,1446-1463.

68. Pluronic F68 Block copolymer surfactant. www. Performance. BASF-Corp.com.

69. Purified water. www. Wikepedia.com.

70. Prajapati KP., Bhandari A., Spectroscopic Method For Estimation of Atorvastatin Calcium in Tablet Dosage Form; Indo Global Journal of Pharmaceutical Sciences, 2011; 1(4): 294-299.

71. Arunkumar N., Deecaraman M., Rani C., Nanosuspension technology and its applications in drug delivery; Asian Journal of Pharmaceutics, 2009; 3: 168-173.

72. Dorothée SC., Dalton CR., Hancock BC., Differential scanning calorimetry:applications in drug development; Journal of Placental site trophoblastic tumor,1999; 2: 311-320.

73. Nagavarma BVN., Yadav HKS., Ayaz A., Vasudha LS., Shivakumar HG., Different techniques for preparation of polymeric nanoparticles- a review; Asian Journal of Pharmaceutical and Clinical Research, 2012; 5 (3): 16-23.

74. Wilson B., Samanta MK., Santhi K., Kumar KPS., Paramakrishnan N., Suresh B. Targeted delivery of tacrine into the brain with polysorbate 80 coated poly (n-butylcyanoacrylate) nanoparticles; European Journal of Biopharmaceutics, 2008; 70: 75-84.

75. Zhu Z., Li Y., Li X., Li R., Jia Z., Liu B., Paclitaxel loaded poly (n-vinylpyrrolidone)-b-poly (ε-caprolactone) nanoparticles: Preparation and antitumor activity *in vivo*; Journal of Control Release, 2010; 142: 438-446.

76. Kumar PV., Jain NK., Suppression of agglomeration of Ciprofloxacin-loaded human serum albumin nanoparticles; American Association of Pharmaceutical Scientist Pharmascience and Technology, 2007; 8(1): E_1-E_2.

77. Costa P., Lobo JMS., Modelling and comparison of dissolution profile; European Journal of Pharmaceutical Science, 2001; 13: 123-133.

78. Sahana B., Santra K., Basu S., Mukharjee B., Development of biodegradable polymer based Tamoxifen citrate loaded nanoparticles and effect of some manufacturing process parameters on them: a physicochemical and *in vitro* evaluation; International Journal of Nanomedicine, 2010; 5: 621-630.

79. Thangaraja A., Savitha V., Jegatheesan K., Preparation and Characterisation of Polyethylene glycol coated silica nanoparticles for drug delivery application; International Journal of Nanotechnology and Application, 2010; 4(1): 31-38.

80. Chouksey R., Jain AK., Pandey H., Maithil A., Development and bioavailability studies of Atorvastatin nanoemulsion; International Journal of Pharmacy & Life Sciences, 2011; 2(8): 982-988.

81. Senthilkumaran K., Enhancement of Bioavailability Atorvastatin Calcium by Micro and Nanoparticle preparation- Design and Evaluation; INTI International University College.

82. Ahmed M., Manohara YN., Ravi MC., RP-HPLC method development and validation for simultaneous estimation of Atorvastatin calcium and Amlodipine besylate; International Journal of ChemTech Research, 2012; 4(1): 337-345.

83. ICH, Q2B, Validation of Analytical Procedures: Methodology, International Conference on Harmonization; Geneva, 1996; 1-8.